AD-A038 068 NORTHROP CORP HAWTHORNE CALIF AIRCRAFT DIV F/G 11/3
FUNDAMENTAL INVESTIGATION OF ANODIC OXIDE FILMS ON ALUMINUM ALL--ETC(U)
AUG 76 R E HERFERT F33615-75-C-5121
UNCLASSIFIED NOR-76-101 AFML-TR-76-142 NL

1 OF 2
AD A038068

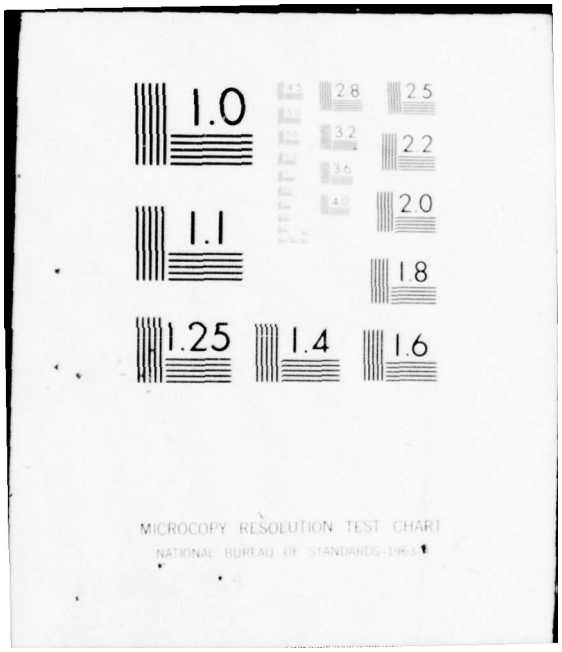
1.0
1.1
1.25
1.4
1.6
2.8
2.5
3.2
2.2
3.6
2.0
4.0
1.8
MICROCOPY RESOLUTION TEST CHART
NATIONAL BUREAU OF STANDARDS-1963-A

AFML-TR-76-142

FUNDAMENTAL INVESTIGATION OF ANODIC OXIDE FILMS ON ALUMINUM ALLOYS AS A SURFACE PREPARATION FOR ADHESIVE BONDING

Northrop Corporation, Aircraft Division
3901 W. Broadway
Hawthorne, California 90250

AUGUST 1976

TECHNICAL REPORT AFML-TR-76-142

Final Report for Period April 1975 – August 1976

Approved for public release; distribution unlimited.

AIR FORCE MATERIALS LABORATORY
AIR FORCE WRIGHT AERONAUTICAL LABORATORIES
AIR FORCE SYSTEMS COMMAND
WRIGHT-PATTERSON AIR FORCE BASE, OHIO 45433

NOTICE

When Government drawings, specifications, or other data are used for any purpose other than in connection with a definitely related Government procurement operation, the United States Government thereby incurs no responsibility nor any obligation whatsoever; and the fact that the Government may have formulated, furnished, or in any way supplied the said drawings, specifications, or other data, is not to be regarded by implication or otherwise as in any manner licensing the holder or any other person or corporation, or conveying any rights or permission to manufacture, use, or sell any patented invention that may in any way be related thereto.

This technical report has been reviewed and is approved for publication.

Neil T. McDevitt

NEIL T. MCDEVITT
Project Engineer

FOR THE DIRECTOR

S. W. Tsai

S. W. TSAI, Chief
Mechanics & Surface Interactions Branch
Nonmetallic Materials Division

Copies of this report should not be returned unless return is required by security considerations, contractual obligations, or notice on a specific document.

AIR FORCE - 30 MARCH 77 - 175

UNCLASSIFIED

SECURITY CLASSIFICATION OF THIS PAGE *(When Data Entered)*

REPORT DOCUMENTATION PAGE	READ INSTRUCTIONS BEFORE COMPLETING FORM
1. REPORT NUMBER: AFML-TR-76-142	2. GOVT ACCESSION NO. / 3. RECIPIENT'S CATALOG NUMBER
4. TITLE *(and Subtitle)*: FUNDAMENTAL INVESTIGATION OF ANODIC OXIDE FILMS ON ALUMINUM ALLOYS AS A SURFACE PREPARATION FOR ADHESIVE BONDING.	5. TYPE OF REPORT & PERIOD COVERED: Final Report. 1 Apr 75 - 30 Jun 1976.
	6. PERFORMING ORG. REPORT NUMBER: NOR-76-101
7. AUTHOR(s): R. E. Herfert	8. CONTRACT OR GRANT NUMBER(s): F33615-75-C-5121
9. PERFORMING ORGANIZATION NAME AND ADDRESS: Northrop Corporation, Aircraft Division, 3901 W. Broadway, Hawthorne, California 90250	10. PROGRAM ELEMENT, PROJECT, TASK AREA & WORK UNIT NUMBERS: Project No. 7342, Task No. 73420215
11. CONTROLLING OFFICE NAME AND ADDRESS: Air Force Materials Laboratory (AFML/MBM), Air Force Wright Aeronautical Laboratories, Wright-Patterson AFB, Ohio 45433	12. REPORT DATE: Aug 1976 / 13. NUMBER OF PAGES: 109 (12) 111 p.
14. MONITORING AGENCY NAME & ADDRESS *(if different from Controlling Office)*	15. SECURITY CLASS. *(of this report)*: Unclassified
	15a. DECLASSIFICATION/DOWNGRADING SCHEDULE

16. DISTRIBUTION STATEMENT *(of this Report)*

Approved for Public Release; distribution unlimited.

17. DISTRIBUTION STATEMENT *(of the abstract entered in Block 20, if different from Report)*

405 228

18. SUPPLEMENTARY NOTES

19. KEY WORDS *(Continue on reverse side if necessary and identify by block number)*

Adhesive Bonding	Aluminum Anodizing
Anodic Films	Oxide Coatings
Surface Characterization	Auger Spectroscopy
Scanning Electron Microscopy	Electron Diffraction

20. ABSTRACT *(Continue on reverse side if necessary and identify by block number)*

This study was structured to define the physical, chemical, and mechanical characteristics of anodized films by selecting widely differing anodic processes, systematically varying these processes, and carefully characterizing the resultant surfaces using the most advanced instrumental techniques. After defining the structure and character of the anodic film from the surface to the metal interface, a comparison of the relative stability of these surfaces was made by defining the point at which breakdown or hydration of the film occurred in salt spray and humid environments.

over

DD FORM 1 JAN 73 1473 EDITION OF 1 NOV 65 IS OBSOLETE

UNCLASSIFIED

SECURITY CLASSIFICATION OF THIS PAGE *(When Data Entered)*

20. Abstract (Continued)

Five distinct anodic systems were chosen for study in this program. These represented two porous systems, phosphoric acid and chromic acid, and three barrier layer systems: (1) ammonium chromate, (2) potassium/lithium nitrate eutectic salt, and (3) ammonium pentaborate in ethylene glycol. In each anodic system, electrical properties were recorded during anodization. Surfaces of each anodic coating were analyzed using electron diffraction to determine crystal structure, Auger electron spectroscopy to determine the chemistry, and scanning electron microscopy to characterize the thickness and morphology of the oxide. The oxide layers formed by the phosphoric acid, chromic acid and ammonium chromate systems were all of the $\alpha Al_2O_3 \cdot H_2O$ (boehmite) type. The oxide formed in the ammonium pentaborate was γAl_2O_3 (gamma) oxide, while the oxide formed in the eutectic salt was αAl_2O_3 (corundum) oxide. Thickness and oxide character varied widely as a function of voltage, time, bath concentration, and temperature. Auger electron spectrographic analysis was used to determine thickness, surface contamination, and active elemental diffusion during anodization. Both Mg and Zn were the most active elements in the 7075 system, whereas Cu was the most active in the 2024 system.

Representative specimens of each anodic condition were exposed to environmental testing in stressed and unstressed conditions. Breakdown of the anodic coating by oxide hydration was greatest in the chromic acid and ammonium chromate systems. Stressing the oxide layer accelerated the rate of breakdown.

The significance of this program lies in the subsequent use of this data in studies on the durability of oxide films in conjunction with adhesives. This program has developed the basic relationship between the parameters and the physical, chemical, and crystallographic character of the oxide films. The next step is to use these parameters in the development of a durable interface for adhesive bonding.

PREFACE

This report was prepared by Northrop Corporation, Aircraft Division, Hawthorne, California under USAF Contract F33615-75-C-5121. The contract work was administered under Project No. 7342, Task No. 73420215, under the direction of the Air Force Materials Laboratory, Wright Patterson AFB, Ohio. The program monitor was Mr. N. T. McDevitt (AFML/MBM) of the Mechanics and Surface Interactions Branch of the Nonmetallic Materials Division.

Mr. R. E. Herfert served as the Principal Investigator on this program. Other Northrop personnel who made major contributions in this research program were T. P. Remmel, P. A. Honeycutt, J. Schifando, H. W. Willis, B. B. Bowen, S. L. Feenstra, R. R. Wells, and J. W. Lewis.

The contractor's report number is NOR 76-101. This covers work from 1 April 1975 through 30 June 1976. This report was submitted in August 1976.

TABLE OF CONTENTS

TABLE OF CONTENTS (Continued)

LIST OF ILLUSTRATIONS

LIST OF ILLUSTRATIONS (Continued)

LIST OF ILLUSTRATIONS (Continued)

LIST OF TABLES

SECTION I

INTRODUCTION

Anodic aluminum oxide films are commonly classified as "porous" or "barrier-type" (i.e., "non-porous") according to the electrolyte in which they are formed. Barrier-type films are formed by anodically polarizing aluminum in electrolytes such as aqueous borates, tartrates, chromates, or nitrates. These electrolytes exert little solvent action on the base material and oxide film, and therefore the thickness of the oxide is proportional to the applied voltage. Porous films, on the other hand, are formed by anodic polarization of aluminum in electrolytes such as aqueous sulfuric, chromic, oxalic, or phosphoric acids. These electrolytes exert appreciable solvent action on the base material and oxide film, and the oxide growth is time-dependent due to the dissolution and growth processes occurring. The structure of porous films has been characterized by Keller, Hunter, and Robinson[1], and later by O'Sullivan and Wood[2], as a close-packed array of columnar hexagonal cells, each containing a central pore normal to the substrate surface and separated from it by a layer of barrier-type film. The dimensions of these structural features are dependent on the formation potential as well as the electrolyte[2]. The thickness of the barrier layer formed beneath the porous layer in the initial stages of porous oxide film growth is proportional to the applied potential, with the proportionality constant being on the order of 10 to 20Å V^{-1}. This is in contrast to the value of approximately 13Å V^{-1} for 100% barrier layer oxides [3, 4, 5].

A number of investigators have studied the mechanism of pore formation and growth in anodic films. Keller, Hunter, and Robinson[1] proposed that pore growth occurs by simultaneous formation and dissolution of oxide. This occurs initially at regions experiencing a locally high dissolution rate; Joule heating in the adjacent electrolyte then enhances the process at these sites.

While Hunter and Fowle [6] explained pore formation simply in terms of chemical dissolution, Hoar and Mott[7] postulated that the dissolution was electrical-field assisted and that both formation and dissolution of oxide were enhanced by the locally high field at the pore bases. The mechanism appears most generally accepted at

present[2]. To explain the observation that pores do not initiate until a barrier-type layer of at least a critical thickness has formed, Hoar and Yahalom[8] have suggested that proton entry into the oxide film is necessary to pore formation and that this is possible, against the anodic field, only when the field has decreased to a value characteristic of the critical thickness. Random local defects in the initial barrier film are seen as important to pore nucleation by Arrowsmith, Culpan, and Smith[9] who studied pore nucleation in films formed on aluminum substrates of varying purities.

Hoar and Yahalom[8] have reported that both barrier-type films (formed in 3% ammonium tartrate at pH 7.3, 25°C, 14.4V) and porous films (formed in 15% sulfuric acid, 25°C, 14.4V) develop their structures after only a few seconds of anodizing. Several investigators have reported the formation of porous-like cellular structures in films formed in borate or tartrate solutions at high formation voltages or prolonged anodizing times. Franklin[10] observed an irregular polygonal cell structure in films formed at 500V in aqueous 3% boric acid by weight. In this investigation the cell diameter was proportional to the formation voltage and the cells grew into both the electrolyte and the substrate. Stirland and Bicknell[11] confirmed this observation and, through electron diffraction of thin films, demonstrated that the centers of the cells were amorphous, while the edges were γ-Al_2O_3. Hoar and Yahalom[8] reported pore formation in films formed in 3% ammonium tartrate, pH 7.3, at 14.4V for 10 minutes. Hunter and Towner[12] found a porous layer had formed above the barrier layer on aluminum which was anodized in 3% ammonium tartrate, pH 5.5, for times up to 90 minutes. The substrate surface after anodizing was seen to have a cellular pattern similar to that seen in the case of porous films. They observed that the barrier layer reached a limiting thickness after twelve minutes, after which the porous layer formed at a linear rate of about 175 Å/hr. Leach and Neufeld[13] observed pore formation in films formed in aqueous borate at pH 9.7 subsequent to attainment of a steady leakage current under constant applied potential. Pore growth was affected both by formation rate and electrolyte temperature.

Many studies have emerged in recent years on the durability of adhesive bonded structures. Most of these studies have been related to the definition of the capability of various adhesive systems and corrosion-inhibiting primers to withstand the combination of applied load and corrosive environment. They have shown that failure will occur in a corrosive environment much more rapidly if the structure is placed under load at the same time. Very few studies have been concerned with the definition of the surface chemistry of the adherend and the effectivity of corrosion inhibition by the surface preparation process.

Up to a very few years ago, the two major advances in adhesive bonding were:

1. The development of the FPL etch treatment for aluminum to improve the humidity and salt spray durability of adhesive bonds.
2. The development of corrosion-inhibiting primers for adhesives.

The FPL etch system was developed about 20 years ago. At present, numerous variations of both the pretreatment FPL etch processes exist throughout the industry. Corrosion resistant primers were developed in the last five years in response to DOD requirements. Work on these primers is continuing. A combination of the FPL etch system and a corrosion resistant primer results in an adhesive bonding system that has good corrosion resistance in humidity and salt spray environments.

Up until a few years ago, good techniques were not available for analyzing and studying the oxide layer on aluminum surfaces. The anodic film can be anywhere from 50Å to 5000Å thick; it can be an amorphous hydrated oxide, a mixture of specific crystalline hydrates, or mixtures of these materials; it can be amorphous or crystallized; it can vary from nearly uncontaminated aluminum hydrate to a hydrate containing 20% impurity; and, it can be either a very dense "barrier" layer, a weak bulky "porous" layer, or a combination of both. With the advent of techniques such as scanning electron microscopy, Auger electron spectroscopy, electron diffraction, and others, all of these characteristics of the oxide film can be determined. Processing can now be varied to produce changes in the oxide film which can be observed directly instead of by indirect corrosion or adhesion tests. A "model" oxide surface may be postulated for adhesive bonding and developed through processing changes and direct observation of the surface.

Based on current knowledge, experience, and the state-of-the-art, the following characteristics were postulated as being most desirable for producing a durable anodic film on aluminum for adhesive bonding.

Crystalline form:

1. Corundum (preferred) — $\alpha \cdot Al_2O_3$
2. Diaspor (second choice) — $\beta \cdot Al_2O_3 \cdot H_2O$
3. Boehmite (most readily achieved) — $\alpha \cdot Al_2O_3 \cdot H_2O$

Structure:

1. "Barrier" film (very dense, crack-free, moisture-proof)
2. "Barrier" film with adherent porous oxide (second choice)

Thickness:

1. 1000Å or less (for good bond strength at -65° F)

Chemical properties:

1. Chromium, added for corrosion inhibition. The presence of catalytic ions forces the parent metal to form the same oxide in open crack areas as the stable oxide film; thus, a self-healing oxide film is formed.

Mechanical properties:

1. High strength, "hard" porous oxide film. Good bond to "barrier" film. Porosity sufficient for good adhesive penetration or a "barrier" film that bonds well to adhesives.

For this program, it was intended to produce anodic films on aluminum that are environmentally stable. The basic premise for this program was that the most readily achieved stable form of anodic coating was a "barrier" film of alpha-aluminum oxide monohydrate called boehmite. The corrosion resistance of this type of oxide film should be proportional to its thickness. It was felt that an alpha-aluminum oxide (corundum) film or a beta-aluminum oxide monohydrate (diaspore) film may be equal to or better than a "barrier" layer of boehmite. However, it is difficult to prepare these films under conditions which are suitable for use in production adhesive bonding. Nevertheless, anodizing processes were selected which produced a maximum variation in crystal structure, composition, and physical or mechanical properties.

In this program, we selected baseline conditions for anodizing by five different electrolytic methods. Samples were prepared on two aluminum substrates by these baseline conditions and completely characterized and evaluated for environmental resistance. We also screened the processing variables for each of the five anodizing systems to determine what changes in physical, chemical, and mechanical characteristics were achieved. Processing conditions that produced extreme variations in characteristics of anodic films were selected for continued characterization and determination of environmental durability. The resulting data were compared to those obtained on the specimens made under baseline anodizing conditions. The relationship between anodic film characteristics and environmental durability was determined.

To achieve the above goals, a systematic investigation was conducted which followed the abbreviated Program Plan presented here. This plan will serve the reader as an outline of the work reported herein.

Task I - Select Anodization Treatments

1. Review anodizing literature and experience
2. Select metal substrates and pretreatment
3. Define FPL etch comparison system
4. Select anodizing system

Task II - Study Anodizing Processing Parameters

1. Define criteria for selection of process variables
2. Define effects of process variables
3. Process specimens under baseline conditions
4. Screen processing variables; prepare specimens
5. Select extreme processing conditions and prepare specimens

Task III - Characterize Anodic Films

1. Select oxide film characterization techniques
2. Characterize baseline systems
   a. FPL etch
   b. Phosphoric acid anodize
   c. Chromic acid anodize
   d. Ammonium chromate anodize
   e. Ammonium pentaborate/ethylene glycol anodize
   f. Potassium/sodium nitrate anodize

Task IV - Determine Environmental Durability of Anodic Films

1. Develop corrosion resistance evaluation technique
2. Determine corrosion resistance of baseline anodic systems
3. Determine corrosion resistance of anodic films made under extremes of processing
4. Correlate anodic film character to corrosion resistance
5. Select and recommend optimum anodizing process for corrosion resistance for each alloy

SECTION II

TEST PROCEDURES

This section describes the various procedures that were used to clean and anodize the aluminum alloys, to evaluate the electrical properties during anodization, to prepare the specimens for examination, and to examine the specimens with the scanning electron microscope, the Auger electron spectrograph, and the transmission electron microscope (electron diffraction).

ANODIZATION CONDITIONS

Material

Four substrate compositions were used in this program including 2024-T3 bare and clad and 7075-T6 bare and clad 0.063-inch sheet. Upon receipt of these alloys in the form of 48-inch by 96-inch by 0.063-inch sheets, the material was sheared into 12-inch by 12-inch panels for storage. Prior to anodizing, this material was sheared into 1-inch by 4-inch strips, which was the standard specimen size for all anodizing.

Electrolytes Selected

The following five electrolytes were selected for aluminum anodizing in the program. They will be compared to each other and to the FPL etch (sulfuric acid/dichromate) baseline system in later sections of this report.

Phosphoric acid anodizing
Chromic acid anodizing
Ammonium chromate anodizing
Ammonium pentaborate-ethylene glycol anodizing
Potassium-lithium nitrate eutectic salt anodizing

Deionized water was used in making up all aqueous solutions. In all chemical treatments and anodizing baths, chemical composition was controlled by periodic wet chemical analysis. Low temperature and high temperature anodizing solutions were constantly agitated by stirring. PH was controlled by bath additions or dilutions.

FPL Etch

The FPL etch process used for this program is in use at Northrop. Processing is as follows:

1. Degrease: Trichlorethane vapor (3-4 minutes)
2. Alkaline Clean: 10-15 minutes

   Turco 4215-S: 6-8 ± 1 wt. oz/gal of solution
   Operate at: 155F ± 10F
3. Rinse: 5 minutes in DI water
4. Etch: 10 ± 1 minute

   Sulfuric acid: 38.5-41.5 fl. oz/gal of solution
   Sodium dichromate: 4.1-4.9 wt. oz/gal of solution
   Operate at: 145F-160F
5. Rinse: 5 minutes in DI water
6. Oven dry: 150F-160F for 30 minutes

This system was the baseline for comparison of all surface characterization performed during the program.

Phosphoric Acid Anodizing System

This is a system that has been used for years both for electropolishing and for producing a thin porous oxide film which can be electroplated. One anodizing technique is based upon the use of a 25-30% phosphoric acid solution at room temperature and 30-60 volts for 10 minutes to produce a porous oxide about 3 microns or 30,000Å thick. Recently, the Boeing Aircraft Company has found that thin phosphoric acid anodized coatings have excellent corrosion resistance and are good surfaces for adhesive bonding. Northrop has used a somewhat similar system for adhesive spot-weld bonding [14] (weldbonding) and has generated both characterization and durability data on this type of anodize layer. The baseline phosphoric acid system used in this program follows:

1. Degrease: Trichlorethane vapor (3-4 minutes)
2. Alkaline Clean: 10-15 minutes

   Turco 4215-S: 6-8 wt. oz/gal of solution
   Operate at: 155F ± 10F

3. Rinse: 5 minutes in DI water

4. Deoxidize: 7 minutes

   Amchem 7: 2.7-3.3 wt. oz/gal of solution
   Nitric Acid: 8-16% by volume
   Operate at: R.T.

5. Rinse: 5 minutes in DI water

6. Anodize: 20-25 minutes

   Phosphoric Acid: 11-16 fl. oz/gal of solution
   10 ± 1 volt D.C.
   Operate at: R.T.

7. Rinse: 5-10 minutes in Dl water

8. Oven dry at: 150F-160F for 30 minutes

Anodizing was conducted in a lead-lined stainless steel tank.

Chromic Acid Anodizing System

Many modifications of the chromic acid anodizing process have been used. Concentration, temperature, and voltage can vary widely and sulfuric acid can be substituted for some of the chromic acid. The following chromic acid anodizing procedure was used on this program.

1. Degrease: Trichlorethane vapor (3-4 minutes)

2. Alkaline Clean: 10-15 minutes

   Turco 4215-S: 6-8 wt. oz/gal of solution
   Operate at: 155F ± 10F

3. Rinse: 5 minutes in DI water

4. Deoxidize: 7 minutes

   Amchem 7: 2.7-3.3 wt. oz/gal of solution
   Nitric Acid: 8-16% by volume
   Operate at: R.T.

5. Rinse: 5 minutes in DI water

6. Anodize: 40 minutes (see schedule below)

Chromic Acid: 10 wt. oz/gal of solution
Operate at: 104F ± 4F
Voltage: D.C.

Gradually increase voltage for first 10 minutes from 0 to 40 volts in steps of not more than 5 volts.

Hold at 40 volts for 20 minutes.
Increase to 50 volts within 5 minutes.
Hold at 50 volts for 5 minutes.

(Note: The current density at the higher voltage should be 2.5 amps/sq.ft. of anode surface).

7. Rinse: 5 minutes in DI water

8. Dichromate Seal: 15 minutes

Sodium Dichromate: 5.0-6.5% by weight/gal of solution

9. Rinse: 5-10 minutes in DI water

10. Oven dry: 150F-160F for 30 minutes

Anodizing was conducted in a lead-lined, stainless steel tank.

Ammonium Chromate

The baseline process used for ammonium chromate anodizing is as follows:

1. Degrease: Tricholorethane vapor (3-4 minutes)

2. Alkaline Clean: 10-15 minutes

Turco 4215-S: 6-8 wt. oz/gal of solution
Operate at: 155F ± 10F

3. Rinse: 5 minutes in DI water

4. Deoxidize: 7 minutes

Amchem 7: 2.7-3.3 wt. oz/gal of solution
Nitric Acid: 8-16% by volume
Operate at: R.T.

5. Rinse: 5 minutes in DI water

6. Anodize: 10 minutes

   Ammonium chromate: 3% by weight
   pH: 5.5 (adjust with ammonia or chromic acid)
   Voltage: 50 volts D.C.
   Operate at: R.T.

7. Rinse: 5-10 minutes in DI water

8. Oven dry: 150F-160F for 30 minutes

This anodizing process produces a "barrier" layer oxide with a film thickness of about 1000Å. All anodizing was performed in a stainless steel tank.

Ammonium Borate in Ethylene Glycol

"Barrier" layer films were thought to be a mixture of gamma-aluminum oxide (anhydrous) and boehmite, with possibly some additional water which could make the film amorphous. Decreasing the water content in this electrolyte makes possible the formation of an almost pure, anhydrous gamma-aluminum oxide. Two typical systems of this type are oxalic acid in alcohol solutions and boric acid or ammonium borate in ethylene glycol. The use of ethylene glycol as the non-water solvent in the electrolyte permitted us to use temperatures below 0°F. The baseline system used was as follows:

1. Degrease: Trichlorethane vapor (3-4 minutes)

2. Alkaline Clean: 10-15 minutes

   Turco 4215-S: 6-8 wt. oz/gal of solution
   Operate at: 155F ± 10F

3. Rinse: 5 minutes in DI water

4. Deoxidize: 7 minutes

   Amchem 7: 2.7-3.3 wt. oz/gal of solution
   Nitric Acid: 8-16% by volume
   Operate at: R.T.

5. Rinse: 5 minutes in DI water, followed by 5 minutes in ethylene glycol

6. Anodize: 10 minutes

Ammonium Borate: 25% by weight in ethylene glycol
Voltage: 50 volts D.C.
Operate at: R.T.

7. Rinse: 5 minutes in DI water

8. Oven dry: 150F-160F for 30 minutes

All anodizing was performed in a stainless steel tank.

This system produced an anhydrous gamma-aluminum oxide "barrier" layer. The main consideration in using this system was in gaining a second method of control of the degree of hydration of the oxide layer on the aluminum surface.

Potassium/Lithium Nitrate Eutectic Salt Anodizing System

Three anhydrous salt mixtures have been found which can be used as electrolytes in the fused condition for producing anhydrous aluminum oxides; these are: (1) the lithium acetate/lithium acrylate system, (2) the potassium bisulfate/sodium bisulfate system, and (3) the potassium nitrate/lithium nitrate system.

The lithium acetate system melts at 155F and decomposes at slightly over 212F. The bisulfate system melts at 350F and the nitrate system melts at about 300F. These systems produce a white matte anodic oxide coating which is a highly porous and very hard corundum oxide. The corundum formed is insoluble in hydrofluoric, sulfuric, or phosphoric acids or by caustic soda. It is non-hydroscopic and is not sealable in boiling water or dichromate solution. The lithium acetate system is expected to produce more gamma-aluminum oxide than the other two systems.

The bisulfate system is probably safer to handle than the nitrate system since the nitrate is a powerful oxidizing agent. However, the sulfate system operates at a temperature where the 7075-T6 aluminum alloy may become "overaged." Therefore, we used the nitrate eutectic salt anodizing system. This system produced a dense, tenacious, adherent anhydrous film of almost pure corundum, alpha-aluminum oxide. The procedure for the potassium/lithium nitrate anodizing process is as follows:

1. Degrease: Trichlorethane vapor (3-4 minutes)

2. Alkaline Clean: 10-15 minutes

Turco 4215-S: 6-8 wt. oz/gal of solution
Operate at: 155F ± 10F

3. Rinse: 5 minutes in DI water

4. Deoxidize: 7 minutes

   Amchem 7: 2.7-3.3 wt. oz/gal of solution
   Nitric Acid: 8-16% by volume
   Operate at: R.T.

5. Rinse: 5 minutes in DI water

6. Anodize: 30 minutes

   Potassium nitrate: 60% by weight
   Lithium nitrate: 40% by weight
   Voltage: 50 volts D.C.
   Operate at: 300F

7. Rinse: 5-10 minutes in DI water

8. Oven dry: 150F-160F for 30 minutes

All anodizing was performed in a stainless steel tank.

ELECTRICAL PROPERTIES

A relatively simple system was used to record voltage, current, surface potential, and temperature as a function of time. A Moseley X-Y and a Hitachi strip chart recorder were used to record electrical information. The Hitachi recorder was a dual pen recorder, whereas the Moseley X-Y recorder was a single pen unit. The voltage was read directly across the input leads to the anode and cathode of the anodizing bath. Current was recorded as voltage drop across a resistor and was calibrated for the recorder system. Surface potential was measured directly from surface contact with a liquid potential probe. A schematic of the electrical arrangement is shown in Figure 1. The anodizing bar with the specimen holders is shown in Figure 2. The specimens were immersed into the electrolyte about 3.5 in. of the 4.0 in. length.

ANALYTICAL CHARACTERIZATION

Scanning Electron Microscopy (SEM)

Scanning electron microscopy (SEM) was used to investigate the physical characteristics of the oxide layer. The 90-degree bend technique prior to SEM analysis was employed, the purpose being to crack the oxide layer so the substrate adhesion

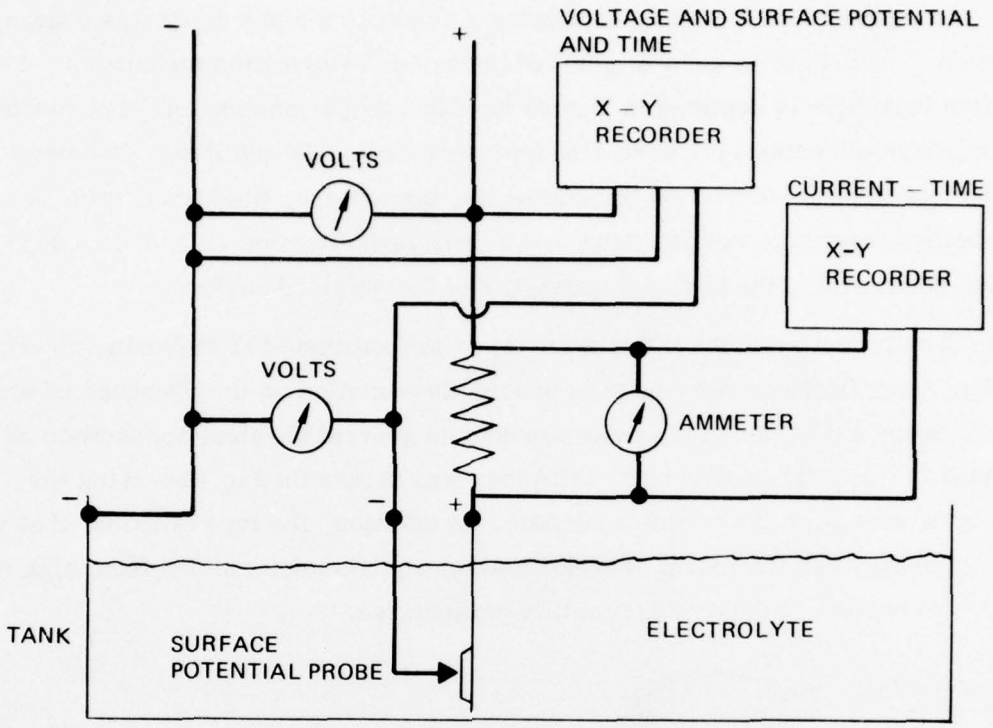

FIGURE 1. ELECTRICAL SCHEMATIC FOR ANODIZING OF ALUMINUM SAMPLES

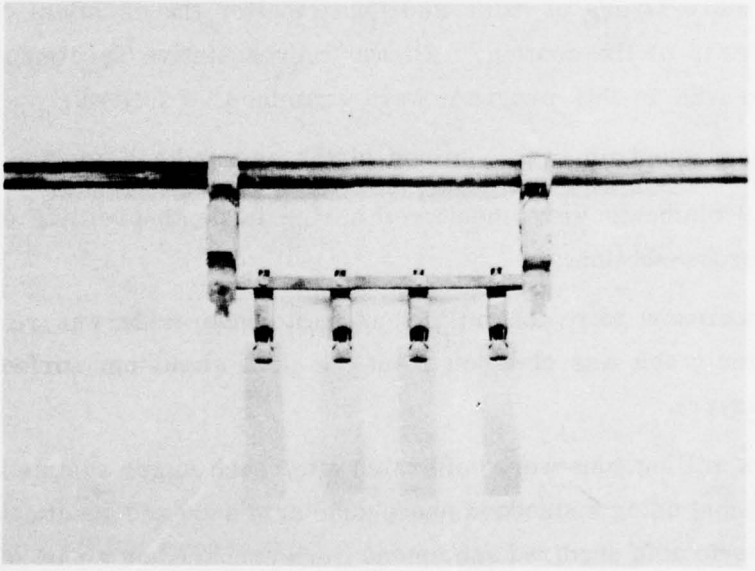

FIGURE 2. HOLDER USED FOR ANODIZING ALUMINUM SPECIMENS

properties, mechanical strength, and thickness could be evaluated. The specimen was mounted on a standard SEM sample stub using a conductive cement. It was coated, in all directions, with 200Å to 400Å of gold using vacuum evaporation techniques. This examination technique is depicted in Figure 3. The sample was examined perpendicular to the surface (A-direction) for pore size type measurements and it was examined across the thickness (B-direction) for continuity, pore shape, thickness, etc. A series of SEM photomicrographs ranging from low to high magnification (50X to 19,000X) were taken documenting the physical character of the oxidized surface.

The density and porosity of the oxide layer was evaluated at high magnification while lower magnifications were used to provide information on the presence of flaws and cracks in the oxide, as well as cleanliness and general physical appearance of the oxide surface layer. The oxide layer thickness was determined by observing the cracked oxide normal to the fracture surface. In addition, the type of oxide, that is, barrier or porous, and the extent of stratification was also determined from high magnification observation of the oxide from this perspective.

Auger Electron Spectroscopy (AES)

The Physical Electronics Industries Inc. Auger spectrograph with cylindrical mirror analyzer (CMA) was used to chemically characterize the outer 15Å-25Å of the surface of the material. In many cases this surface was then bombarded with argon ions to remove layers of oxide and thus monitor the chemical content through the thickness of the coating. All the representative specimens which were analyzed with the AES in this program were examined as follows:

1. An Auger spectrum was obtained of the as-anodized surface.
2. Up to 6 elements were monitored during in depth-profiling of the oxide cross-section.
3. The specimens were ion milled until after the oxide was removed then an Auger trace was obtained from the final aluminum surface (below the oxide layer).
4. The ion milling guns were calibrated after each Auger sample loading (10 specimens) using a standard phosphoric acid anodized specimen. The phosphoric acid anodized specimens were prepared as a part of this program and they provided a very reliable (4000Å) aluminum oxide thickness.

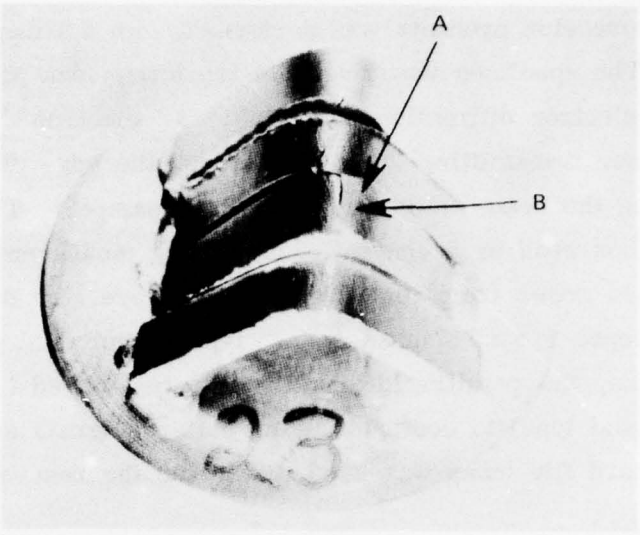

FIGURE 3. SEM 90° BEND SAMPLE CONFIGURATION FOR OXIDE THICKNESS EXAMINATION, 2X

Electron Diffraction

The morphological character of the oxide films was determined using high resolution electron diffraction. Crystallographic characterization of the developed oxide surfaces or corrosion products was performed with a Hitachi HU-11A electron microscope. The specimen was placed in the lower lens position to obtain the high resolution electron diffraction reflection. An electron diffraction pattern was obtained by either transmitting the beam through the edge of the oxide at the bend or by reflecting the beam off of the face of the sample. The resulting diffraction plate was then read on a conventional rotating measurement stage. Since the oxide layers were grown from the bare metal outward, the diffraction patterns show a great prevalence for a "single crystal" type or epitaxial growth pattern of crystallization. Thus, the resulting diffraction patterns varied from complete spot patterns (single crystal type) to continuous ring patterns (grain size 10^{-4} to 10^{-5} mm). The ASTM card file index was used to analyze the results and diffraction patterns.

Corrosion Resistance Testing

The corrosion resistance of the anodic films was evaluated by determining the time required for initial formation of bayerite on the surface and by qualitatively determining the rate of growth under various conditions. To accomplish these measurements, simple specimens, 0.063-inch by 1-inch by 4-inches, were prepared and exposed to standard humidity conditions (140F at 100% R.H.). These specimens were exposed in a flat, unstressed condition and in a bent condition similar to that shown in Figure 4 to provide a constant stress level of 35,000 psi on the aluminum surface. These surfaces were then examined with SEM and electron diffraction after various exposure times to determine the time of initial bayerite formation and a rate of bayerite growth. Anodize treatments were ranked in accordance with a relative time frame based on initial appearance of bayerite and the time at which approximately 50% of the surface has been converted. Comparisons were similarly drawn between stressed and unstressed conditions.

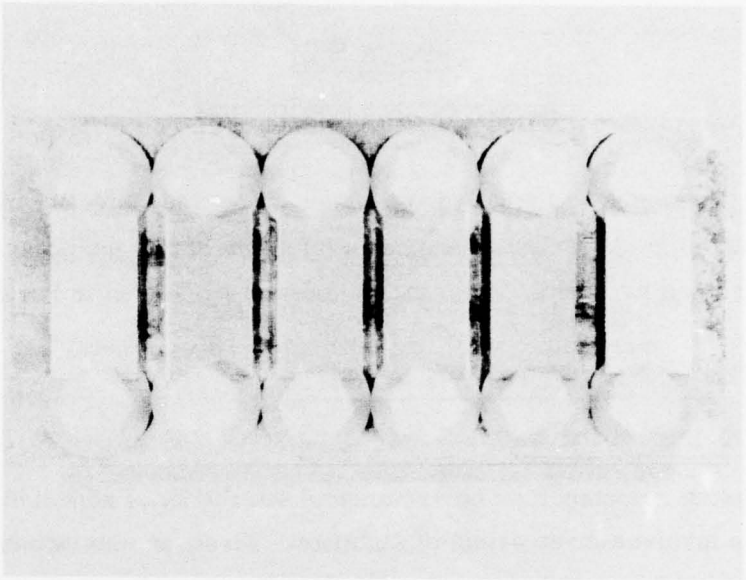

FIGURE 4. FIXTURE FOR CORROSION TESTING

SECTION III

RESULTS AND DISCUSSION

In order to present a logical progression from the selection of anodization treatments through the characterization and evaluation of the anodic systems, the results are presented by Tasks, following the outline presented in Section I.

TASK I — SELECT ANODIZATION TREATMENTS

Comparison of Aluminum Oxides

The corrosion resistance or environmental durability of adhesive bonds on aluminum alloys involves three areas of stability. First, moisture can be absorbed through the adhesive layer and accumulate at the adhesive/aluminum oxide interface. Here, it can be mechanically absorbed or be chemically combined with the oxide. The preferred oxide film is one that will mechanically absorb the minimum amount of moisture and that will not chemically combine with absorbed moisture. Second, the aluminum oxide layer should be thermodynamically and environmentally stable. Third, when a crack, flaw, or scratch extends through the aluminum oxide layer to the bare metal, the new oxide that grows on the exposed bare metal surface should be either the same as the surrounding oxide layer or it should be morphologically and mechanically compatible with it.

Many oxide and oxide-hydrates of aluminum exist; however, we can categorize their usefulness in adhesive bonding by considering all of them to be essentially one of the following six oxide combinations.

Stable below 200F: alpha-aluminum oxide trihydrate - Gibbsite
beta-aluminum oxide trihydrate - Bayerite

Both of these oxides are natural forming at room temperature. Recently work has shown that bayerite forms in cracks on bare aluminum in an environment of either humidity or a corrosive medium.

Stable above 200F: alpha-aluminum oxide monohydrate - Boehmite
beta-aluminum oxide monohydrate - Diaspore
gamma-aluminum oxide (anhydrous)
alpha-aluminum oxide (anhydrous) - Corundum

Based upon our current experience and a review of the literature, we feel that all of these latter oxides and hydrates are also stable at low temperatures. By this, we mean that they will not change their crystalline form when cooled below room temperature. For example, gibbsite may change to boehmite by heating above 200F, but boehmite will not revert to gibbsite in a moist atmosphere at temperatures between RT and 200F.

Also, any of the anhydrous or partially dehydrated oxides, like gamma-aluminum oxide, are very porous and hygroscopic. They are used as desiccants and act like a sponge in the presence of moisture. However, so far, we have found no evidence that gamma oxides or partially dehydrated oxide-hydrates will convert back to a specific hydrate in the presence of water or moisture. The most stable aluminum oxide is corundum, but there is currently no economically practical procedure for forming this oxide on aluminum under production conditions.

Currently after 2 hours at 200F only boehmite, diaspore, and corundum films are stable. Gamma-aluminum oxides are stable at 200F, but unless they can be densified and made almost non-porous, they are too hygroscopic.

The second very important factor is that some of the oxide-hydrates can be formed in either a very dense, non-porous "barrier" layer or as a "porous" oxide layer; and, in many cases, a "barrier" layer will be obtained at the metal surface with a "porous" oxide layer on top of it. Processing parameters can be used to vary the relative proportions of "barrier" and "porous" oxide layers, and they can be used to essentially eliminate the "porous" oxide layer. The "porous" oxide layer might improve bond strength by improving the mechanical interlocking of the adhesive and the oxide layer, whereas the "barrier" layer does not appear to have this capability. However, our results indicate that the adhesive lap shear strengths of "barrier" layers are 5000 to 6000 psi which are as high as those which can be obtained with "porous" oxide layers.

Selection of Aluminum Alloys

The 2024-T3 and 7075-T6 alloys were selected because they represent over 90% of the aluminum alloy used for aircraft structural adhesive bonding in the United States. Chemically and metallurgically, these alloys are widely different. The 2024 (4.3% Cu, 0.6% Mn, 1.5% Mg) is a precipitation strengthened aluminum base alloy. In the T3 condition, it consists of a microstructure of S-$CuAl_2$ platelets and Guinier-Preston zones (copper concentration areas) in the aluminum grains. These copper concentration zones in the grains should produce a different reaction to the processing and anodizing treatments than that which occurs in the 7075 alloy. The 7075 (5.7%, Zn, 2.6% Mg, 1.5% Cu) is also a precipitation strengthened aluminum base alloy. It is strengthened, however, by the precipitation of an Al-Mg-Zn intermetallic phase. In the T6 condition it is fully aged and stable.

The use of bare alloys represents a major trend in structural bonding today due to the increased bond durability in highly stressed environments. However, it was unknown why the clad alloys anodized so differently. It was our contention that the major differences occurred in the formation and morphology of the oxide layer. These differences were characterized in this program using 2024-T3 bare and clad alloy and 7075-T6 bare and clad alloy.

Other major differences that occur in production and that have an effect on the anodizing results obtained in this program are the conditions of the starting surface, e.g., light corrosion, mill conditioning, machining, etc. Since this program was designed to develop basic data on anodizing characteristics related to bonding, these other variables were kept to a minimum by cutting all test samples from the same sheet. A nominal sheet thickness of 0.063-inch was used (standard lap shear panel thickness) and the anodizing sample size was 1-inch by 4-inches. Test specimens for surface analysis were cut from the processed 1-inch by 4-inch sample. Samples were carefully analyzed for uniformity of anodic coatings and typical areas representing the surface were selected.

A major effect on the anodic coatings, exclusive of the previously discussed variables, is caused by the pretreatment conditioning of the sheet surface. A sequence of vapor degreasing, alkaline cleaning, and acid deoxidizing was used prior to anodizing. Rinsing after cleaning and deoxidizing is done with room temperature deionized water. The importance of each of these pretreatment steps is shown in the following SEM photographs, Figures 5 through 7. The first photo, Figure 5, shows the surface of an "as-received" vapor degreased aluminum sheet bent 90° to fracture the oxide layer.

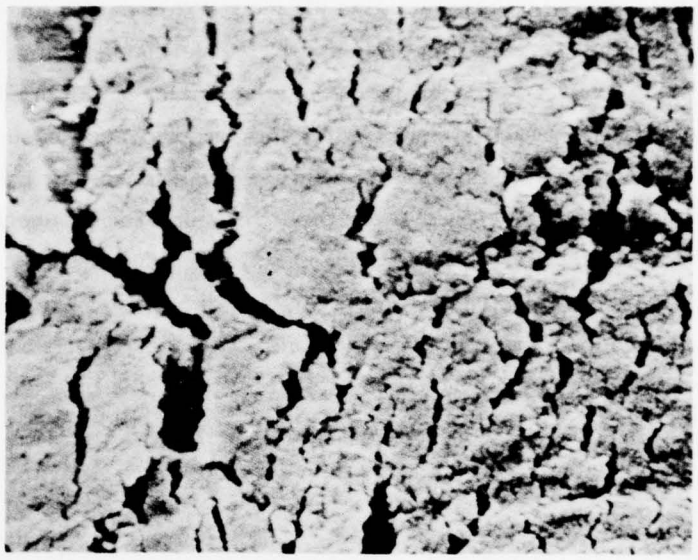

FIGURE 5. SURFACE CHARACTER OF BARE 7075-T6, VAPOR DEGREASED (14,000X)

This surface is primarily bayerite, fairly thick, and loosely adhering. Figure 6 shows a similar surface which has been alkaline cleaned. This surface has now been lightly etched and broken up to a condition which will enhance the deoxidizer attack. Figure 7 shows the surface after deoxidizing. No surface oxide layer is now visible, meaning that the layer (still characterized primarily as bayerite) has been removed to a thickness of less than 60Å, which is the resolution capability of the microscope. This surface condition is especially critical for the formation of subsequent non-reactive or "barrier" layers. Since barrier layer anodizing solutions do not react with the surface to dissolve the residual oxide layer remaining after pretreatment, anodizing in these solutions will merely add oxide onto the bayerite. The residual bayerite layer is loosely adhering, which is undesirable; thus, the bayerite must be removed as completely as possible. This requirement may not be as critical for the acid anodizing solutions, since these solutions remove some of the sub-oxide layer during the anodizing process.

Selection Criteria

The objective of this study was to determine the characteristics of the anodic films on aluminum alloys which have a relationship to adhesive bonding technology and that might have excellent environmental stability. Evaluation of durability in this study was done on the anodic films themselves and not on primer- or adhesive-coated films. Since we evaluated only the anodic films, our first criterion for the selection of anodic films was to obtain as many different crystalline types of films as possible. These were:

Two aluminum oxide trihydrates - bayerite and gibbsite
Two aluminum oxide monohydrates - boehmite and diaspore
Two anhydrous aluminum oxides - gamma and alpha (corundum)

The second criterion used for the selection of the anodizing systems was the physical character of the oxide film formed. This was either a very dense "barrier" layer oxide film, or a "porous" less dense film, or a stratified oxide of a "barrier" layer on the metal surface with a "porous" layer on top of it. The "barrier" layer films, as the name implies, are a continuous thin oxide coating over the metal and they effectively prevent entrance of moisture or other corrosion media to the aluminum surface. However, there are some cracks and flaws in the "barrier" layer and flexing

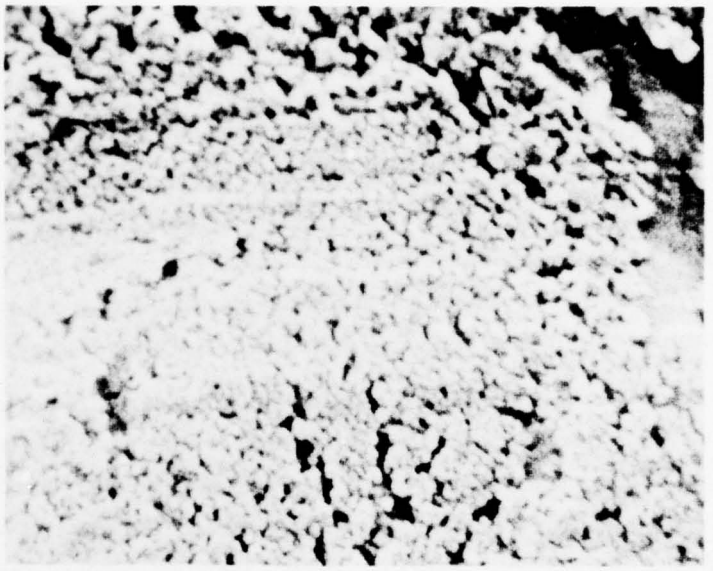

FIGURE 6. SURFACE CHARACTER OF BARE 7075-T6, ALKALINE CLEANED (14,000X)

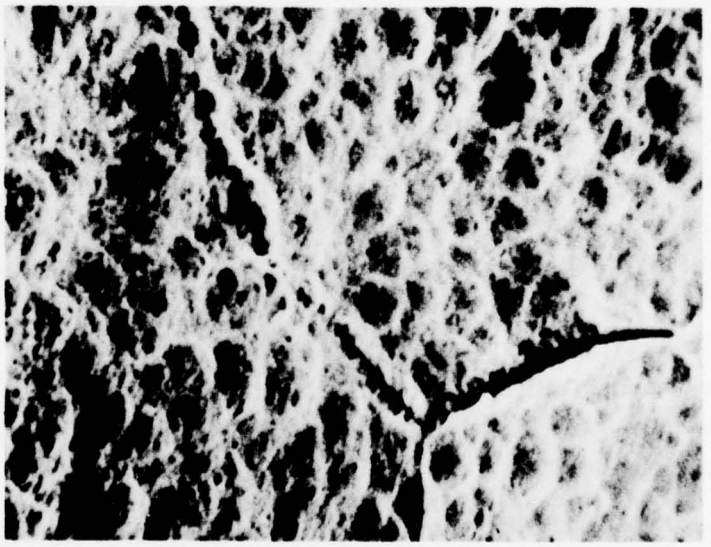

FIGURE 7. SURFACE CHARACTER OF BARE 7075-T6, DEOXIDIZED (14,000X)

or stressing of the parent metal may produce additional flaws or cracks in the "barrier" layer. As a goal, we wanted to obtain the maximum corrosion resistance or environmental durability in the anodic film, with a flawless, flexible, "barrier" layer. Since "flawless" and "flexible" probably cannot be achieved, we compromised by using a thicker film which incorporated the properties of "self-healing." When a crack, flaw, or scratch penetrates through the oxide film to the parent metal, the "self-healing" aspect of the film will cause the exposed parent metal to oxidize to a crystalline form completely compatible with the existing surrounding "barrier" layer film.

The third characteristic of the anodic film that is considered important is its moisture absorptivity. This may or may not be related to its crystalline structure and its mechanical strength. Low temperature anodization produces "hard" films that may have high mechanical strengths. High temperature molten salt electrolytes produce gamma or possibly alpha-aluminum oxide (corundum). Other anodizing conditions produce various aluminum oxide hydrates, but none of these anodizing systems appears to produce a pure, high density crystalline form. Porosity, cell size, density, and other physical properties can vary widely. Even when these physical properties are nearly the same, the absorptivity of the anodic film on different alloys may vary widely. So also, the ability of the anodic film to pick up moisture may vary considerably, even when morphology, chemical composition, and physical properties are nearly the same. Thus, variations in processing conditions were used to permit the production of films from the same electrolyte system that varied widely in moisture absorptivity.

The fourth criterion that was used to select the anodizing processes was the ease of process control. The system had to be accurately reproducible with easy control over the range of thickness of anodic film desired. This included a factor such as degree of oxide contamination with electrolyte anions or cations. These may catalyze crystal formation, improve corrosion resistance, or they may be left over as ordinary absorbed contamination from the anodizing process. However, the systems which were selected were controllable such that the type and degree of processing was the same as each batch of samples.

Additional factors affecting the selection of anodizing systems were:

1. The known corrosion resistance of systems like the phosphoric acid anodizing system.

2. The adhesive bondability of the anodic film.

3. Adherence of the anodic film to the base metal.

Currently, we know of no anodic films that produce poor bondability because of their chemical nature. The poor bondability observed in practice is due to surface contamination, poor mechanical strength of the oxide layer, or poor adhesion to base metal. To summarize, the main criteria used for the selection of the anodizing systems capable of forming thin, corrosion resistant anodic films for adhesive bonding were:

1. Maximum number of crystalline forms.
2. Control over ratio of "barrier" layer to "porous" layer.
3. Minimum absorptivity for moisture.
4. Ease of process control.
5. Degree of known corrosion resistance.
6. Bondability of anodic film to adhesives.

Characterization of FPL System

The FPL (Forest Products Laboratories) surface preparation (ASTM/D2651-67-A) is not an anodic coating system but rather a chemical treatment method for forming a surface oxide on aluminum. The procedure is fully described in the Test Procedures, Section II. Since this treatment has been the mainstay of aluminum surface treatment for the past several years, it was used as the baseline for comparison of the physical, chemical and crystallographic character of the five anodic surface treatments.

Scanning electron microscopic characterization of the resultant oxide is shown in Figure 8. The oxide was measured to be 100Å-400Å thick. This measurement was confirmed by Auger profiling as well as by ellipsometry[15] methods. The oxide appears to be porous in nature when observed at higher magnifications. Reflected high energy electron diffraction analysis (RHEED) was performed on the surface of a FPL etched specimen. Figure 9 shows the resulting diffraction pattern from the oxide layer on the FPL etched surface. Analysis of the pattern showed the oxide to be $\alpha Al_2O_3 \cdot H_2O$.

The 2024-T3 bare and clad and 7075-T6 bare and clad alloys which were treated by the FPL process were analyzed using Auger electron spectroscopy (AES). Data from the 7075-T6 bare alloy surface is shown in Figure 10. The oxide surface (A) shows the normal contaminants of S, C and N_2 which appear in nearly all surface

FIGURE 8. CHARACTER OF BARE 7075-T6 AFTER FPL ETCH TREATMENT

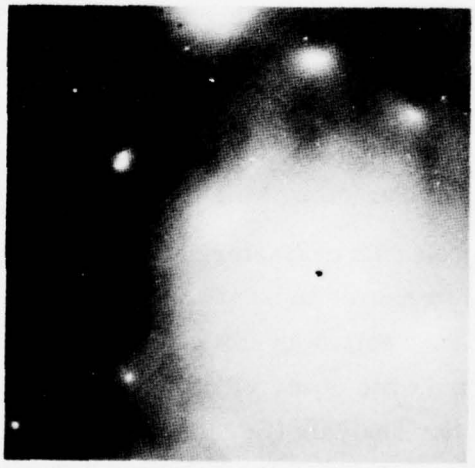

FIGURE 9. RHEED PATTERN FROM OXIDE ON FPL ETCH SURFACE ON BARE 2024-T3

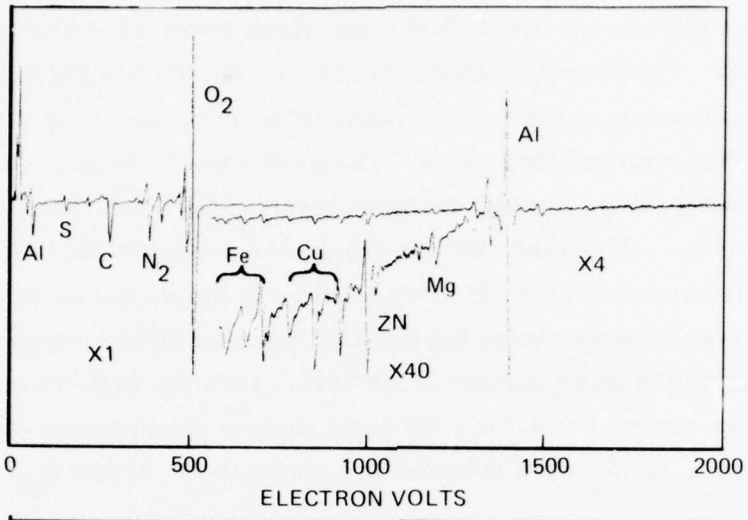

BARE 7075-T6
OXIDE SURFACE

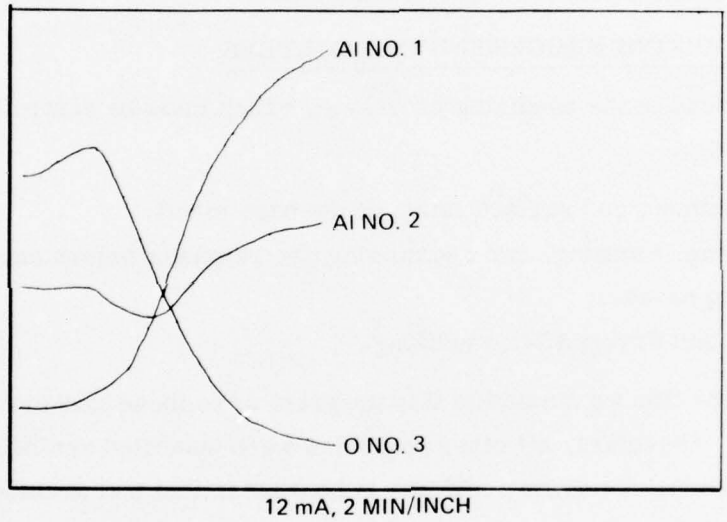

PROFILE
THROUGH
OXIDE ON
BARE 7075-T6

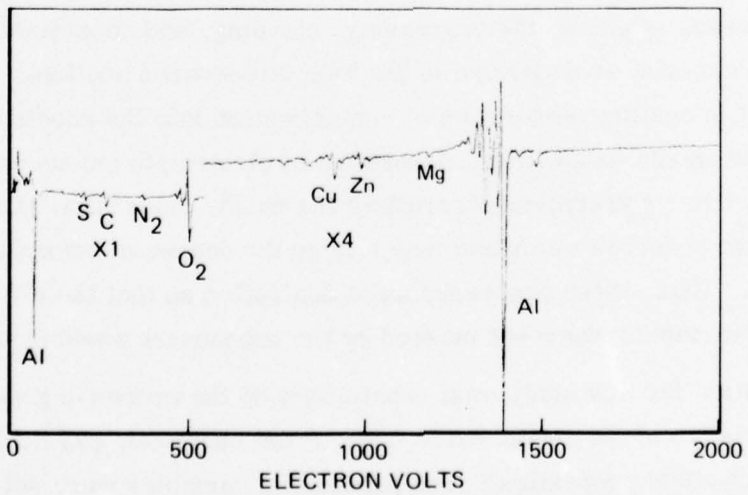

SURFACE OF
BARE 7075-T6

FIGURE 10. AUGER TRACES AND DEPTH PROFILE OF FPL ETCHED BARE 7075-T6 ALLOY

preparations. These elements are from either the rinse water or exposure to atmospheric conditions. The important elements are Fe, Zn, Cu and Mg which come from the as-received aluminum surface. The peaks with the greatest peak-to-peak intensity are for the aluminum and the oxygen. The profile trace (B) shows the two Al peaks and the O_2 peak profiled through the oxide layer. The final trace (C) shows a very slight amount of O_2. Of course, the aluminum alloy contains small amounts of oxides. The FPL treatment of 2024-T3 alloy resulted in the formation of the same oxide thickness and crystalline character but the AES revealed higher concentrations of Cu than that present on the outer surface of the 7075. Both the 7075-T6 clad and 2024-T3 clad conditions showed essentially the same surface chemistries. Only the normal contaminants of S, C, N_2 were detected in addition to the Al and O_2.

TASK II — STUDY ANODIZING PROCESSING PARAMETERS

There are four steps in the anodizing processing which must be controlled to achieve consistent results.

1. The heat treatment and surface finish of the base metal.
2. The degreasing, cleaning, and deoxidizing pretreatment before anodizing.
3. The anodizing process.
4. The washing and drying after anodizing.

The main variables that we studied in this program were those associated with the anodizing process. Therefore, all other variables were specified and held as nearly constant as possible. To avoid problems in heat treatment and surface finish of the base metal, we used one sheet of each alloy for the entire program. For each of the anodizing processes selected, the degreasing, cleaning, and deoxidizing pretreatments were held constant as described in the Test Procedures section. Rinsing procedures can result in sealing, absorption of contamination into the anodic oxide films, hydration of the anodic oxide films, desorption of electrolyte anions and cations from the anodic oxide film, and continued growth of the anodic oxide film. Drying procedures can remove absorbed water and may change the degree of crystallinity in the anodic oxide film. Thus, these processes were controlled so that the effect of anodizing processing variables were not masked by the subsequent washing and drying.

The prime question for this study was: what effect do the processing variables have on the characteristics of the anodic oxide films — the chemical, physical, crystallographic, and mechanical properties? The processing variables were selected to produce the following results:

1. Thickness variation from 1000 to approximately 10,000 Angstroms.
2. Maximum and minimum "barrier" layer/"porous" layer ratio.
3. Varying degrees of hydration of the anodic oxide.
4. Changes in the type and quantity of absorbed ions in the anodic oxide.
5. Change in the degree of crystallinity in the anodic oxide.
6. Effects on the pore size, cell size, density, porosity, and mechanical strength of the anodic oxide.
7. Changes in the "layering" in the anodic oxide.
8. Changes in the crystal structure - corundum instead of gamma-oxide, boehmite instead of bayerite.
9. Minimizes the water absorption of the anodic oxide.

The anticipated effects of some of the process variables on the anodizing systems is given below:

Concentration: (increased)

Acid Systems:	Increased dissolution of aluminum. Thinner anodic oxide layer at the same voltage. Increased contamination of anodic film. Increased porosity.
"Barrier" Layer Systems:	Little effect. May increase contamination in anodic oxide layer. May reduce voltage drop in solution and prevent hot spots on anode. Ratio of ethylene glycol/water in ammonium borate system will change the degree of hydration in the anodic oxide.
Molten Salt System:	No effect as system is 100 percent solids (no concentration change). No water present. Ratio of lithium/potassium nitrate will change the melting point of the system.

Time:

Acid Systems:	Thickness is proportional to anodizing time.
"Barrier" Layer Systems:	Thickness is independent of time — depends on voltage.
Molten Salt System:	Thickness increases with time, but not linearly. Ratio of corundum/gamma-oxide may change with time.

Temperature:

Acid Systems:	Very low temperature, 41F, yields "hard" anodized films. High temperature increases rate of "dissolution," increases porosity, decreases "barrier" layer thickness.
"Barrier" Systems:	Effect of very low temperatures is unknown. High temperatures should decrease hydration and increase crystallinity. High temperature should decrease contamination. Very high temperature and high glycol content may produce corundum.
Molten Salt System:	Temperatures below 300F cannot be used. Higher temperatures should produce purer corundum.

Voltage: (increased)

Acid Systems:	Decreased porosity. Thickness depends on current density, which in turn depends on voltage.
"Barrier" Systems:	Thickness proportional to voltage.
Molten Salt System:	Thickness increases with voltage. High voltage "hot spots" might produce gamma-oxide instead of corundum.

pH of Electrolyte:

All Systems:

High acidity, low pH, decreases "barrier" layer thickness, increases dissolution.
Neutral, pH 5-7, favors "barrier" layer.
Basic electrolyte, pH greater than 10, increases dissolution.
Presence of alkali ions may favor boehmite.

Based on the above considerations, we established the variations in processing for each of the five proposed systems as shown in Table 1. The experimental conditions shown were then used to obtain the specimens which satisfied the desired parameter study for this anodic coating program.

TASK III — CHARACTERIZATION OF ANODIC COATINGS

Phosphoric Acid Anodize System

A total of 10 test series were anodized as described in Table 1. In addition to this, 4 additional series were anodized at 20, 30 and 40 volts at room temperature. Electrical properties were obtained as described in the Test Procedure section for each run of 4 specimens. The most descriptive electrical property which was obtained during these runs was the current density as a function of time for the various anodizing conditions. Figure 11 shows a plot of the current density for the standard 10 volt anodizing of the bare and clad surfaces of 2024-T3 and 7075-T6 in a phosphoric acid electrolyte. In all cases, the bare alloy demands a higher current density than the clad alloy.

The initial "hump" in the current density curve represents the rapid growth of the barrier layer on the aluminum surface. The size of this "hump" is directly proportional to the applied voltage and the entire current density/time plot shifts upward slightly as the voltage increases. The longer the time, the thicker the porous oxide layer that forms on top of the barrier layer. As the anodizing temperature was increased to 180F, the current density increased dramatically. As the anodizing temperature was decreased to 41F, the current density was reduced. Increased voltages at all temperatures shifted the entire density/time curve upward.

The scanning electron microscope (SEM) was used to measure the oxide thicknesses for each anodizing condition. Table 2 shows the measured thickness values.

TABLE 1. CONDITIONS FOR PROCESSING SCREENING TEST VARIABLES

ANODIZING SYSTEM	BASELINE	MAXIMIZE THICKNESS	MINIMIZE THICKNESS	MAXIMIZE DENSITY	MAXIMIZE BOEHMITE
Phosphoric Acid					
Concentration, oz./gal.	14	14	3	14	14
Time, Minutes	20	50	10	50	50
Temperature, °F	RT	RT	180	41	180
Voltage, D.C.	10	50	10	50	50
pH	as is	as is	as is	as is	as is
Chromic Acid					
Concentration	10	50	50	10	10
Time	40	80	10	40	30
Temperature	104	104	104	41	180
Voltage	50	50	10	50	40
pH	as is	as is	as is	as is	as is
Ammonium Chromate					
Concentration,	3	3	3	3	sat'd.
Time	30	30	30	30	30
Temperature	RT	RT	RT	41	180
Voltage	50	100	10	150	150
ph	5.5	5.5	5.5	5.5	5.5
Ammonium Pentaborate in Ethelene Glycol					
Concentration, %	25	25	25	25	sat'd.
Time	30	30	30	30	30
Temperature	RT	RT	RT	41	200
Voltage	50	100	10	50, 100	50
Glycol, %	30	30	30	30	max
pH	5.5	5.5	5.5	5.5	5.5
Potassium/Lithium Nitrate Eutectic Molten Salt					
Concentration,	60/40	60/40	60/40	60/40	60/40
Time	30	10	10	30	long
Temperature	315	315	300	500	500
Voltage	50	100	10	50	500
pH	7	7	7	7	7

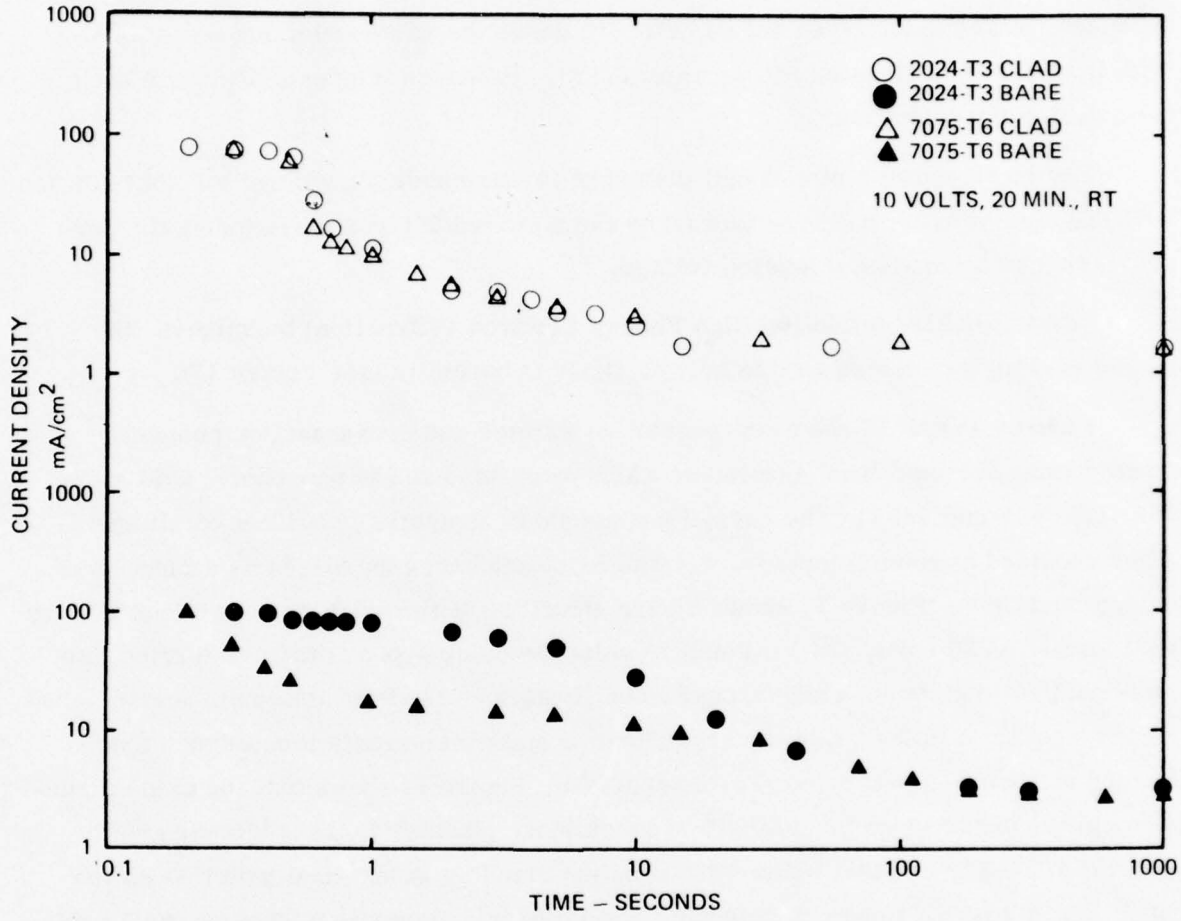

FIGURE 11. CURRENT DENSITY VERSUS TIME FOR 7075-T6 AND 2024-T3 ANODIZED IN PHOSPHORIC ACID

In certain instances both SEM and Auger techniques were used for thickness measurement. The oxide thicknesses on the clad surfaces are, in general, greater than on the bare surfaces for both 7075-T6 and 2024-T3. The 7075-T6, in general, produced thicker oxides than did the 2024-T3 under the same anodizing conditions. Both low (41F) and elevated temperatures (180F) produced thinner oxides than were formed at room temperature

Figure 12 shows a plot of cell diameter versus anodizing voltage for 2024-T3 and 7075-T6 clad alloys. A cell is formed by the solid oxide layer surrounding the pore and varies as a function of applied voltage.

Using RHEED (Reflection High Energy Electron Diffraction) techniques, the anodic coating was determined to be $\alpha Al_2O_3 \cdot H_2O$ boehmite (see Figure 13).

Figures 14 and 15 show representative surface and cross-section photomicrographs obtained from specimens which were anodized in phosphoric acid at 75F(RT), 42F and 180F. The normal porous oxide structure is evident on all specimens anodized at room temperature. The oxide thickness increases as a function of voltage and time. Figure 15 shows a pore structure at the oxide surface which is very well formed at 30 volts. At 180F and 10 volts the oxide appears to have formed into individual solid globules which appear to be floating on the bent aluminum surface. At 42F and 50 volts the oxide is very columnar and considerably thinner than that formed at room temperature. For comparison, Figure 14 shows that the oxide formed at room temperature on the 2024-T3 is much more globular in its columnar growth than the 7075-T6, and that oxide formed on the cladding is identical with that on the 7075-T6. Finite columns can be seen. Even a barrier layer is evident on the 40 volt clad specimen. At 180F and 10 volts the oxide is essentially the same as that formed on the 7075 except that the globules are slightly smaller. At 42F and 50 volts the oxide is definitely of a barrier layer form and only very slight columnar markings are visible on the side of the oxide layer. Even though changes occurred in the physical nature of the oxide as a result of temperature changes, crystallographically they were all $\alpha Al_2O_3 \cdot H_2O$ (boehmite) oxide. Measurements of the barrier layer thickness development as a result of the applied voltage indicated that 17-21Å of oxide formed per volt.

Auger electron spectrographic (AES) analysis was performed on specimens representing each anodic surface condition. The thickness of the oxide was then profiled by ion bombardment milling of the layer until the base metal composition was observed. Figures 16 and 17 show the surface, profile, and final AES traces for the

TABLE 2. ANODIC OXIDE FILM THICKNESS FOR PHOSPHORIC ACID ANODIZE AT VARIOUS TEMPERATURES AND VOLTAGES FOR 20 MINUTES

	2024		7075	
VOLTAGE	BARE	CLAD	BARE	CLAD
		41°F		
30V	1,950-2,620Å	2,100Å	3,400-4,050Å**	2,570-3,140Å
		R. T. (78°F)		
10V	2,250-2,320Å	4,580-5,100Å	3,150Å-3,850	6,300-7,000Å****
20V	2,100Å	11,000-12,000Å	6,050Å	11,100Å
30V	5,250Å*	13,400-16,200Å**	14,700Å	14,900Å
40V	7,370-8,400Å	19,800-23,000Å	19,470Å	16,850-18,400Å
50V	7,900Å	29,500Å	23,600Å	26,800
		180°F		
10V	520-1,150Å	420-520Å (Large particles to 2,000Å)	1,150-1,670Å	520A-850Å

*5,000Å by Auger Profiling
**12,000Å by Auger Profiling
***2,750Å by Auger Profiling
****6,800Å by Auger Profiling

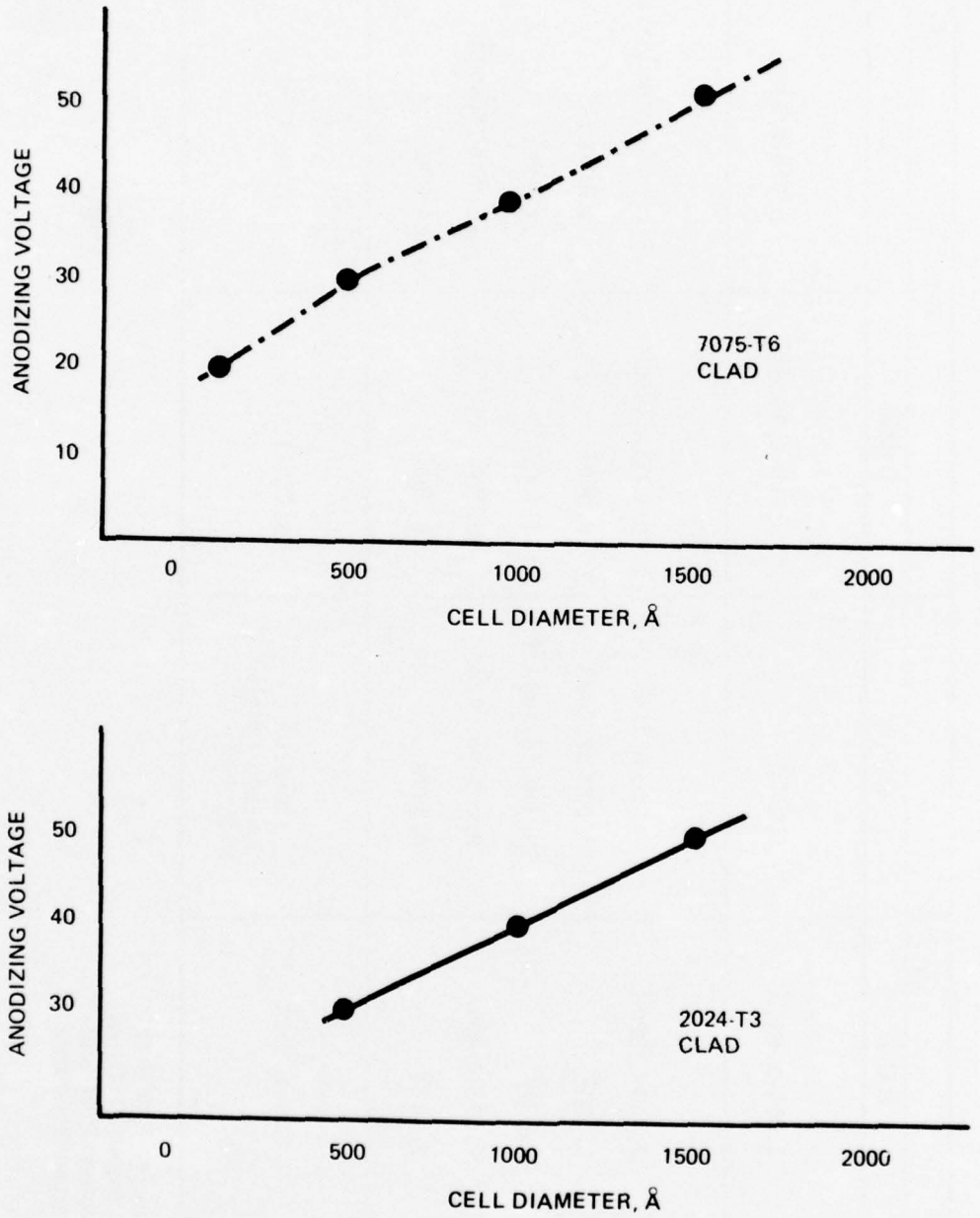

FIGURE 12. EFFECT OF VOLTAGE ON OXIDE FILM CELL SIZE FOR PHOSPHORIC ACID ANODIZE-20 MINUTES AT R.T.

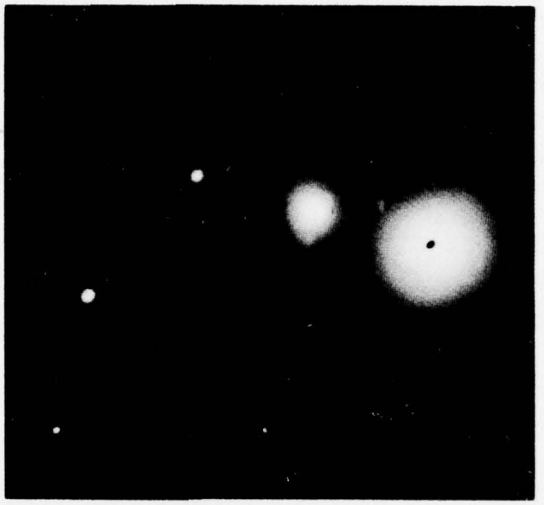

FIGURE 13. RHEED PATTERN FROM OXIDE ON 10 VOLT, R.T., PHOSPHORIC ACID ANODIZE ON BARE 7075-T6

30 VOLTS, 20 MIN., RT 19,000X

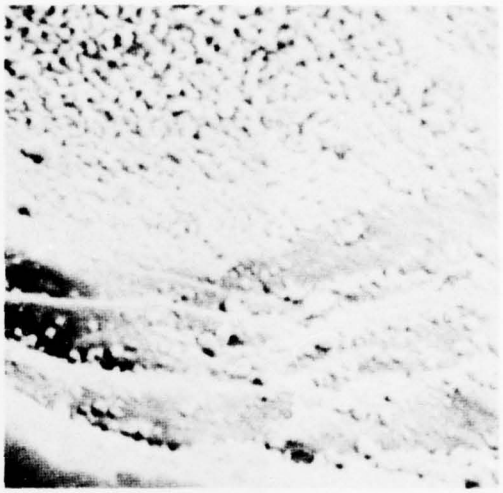

10 VOLTS, 20 MIN., 180F 19,000X

BARE

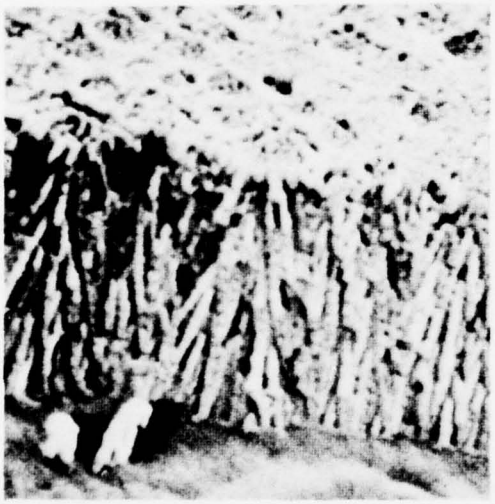

40 VOLTS, 20 MIN., RT 19,000X

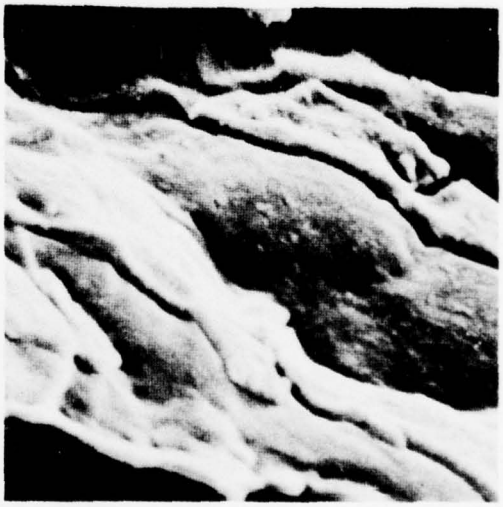

50 VOLTS, 40 MIN., 42F 19,000X

CLAD

FIGURE 14. SURFACE CHARACTER OF 2024-T3 ANODIZED IN PHOSPHORIC ACID

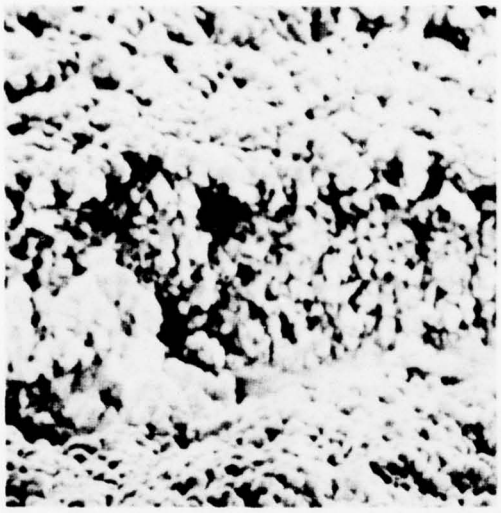

30 VOLTS, 20 MIN., RT 19,000X

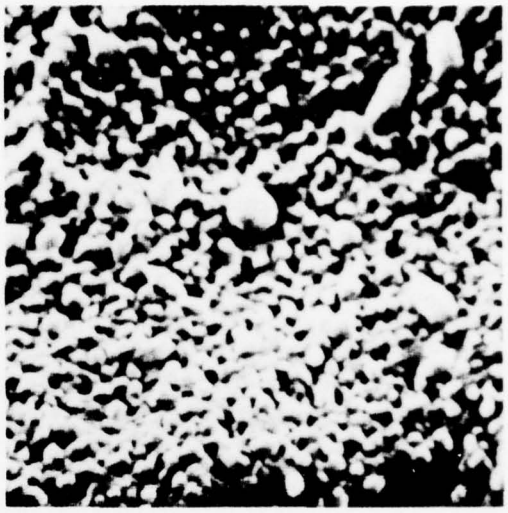

10 VOLTS, 20 MIN., 180F 19,000X

BARE

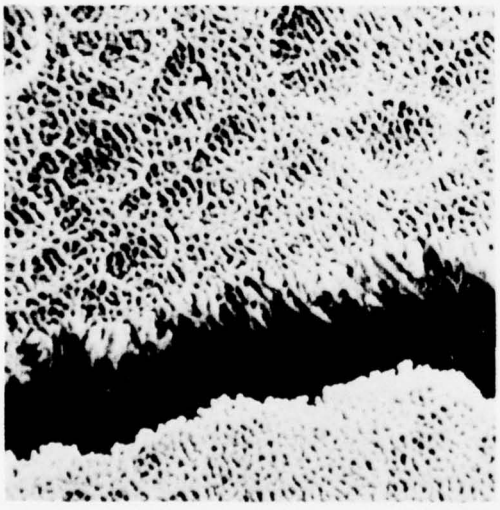

30 VOLTS, 20 MIN., RT 19,000X

50 VOLTS, 40 MIN., 42F 19,000X

CLAD

FIGURE 15. SURFACE CHARACTER OF 7075-T6 ANODIZED IN PHOSPHORIC ACID

bare 7075-T6 and 2024-T3 alloys. The actual AES data are tabulated in Tables 3 and 4. From these data, the Cu content was slightly higher on the oxide surface than it was in the matrix of the 2024-T3 and the Cu content was higher on the 2024 oxide surface than it was on the 7075-T6 oxide surface. Zn and Mg are retained at the oxide surface of the 7075-T6 along with the Cu. The Fe and Ni in the oxide surface are believed to be contaminants from the anodizing bath. Analyses on the clad surfaces showed Al and O_2 with traces of Fe, P, N_2 and Ni appearing.

Chromic Acid Anodize System

Twelve series of specimens were anodized as outlined in Table 1. The standard procedure for anodizing with chromic acid is to apply the voltage in 5 volt steps. During each application of a voltage increment, the current density rises rapidly and then it slowly decays. Figures 18 through 21 show curves for current density versus time for each material condition anodized at 104F, using 50 volts and a 10 oz/gal solution. The upper curve relates to the peak of the current surge and the lower curve the base of the decay curve. Thus, a total energy of current density output is developed in each curve. It is of interest to note that, in general, the current density/time relationships are very nearly the same for all four alloy compositions with the standard 104F operation. As the bath concentration was decreased to 3 oz/gal there was a decrease in the magnitude of current density. Conversely, as the concentration was increased to 50 oz/gal, the current density increased nearly two-fold, but it followed the general shape of the 104F, 10 oz/gal curves. As the temperature was decreased to 41F, the standard 10 oz/gal curves shifted very slightly downward. Similarly, an increase in temperature to 180F caused a rise in current density values and an upward shift in the curves.

The scanning electron microscope (SEM) was used to measure the oxide thickness for each anodizing condition. Table 5 shows the measured thickness values. The thickness of the oxide produced in the 10 oz/gal solution shows that the clad surfaces produced thicker oxide layers than the bare material did. Increased concentrations of chromic acid produced thicker oxides in all specimens, and again the clad surfaces had a thicker layer than did the bare surfaces. The 3 oz/gal solution produced much thinner oxide layers, with those on the clad surfaces being thinner than those on the bare surfaces. The oxides on both 2024-T3 and 7075-T6 were very similar in thickness in this solution at 41F. In the 10 oz/gal solution at 41F, the oxide on the 7075-T6 was thinner than the one on the 2024-T3, but at 104F the reverse was true. In the 50 oz/gal chromic acid solution, the clad alloys developed thicker oxides than the bare material did.

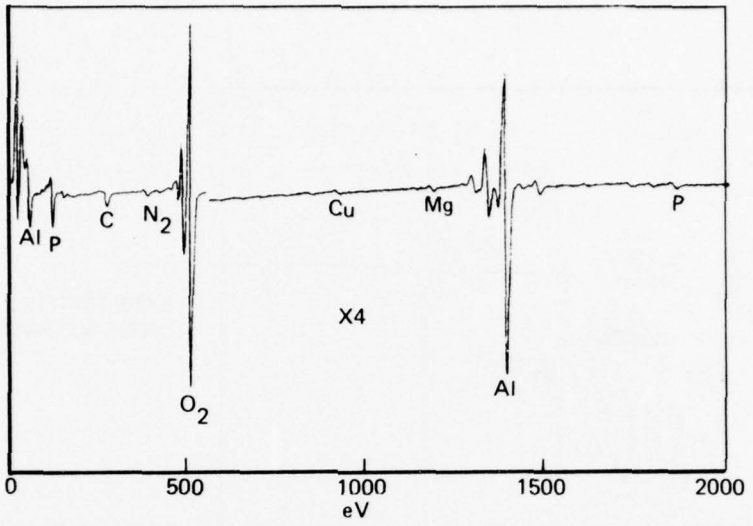

BARE 2024-T3
OXIDE SURFACE

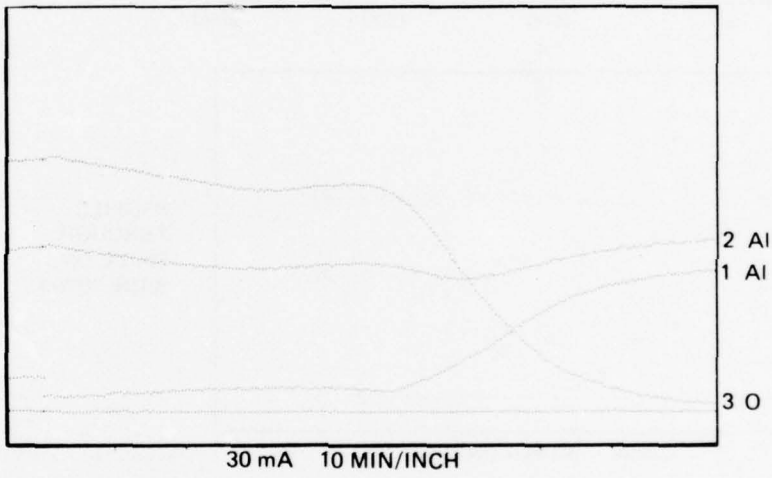

PROFILE
THROUGH
OXIDE ON
BARE 2024-T3

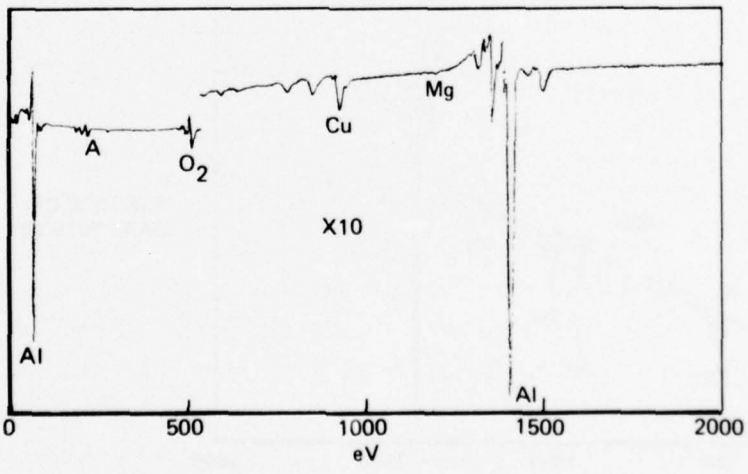

SURFACE OF
BARE 2024-T3

FIGURE 16. AUGER TRACES AND DEPTH PROFILE OF PHOSPHORIC ACID ANODIZED BARE 2024-T3, 40 VOLTS, 20 MIN, R.T.

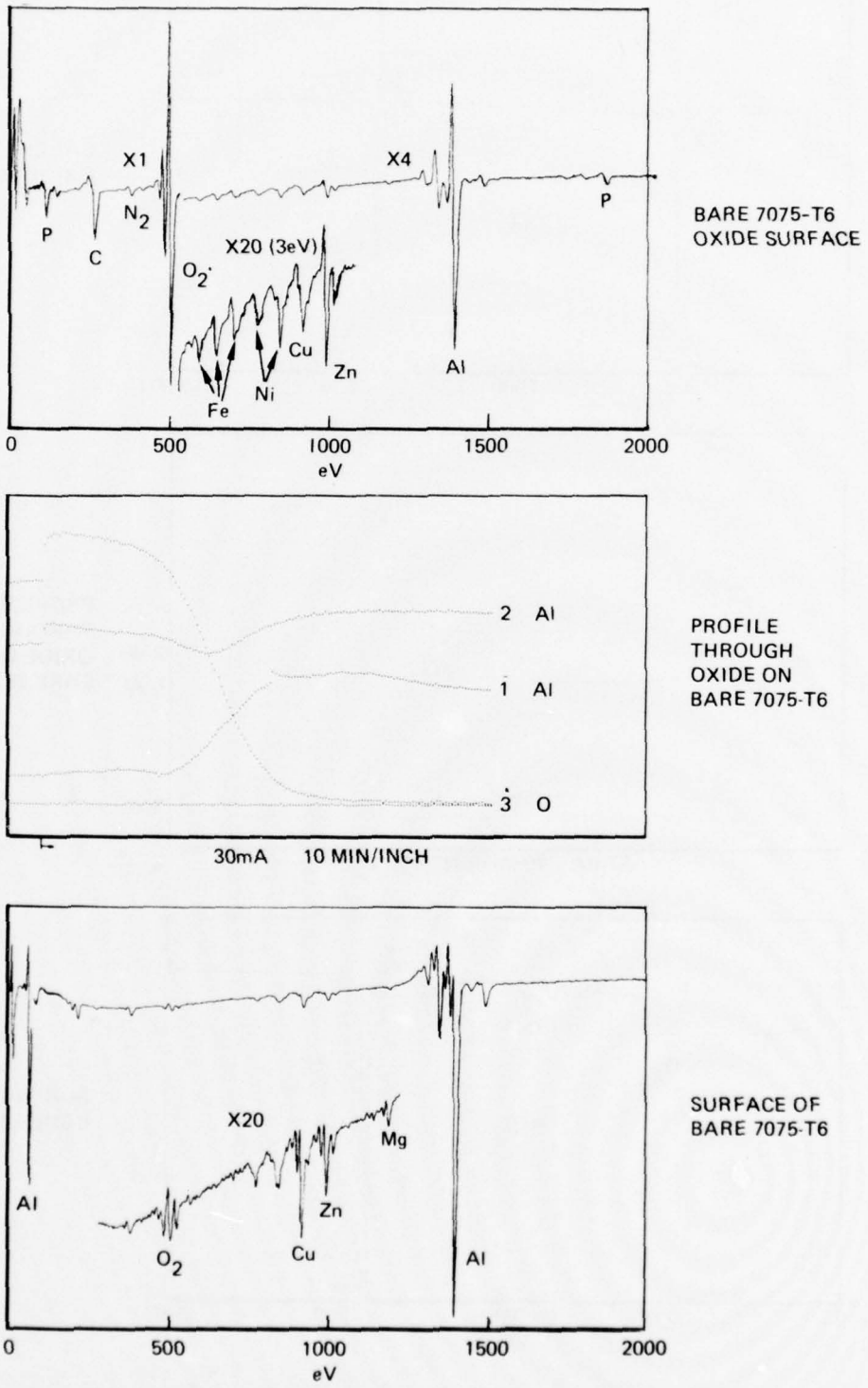

FIGURE 17. AUGER TRACES AND DEPTH PROFILE OF PHOSPHORIC ACID ANODIZED BARE 7075-T6, 20 VOLTS, 20 MIN, R.T.

TABLE 3. TABULATION OF AUGER INTENSITIES OBTAINED FROM SURFACES OF PHOSPHORIC ACID ANODIZED BARE AND CLAD 2024-T3

ANODIZE CONDITION	Al	O_2	Cu	Zn	Mg	Cr	N_2	P	Fe	Ni
Bare										
20 V, 20 Min, RT	VS	VS	MW	---	VVW	---	MW	MW	---	---
50 V, 20 Min, RT	VS	VS	MW	---	VW	---	MW	MW	---	---
50 V, 20 Min, 42°F	VS	VS	W	---	VVW	---	VW	W	---	---
20 V, 20 Min, 180°F	VS	VS	MW	---	VVW	---	VVW	VVW	VW	VW
Clad										
20 V, 20 Min, RT	VS	VS	---	---	---	---	VW	VW	---	---
50 V, 20 Min, RT	VS	VS	---	---	---	---	VW	VW	VVW	VVW
50 V, 20 Min, 41°F	VS	VS	---	---	---	---	VW	W	VVW	VVW
20 V, 20 Min, 180°F	VS	VS	---	---	---	---	---	VVW	VVW	VVW

INTENSITY OF LINE

VS — Very Strong
S — Strong
M — Medium
MW — Medium Weak
W — Weak
VW — Very Weak
VVW — Very Very Weak

TABLE 4. TABULATION OF AUGER INTENSITIES OBTAINED FROM SURFACES OF PHOSPHORIC ACID ANODIZED BARE AND CLAD 7075-T6

ANODIZE CONDITION	Al	O_2	Cu	Zn	Mg	Cr	N_2	P	Fe	Ni
Bare										
10 V, 20 Min, RT	VS	VS	VW	W	VW	---	MW	W	---	---
20 V, 20 Min, RT	VS	VS	VW	W	VW	---	MW	MW	W	W
50 V, 20 Min, RT	VS	VS	VVW	VW	VVW	---	W	MW	---	---
50 V, 20 Min, 42°F	VS	VS	VW	W	W	---	MW	W	W	W
50 V, 20 Min, 180°F	S	S	W	W	W	---	MW	MW	MW	MW
Clad										
10 V, 20 Min, RT	VS	VS	---	---	---	---	VW	W	VW	VW
50 V, 20 Min, RT	VS	VS	---	---	---	---	W	W	W	W
50 V, 20 Min, 42°F	VS	VS	---	---	---	---	VW	VW	---	---
50 V, 20 Min, 180°F	VS	VS	VW	VW	VW	---	W	VW	VVW	VVW

INTENSITY OF LINE

VS — Very Strong
S — Strong
M — Medium
MW — Medium Weak
W — Weak
VW — Very Weak
VVW — Very Very Weak

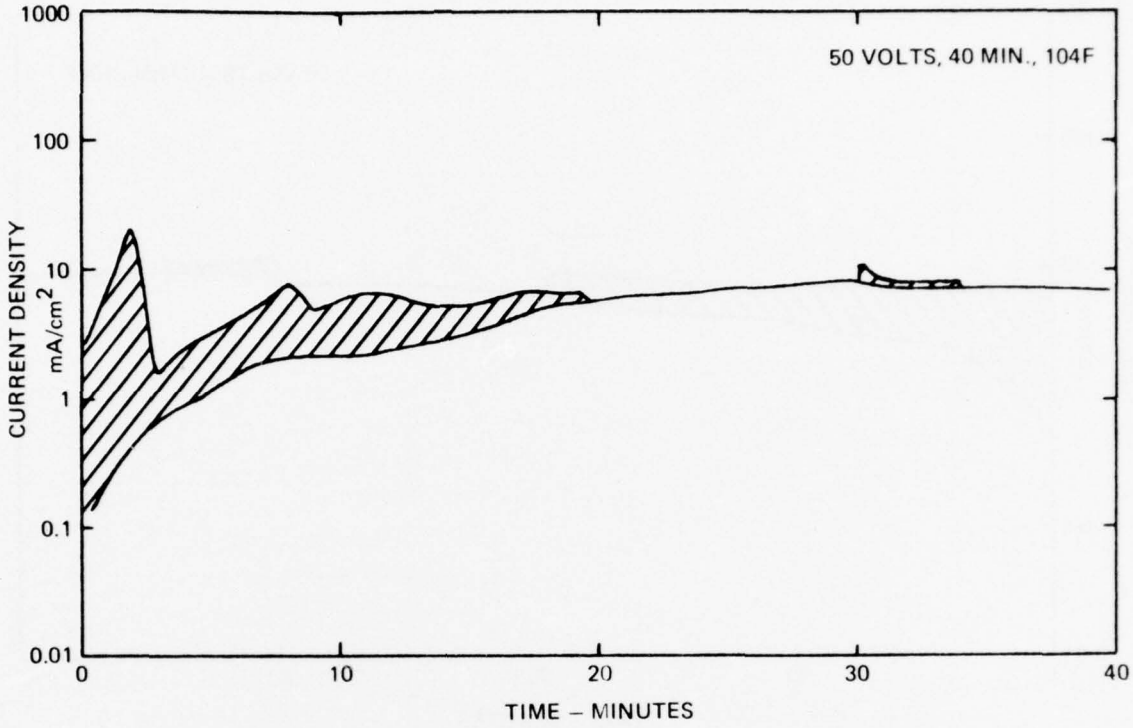

FIGURE 18. CURRENT DENSITY VERSUS TIME CHARACTERISTICS OF BARE 2024-T3 ANODIZED IN CHROMIC ACID

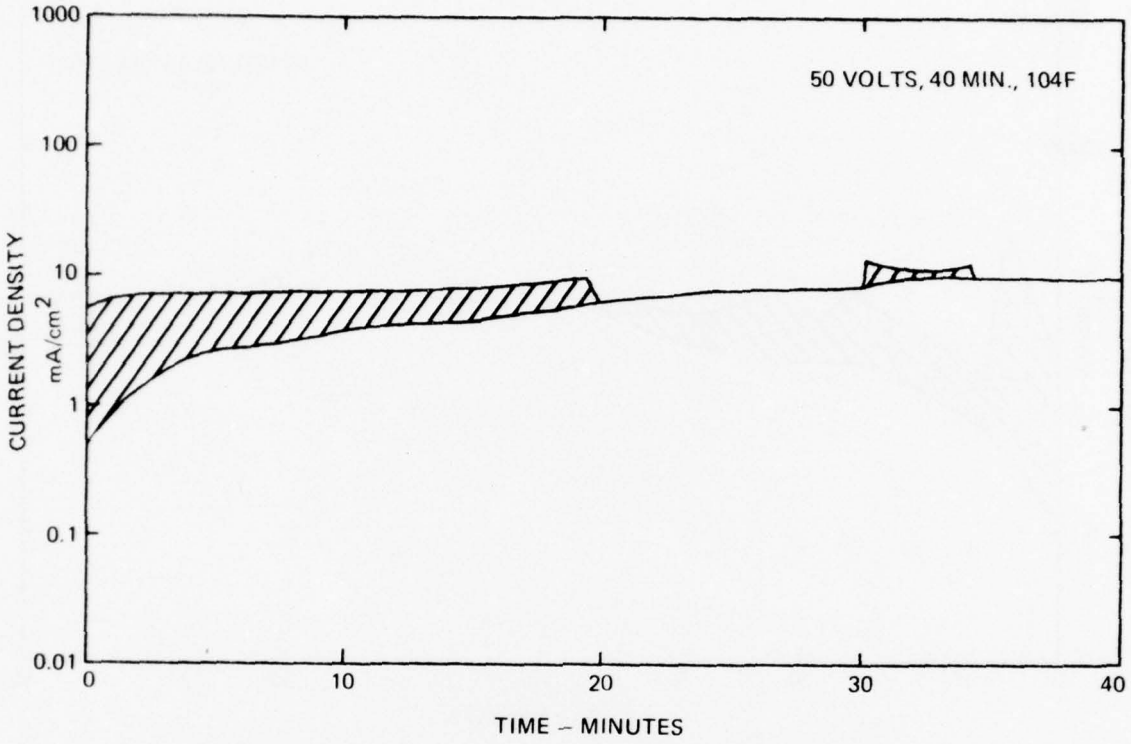

FIGURE 19. CURRENT DENSITY VERSUS TIME CHARACTERISTICS OF CLAD 2024-T3 ANODIZED IN CHROMIC ACID

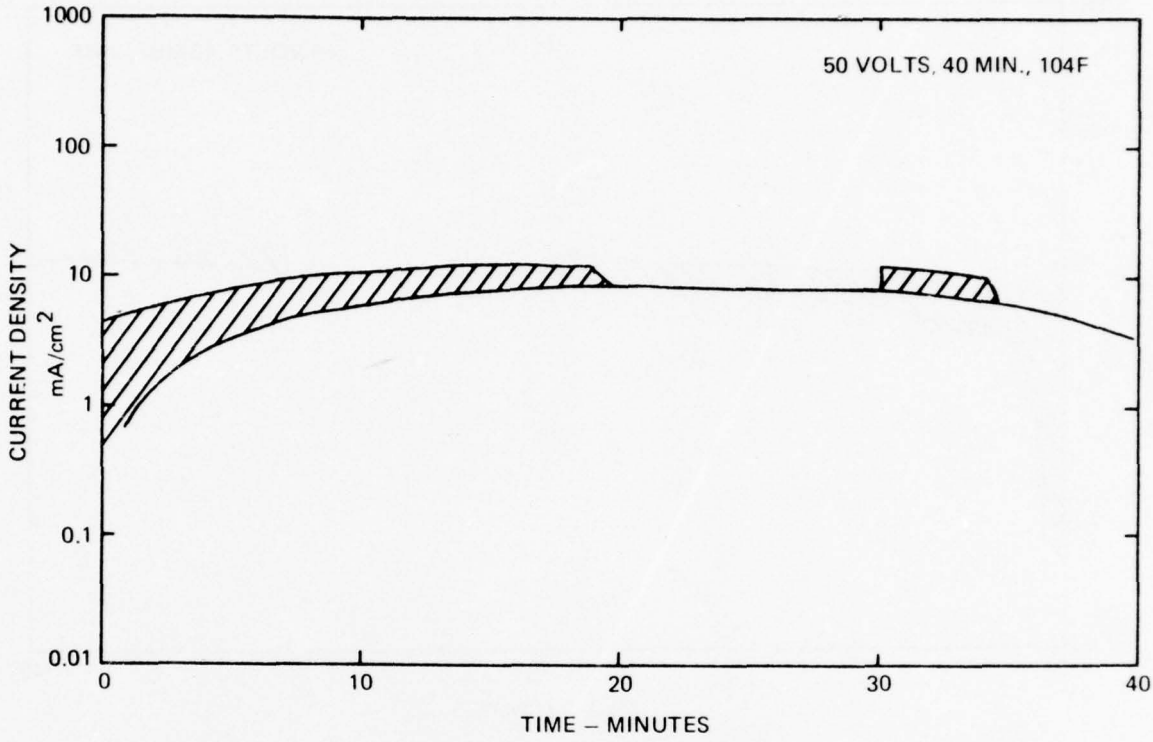

FIGURE 20. CURRENT DENSITY VERSUS TIME CHARACTERISTICS OF BARE 7075-T6 ANODIZED IN CHROMIC ACID

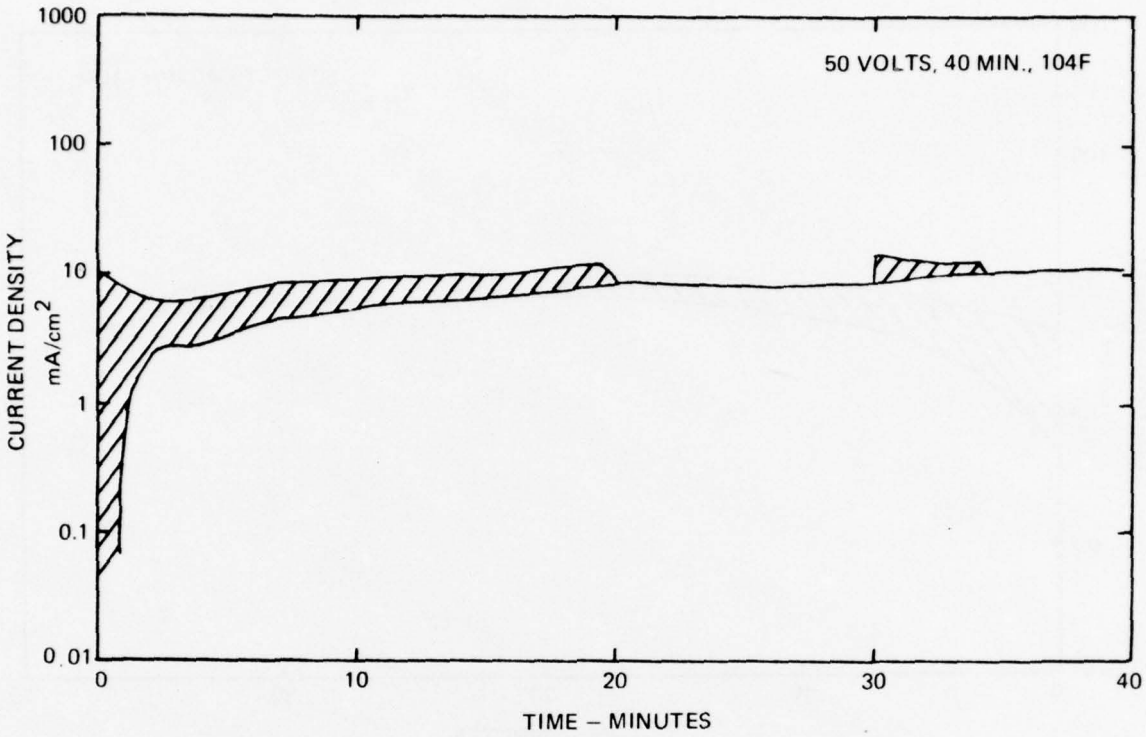

FIGURE 21. CURRENT DENSITY VERSUS TIME CHARACTERISTICS OF CLAD 7075-T6 ANODIZED IN CHROMIC ACID

TABLE 5. ANODIC OXIDE FILM THICKNESS FOR CHROMIC ACID ANODIZING WITH VARIOUS VOLTAGES, TEMPERATURES AND TIMES*

ANODIZE CONDITION	THICKNESS Å 2024-T3 BARE	THICKNESS Å 2024-T3 CLAD	THICKNESS Å 7075-T6 BARE	THICKNESS Å 7075-T6 CLAD
3 Oz/Gal CrO_3				
50 V, 40 Min, 41°F	2,220	1,390	2,500	1,400
3 Oz/Gal CrO_3/Dich. Sealed				
50 V, 40 min, 41°F	2,340	1,670	2,220	1,580
10 Oz/Gal CrO_3				
50 V, 80 Min, 42°F	4,740	6,580	3,680	5,530
50 V, 40 Min, 104°F	43,500	48,000	39,500	60,630
50 V, 40 Min, 125°F	64,000	49,500	52,500	53,130
10 Oz/Gal CrO_3/Dich. Sealed				
50 V, 80 Min, 42°F	3,160	6,320	5,000	6,970
50 V, 40 Min, 104°F	40,750	51,750	52,750	61,000
50 V, 40 Min, 125°F	41,250	57,000	50,000	61,630
50 Oz/Gal CrO_3				
10 V, 10 Min, 104°F	7,630	8,820	8,320	5,790
50 V, 80 Min, 104°F	101,500	196,250	68,000	171,250
50 Oz/Gal CrO_3/Dich. Sealed				
10 V, 10 Min, 104°F	7,370	9,080	8,950	7,500
50 V, 80 Min, 104°F	105,500	167,500	70,000	187,000

*These thicknesses were determined by SEM evaluation.

Representative photomicrographs of the oxide layers which formed on the 2024-T3 bare and clad and the 7075-T6 bare and clad alloys are shown in Figures 22 and 23. At both 104F and 125F, the columnar structure of a typical porous oxide is evident. At 41F the clad oxide of both materials shows a barrier layer structure. The bare alloys produced large columns or globules of oxide. Apparently, the weak concentration of chromic acid is not sufficient to maintain an "acid-like" environment for anodic reaction at the 41F temperature, so a porous layer was not formed. Note the outside diffuse layer on the anodic coating formed in the 10 oz/gal chromic acid anodizing bath. This resulted from the sodium dichromate sealing process.

Using RHEED techniques, both the porous and barrier oxides were $\alpha Al_2O_3 \cdot H_2O$ boehmite (see Figure 24).

Auger electron spectrographic analysis was performed on the surface of the thick oxides and then the oxide layer was ion milled for 10 minutes and re-analyzed. Figures 25 and 26 show representative Auger traces from the surface and just below the surface of the chromic acid anodized coatings. It was found that the impurity elements were all located in this outer 50-100Å layer. Elements such as Cu were found in the oxide on 2024-T3 and Cu, Mg, and Zn were found in the oxide on the 7075-T6 alloy throughout its thickness. The elements Cu, Zn, and Mg appeared in much lower concentrations in the anodic coatings produced in chromic acid than they did in the phosphoric acid. The lower temperature once again retarded elemental migration and negligible amounts of Cu, Mg, and Zn were found on the surface of the oxide. Chromium was found on all oxide surfaces. The Cr content was particularly high in the specimens sealed in sodium dichromate. Tables 6 and 7 show a representative tabulation of the element concentrations detected on the oxide surface under different conditions of anodizing. Due to the thickness of the anodic films, complete profiling was not performed. Scans were made from the surface again after milling for 10 minutes by ion bombardment.

Ammonium Chromate Anodize System

A total of 6 variable test panels were anodized under varying conditions as described in Table 1. Electrical properties were recorded for each run of four specimens. Figures 27 and 28 show the electrical property plots for current density versus time. The typical current curve for this system starts with a surge of current which is proportional to the voltage and then a decay to a low value. It is during the high current surge that most of the oxide is formed in this system. As is the case with the other

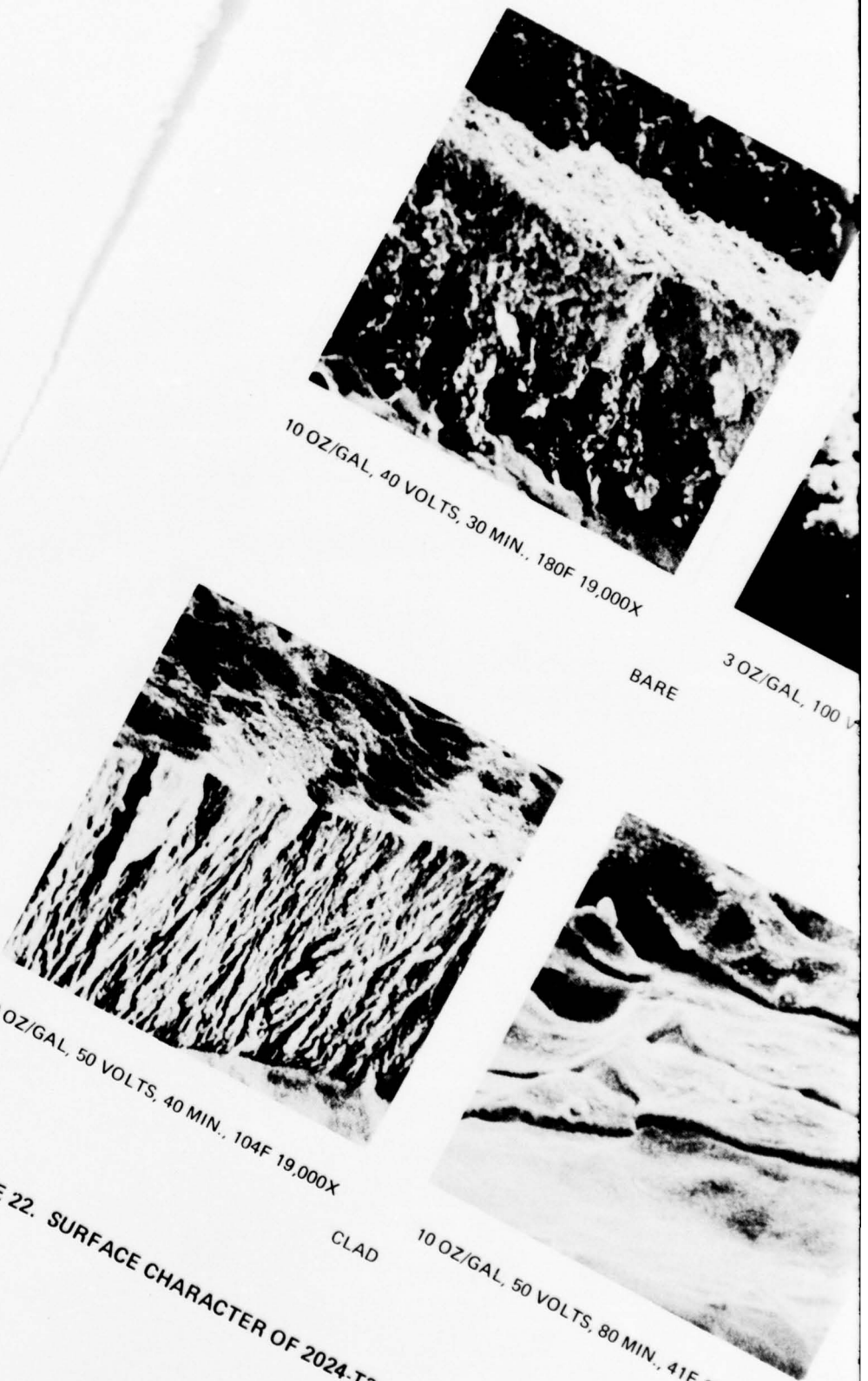

FIGURE 22. SURFACE CHARACTER OF 2024-T3 ANODIZED IN CHROMIC ACID

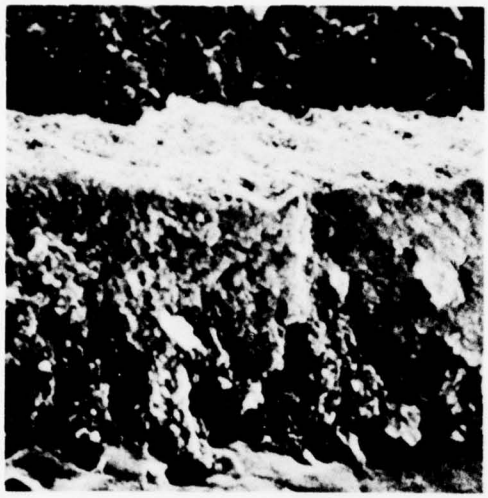

10 OZ/GAL, 40 VOLTS, 30 MIN., 180F 19,000X

3 OZ/GAL, 100 VOLTS, 20 MIN., 41F 19,000X

BARE

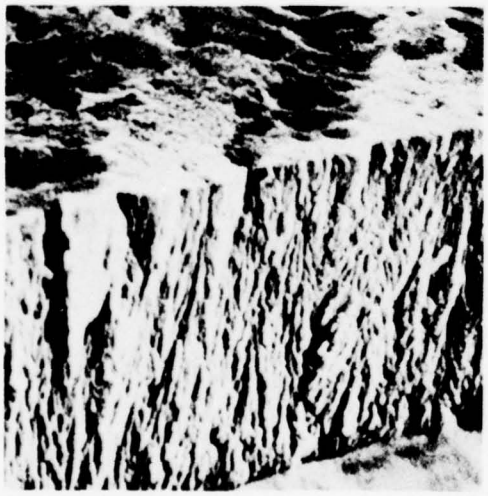

10 OZ/GAL, 50 VOLTS, 40 MIN., 104F 19,000X

10 OZ/GAL, 50 VOLTS, 80 MIN., 41F 19,000X

CLAD

FIGURE 22. SURFACE CHARACTER OF 2024-T3 ANODIZED IN CHROMIC ACID

10 OZ/GAL, 50 VOLTS, 40 MIN., 104F 19,000X

3 OZ/GAL, 50 VOLTS, 40 MIN., 41F 19,000X

BARE

10 OZ/GAL, 50 VOLTS, 40 MIN., 104F 19,000X

3 OZ/GAL, 50 VOLTS, 40 MIN., 41F 19,000X

CLAD

FIGURE 23. SURFACE CHARACTER OF 7075-T6 ANODIZED IN CHROMIC ACID

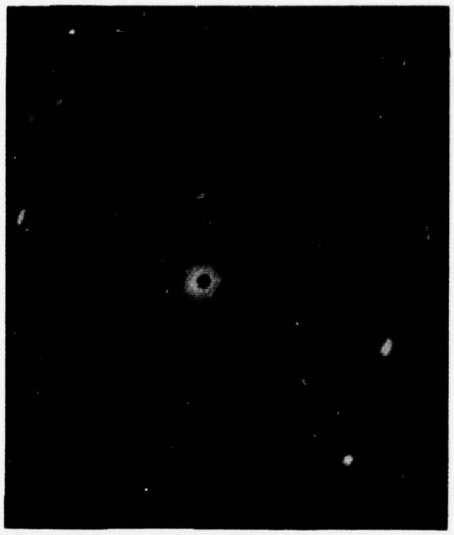

FIGURE 24. RHEED PATTERN FROM OXIDE ON 50 VOLT, 104F, (10 OZ/GAL) CHROMIC ACID ANODIZE ON BARE 7075-T6

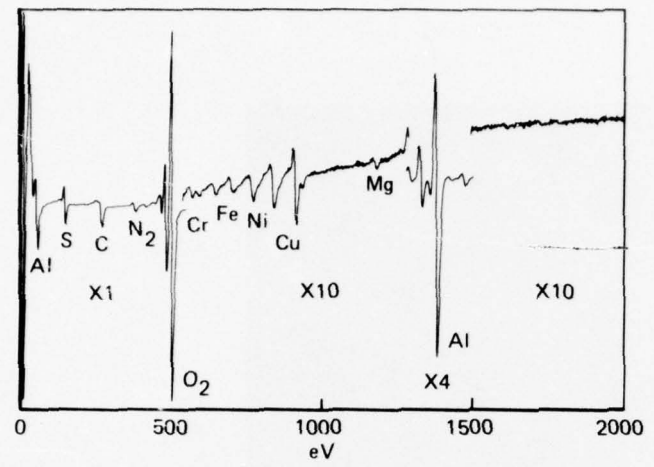

BARE 2024-T3
OXIDE SURFACE
50 VOLT,40 MIN,125F

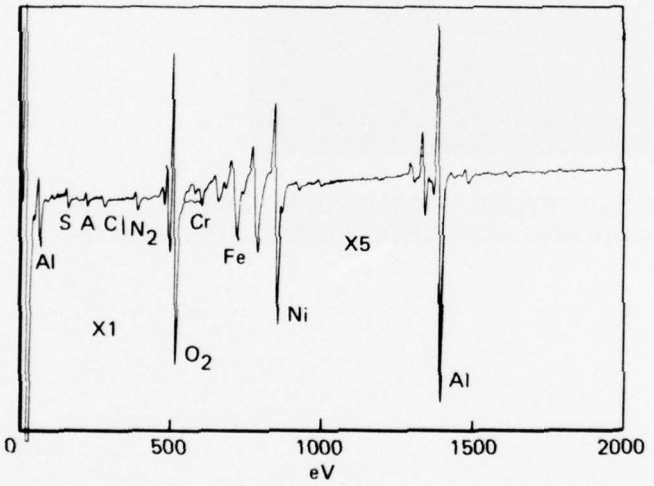

BARE 2024-T3
10 VOLT,10 MIN,104F
OXIDE SURFACE,
SEALED

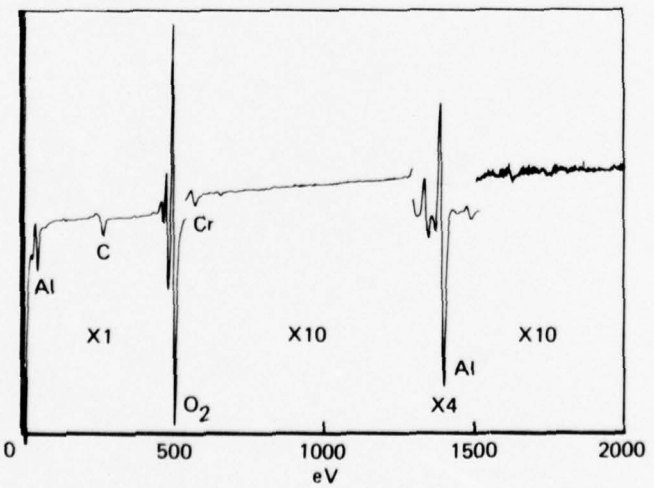

CLAD 2024-T3
50 VOLT 40 MIN 125F
OXIDE SURFACE,
SEALED

FIGURE 25. AUGER TRACES FROM CHROMIC ACID ANODIZED BARE AND CLAD 2024-T3

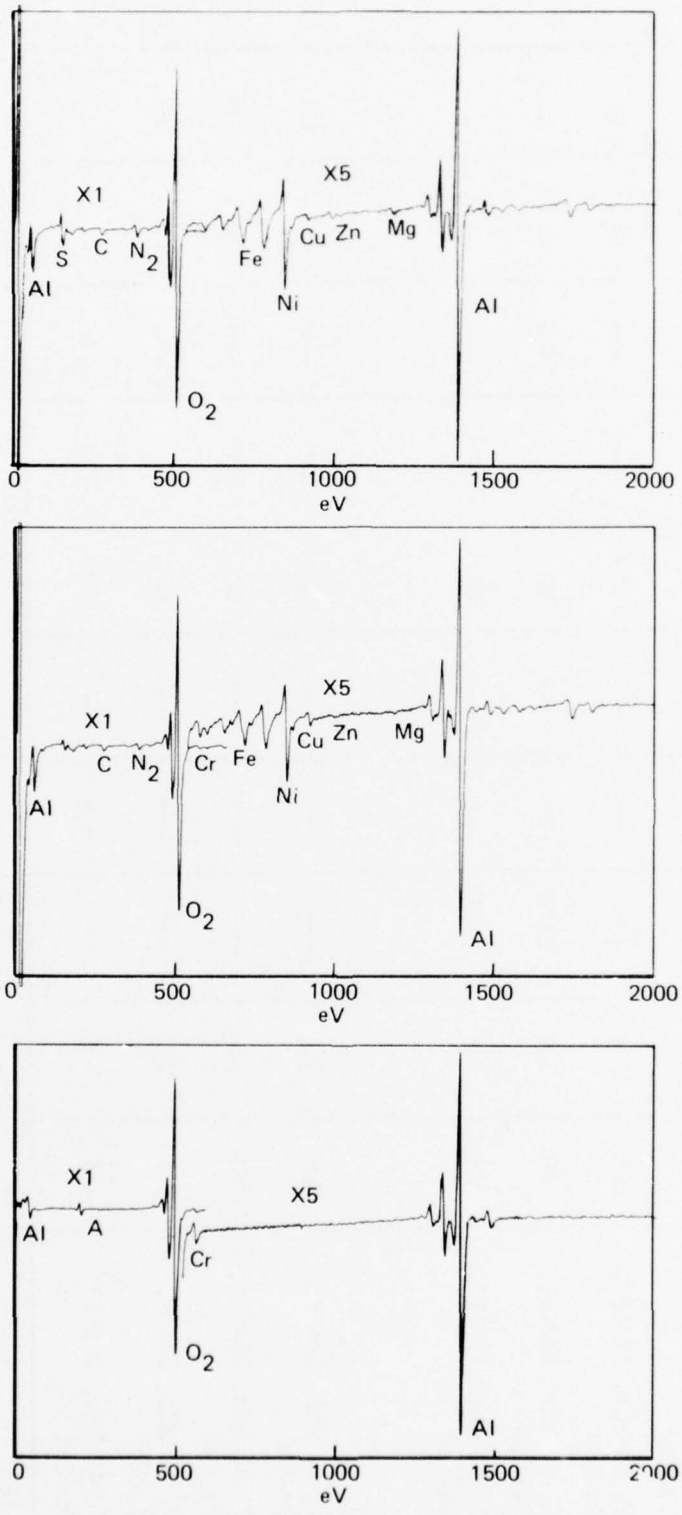

FIGURE 26. AUGER TRACES FROM CHROMIC ACID ANODIZED BARE AND CLAD 7075-T6, 50 VOLTS, 80 MIN, 104F

TABLE 6. TABULATION OF AUGER INTENSITIES OBTAINED FROM SURFACES OF CHROMIC ACID ANODIZED BARE AND CLAD 2024-T3

ANODIZE CONDITION	Al	O_2	Cu	Zn	Mg	Cr	N_2	P	Fe	Ni
Bare										
10 V, 10 Min, 104°F, 10 Oz/Gal	VS	VS	VVW	---	---	W	W	---	W	W
50 V, 80 Min, 104°F, 50 Oz/Gal	VS	VS	M	---	---	VVW	---	---	---	---
50 V, 80 Min, 104°F*, 50 Oz/Gal	VS	VS	VW	---	---	MW	---	---	W	W
50 V, 40 Min, 125°F, 10 Oz/Gal	VS	VS	VVW	---	---	W	W	---	---	---
50 V, 40 Min, 125°F*, 10 Oz/Gal	VS	VS	VVW	---	---	W	W	---	---	---
Clad										
10 V, 10 Min, 104°F, 10 Oz/Gal	VS	VS	---	---	---	W	W	---	W	W
10 V, 10 Min, 104°F*, 10 Oz/Gal	VS	VS	---	---	---	W	VW	---	M	M
50 V, 40 Min, 125°F, 10 Oz/Gal	VS	VS	---	---	---	W	W	---	---	---
50 V, 40 Min, 125°F*, 10 Oz/Gal	VS	VS	---	---	---	MW	VW	---	---	---

*Sealed

INTENSITY OF LINE

VS — Very Strong
S — Strong
M — Medium
MW — Medium Weak
W — Weak
VW — Very Weak
VVW — Very Very Weak

TABLE 7. TABULATION OF AUGER INTENSITIES OBTAINED FROM SURFACES OF CHROMIC ACID ANODIZED BARE AND CLAD 7075-T6

ANODIZE CONDITION	Al	O_2	Cu	Zn	Mg	Cr	N_2	P	Fe	Ni
Bare										
10 V, 10 Min, 104°F	VS	VS	VW	VW	VW	VW	W	---	W	W
10 V, 10 Min, 104°F*	VS	VS	VVW	---	---	W	VW	---	W	W
50 V, 80 Min, 104°F	VS	VS	VVW	VW	VW	W	---	---	W	W
50 V, 40 Min, 125°F, 10 Oz/Gal	VS	VS	VVW	---	VVW	VW	W	---	VVW	VVW
50 V, 40 Min, 125°F*, 10 Oz/Gal	VS	VS	---	---	---	M	VVW	---	VVW	---
Clad										
50 V, 80 Min, 104°F	VS	VS	---	---	---	W	VW	---	W	W
50 V, 40 Min, 125°F, 10 Oz/Gal	VS	VS	VVW	---	---	M	W	---	VW	VW
50 V, 40 Min, 125°F*, 10 Oz/Gal	VS	VS	---	---	---	MW	W	---	W	W

*Sealed

INTENSITY OF LINE

VS — Very Strong
S — Strong
M — Medium
MW — Medium Weak
W — Weak
VW — Very Weak
VVW — Very Very Weak

anodic systems, the current density is directly proportional to temperature. At 180F, the long-time behavior shows a slight rise in current as a function of time. This would indicate a breakdown in the oxide due to the chemical activity of the hot ammonium chromate.

The thicknesses of the oxide layers as measured with the SEM are shown in Table 8. In general, the oxides on the clad surfaces are thicker than those on the bare surfaces. The oxide thickness increased as the applied voltage increased. In general, the oxides formed on 7075-T6 at RT and 41F are thicker than those which formed on the 2024-T3.

Figures 29 and 30 show representative surface and cross-section photomicrographs of the oxide layers which were formed with the ammonium chromate anodize system. The expected barrier layer type of oxide was evident for all conditions investigated. Both the 2024-T3 and 7075-T6 anodize coatings show a "bubble-like" pore structure on the surface of the barrier layer oxide. The 100 volt RT specimen actually shows rows of "pimples" on the oxide surface. This behavior is different from that of a normal barrier layer oxide which is relatively smooth and "slab-like" in nature.

RHEED analysis showed these anodic layers to consist of the $\alpha Al_2O_3 \cdot H_2O$ boehmite form of oxide (see Figure 31).

Auger electron spectrographic analysis was performed on the oxide surfaces and the oxide was then profiled. Figures 32 and 33 show representative Auger traces and profiles. Tables 9 and 10 show a summary of the elements detected on the oxide surface and their relative intensities. The amount of Cu showing on the bare and clad oxide surfaces is less than that which appeared on the phosphoric or chromic acid anodize surfaces. The relative amount of Cu appears greater on the 7075-T6 surface than on the 2024-T3 anodized surfaces. The Zn and Mg appear on the bare 7075-T6 anodized surfaces, and at the higher voltages on the clad surfaces. Chromium appears on the oxide surface of all samples and it must be deposited from the bath itself, and the Cr content appears to be relatively uniform throughout the thickness. Fe and Ni were also detected. They were believed to be associated with the stainless steel container.

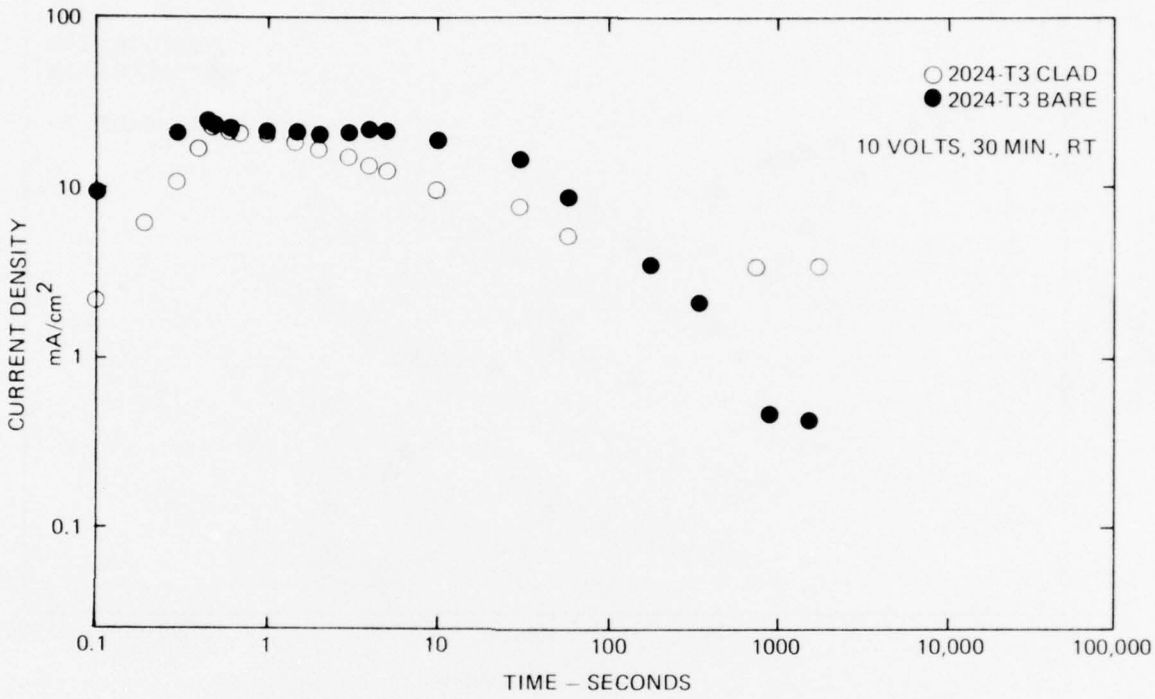

FIGURE 27. CURRENT DENSITY VERSUS TIME CHARACTERISTICS OF BARE AND CLAD 2024-T3 ANODIZED IN 3% AMMONIUM CHROMATE

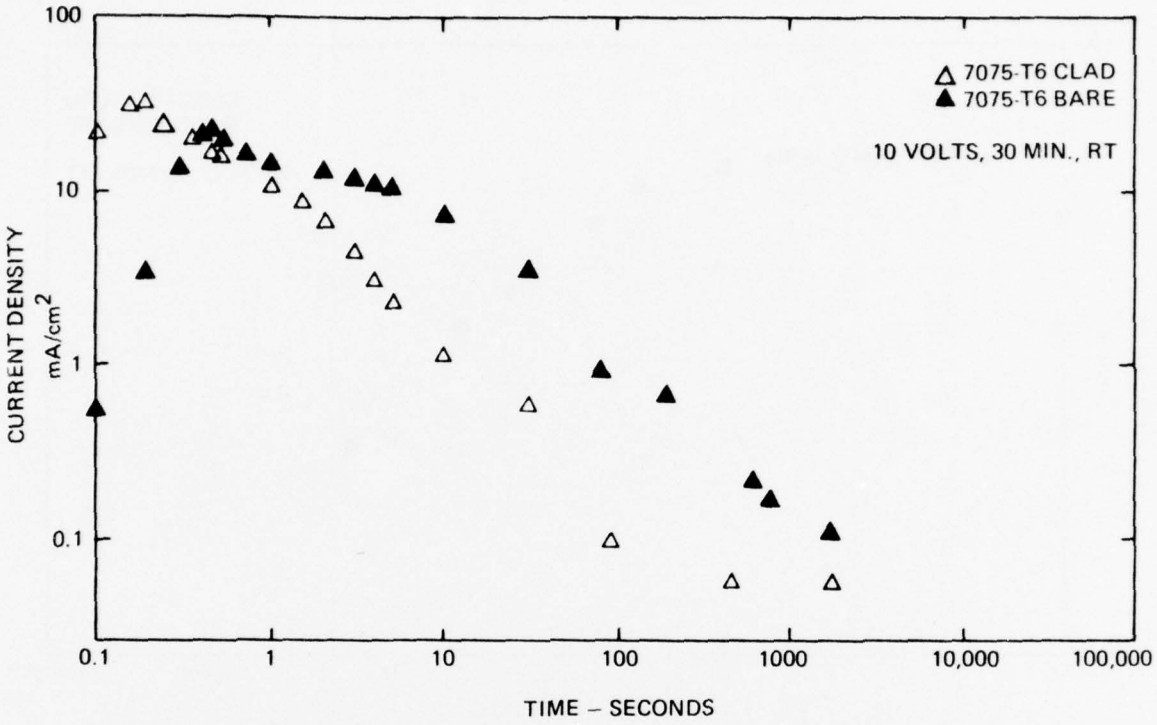

FIGURE 28. CURRENT DENSITY VERSUS TIME CHARACTERISTICS OF BARE AND CLAD 7075-T6 ANODIZED IN 3% AMMONIUM CHROMATE

TABLE 8. ANODIC OXIDE FILM THICKNESS FOR AMMONIUM CHROMATE ANODIZING WITH VARIOUS VOLTAGES AND TEMPERATURES

ANODIZE CONDITION	THICKNESS (Å) 2024-T3 BARE	THICKNESS (Å) 2024-T3 CLAD	THICKNESS (Å) 7075-T6 BARE	THICKNESS (Å) 7075-T6 CLAD
3% Ammonium Chromate				
150 V, 30 Min, 41°F	1,970	2,100	2,370	2,170
10 V, 30 Min, RT	900	900	1,050	660
50 V, 30 Min, RT	1,780	1,710	2,040	1,460
100 V, 30 Min, RT	2,630	2,100	3,160	2,370
10% Ammonium Chromate				
50 V, 30 Min, 180°F	10,530	11,180	8,420	12,630

50 VOLTS, 30 MIN., RT 19,000X

150 VOLTS, 30 MIN., 41F 19,000X

BARE

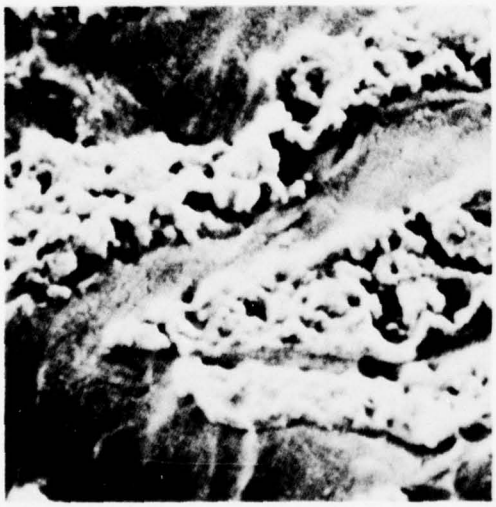

50 VOLTS, 30 MIN., RT 19,000X

100 VOLTS, 30 MIN., RT 19,000X

CLAD

FIGURE 29. SURFACE CHARACTER OF 2024-T3 ANODIZED IN AMMONIUM CHROMATE

50 VOLTS, 30 MIN., RT 19,000X

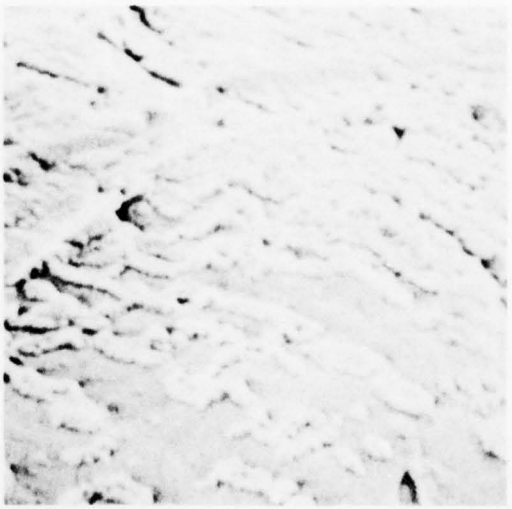

10 VOLTS, 30 MIN., RT 19,000X

BARE

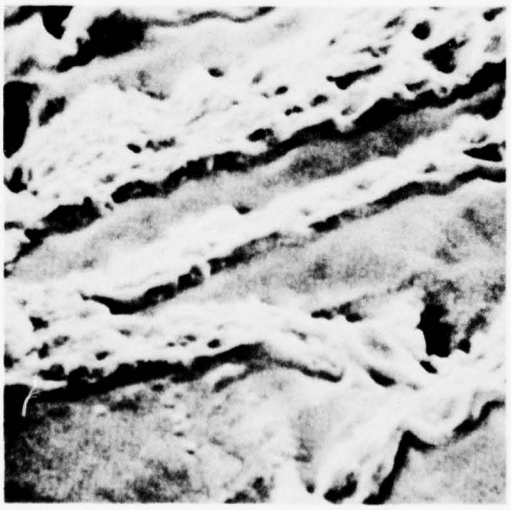

50 VOLTS, 30 MIN., RT 19,000X

100 VOLTS, 30 MIN., RT 19,000X

CLAD

FIGURE 30. SURFACE CHARACTER OF 7075-T6 ANODIZED IN AMMONIUM CHROMATE

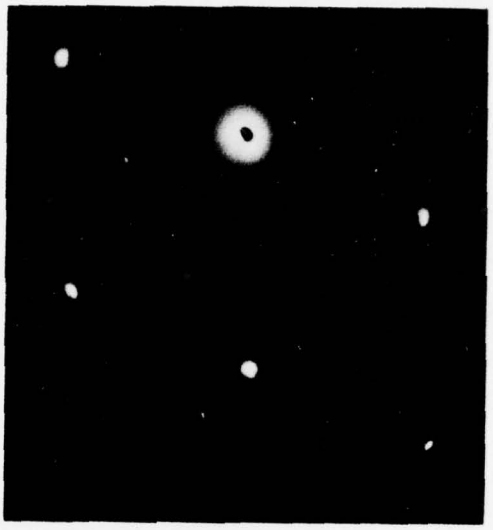

FIGURE 31. RHEED PATTERN FROM OXIDE ON 50 VOLT, R.T., 30 MIN, AMMONIUM CHROMATE ANODIZE ON BARE 7075-T6

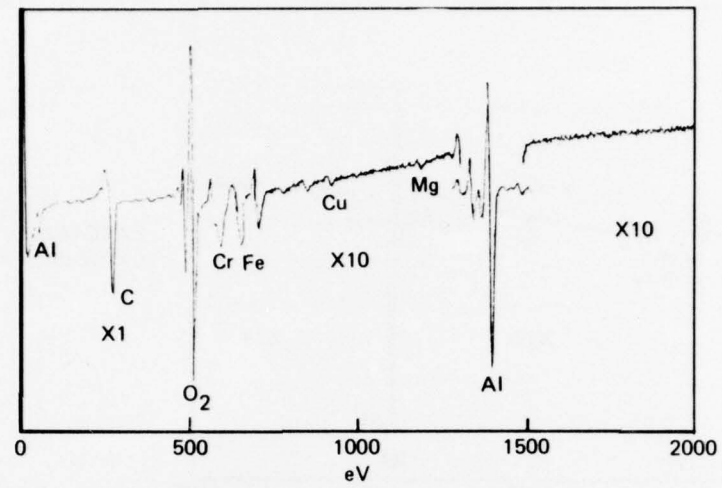

BARE 2024-T3
OXIDE SURFACE

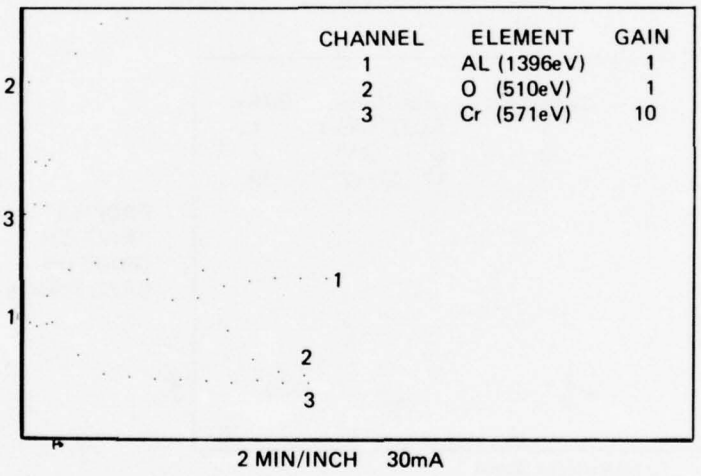

PROFILE
THROUGH
OXIDE ON
BARE 2024-T 3

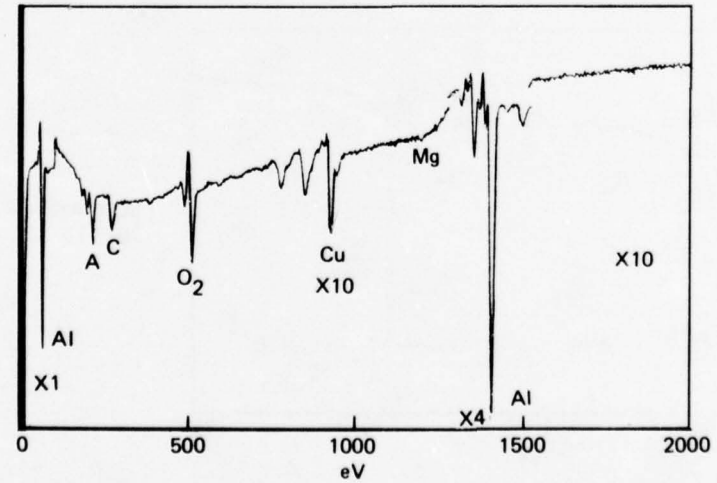

SURFACE OF
BARE 2024-T3

FIGURE 32. AUGER TRACES FROM AMMONIUM CHROMATE ANODIZED BARE 2024-T3, 10 VOLTS, 30 MIN, R.T.

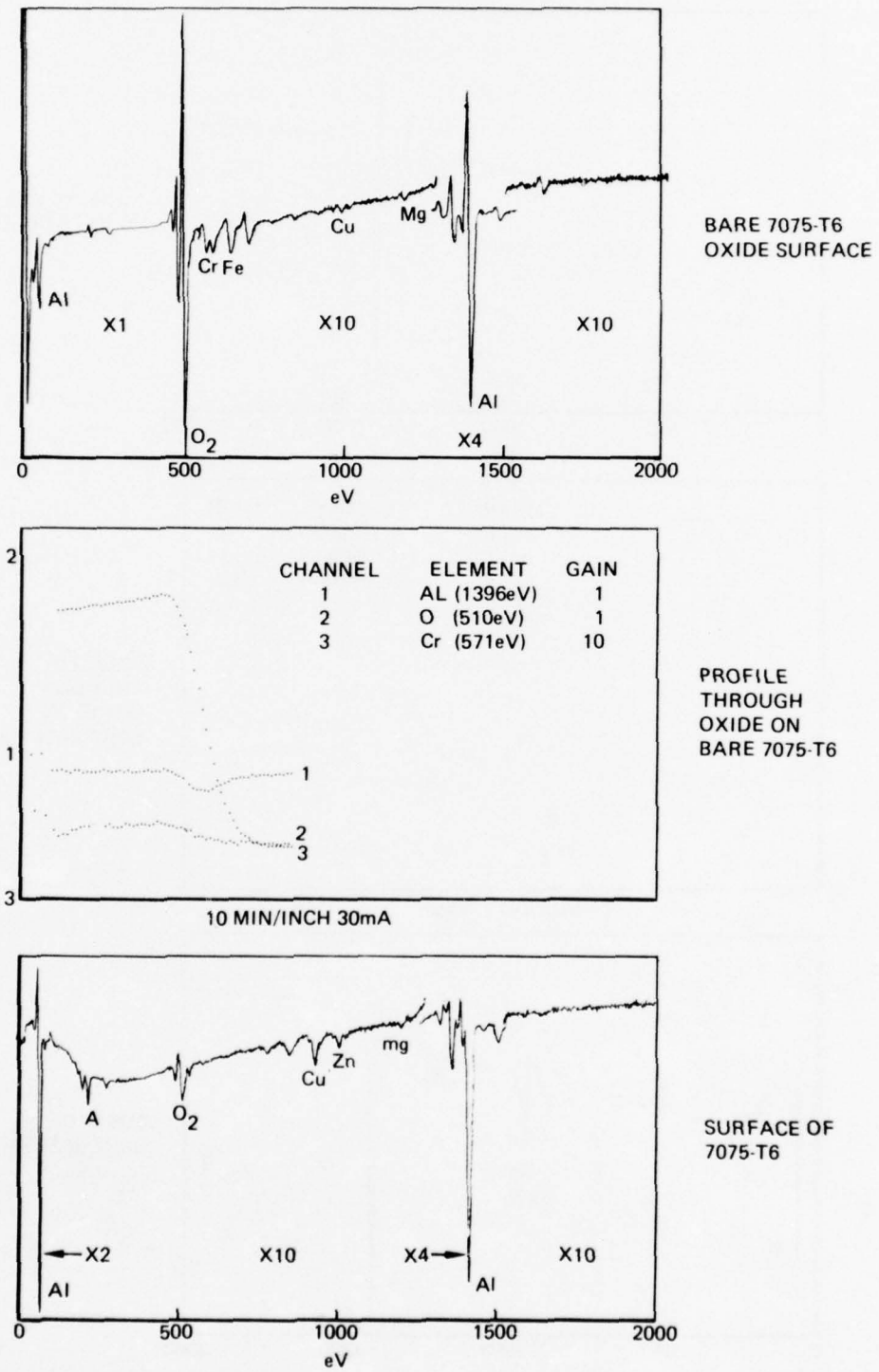

FIGURE 33. AUGER TRACES FROM AMMONIUM CHROMATE ANODIZED BARE 7075-T6, 100 VOLTS, 30 MIN, R.T.

TABLE 9. TABULATION OF AUGER INTENSITIES OBTAINED FROM SURFACES OF AMMONIUM CHROMATE ANODIZED BARE AND CLAD 2024-T3

ANODIZE CONDITION	Al	O_2	Cu	Zn	Mg	Cr	N_2	P	Fe	Ni
Bare										
10 V, 30 Min, RT	VS	VS	VVW	---	---	VW	VW	---	---	---
50 V, 30 Min, RT	VS	VS	VVW	---	---	W	---	---	VVW	---
100 V, 30 Min, RT	VS	VS	VW	---	---	VW	---	---	---	---
150 V, 30 Min, 41°F	VS	VS	VVW	---	---	W	---	---	VW	VW
150 V, 30 Min, 180°F 10% Conc.	VS	VS	VVW	---	---	W	---	---	---	---
Clad										
10 V, 30 Min, RT	VS	VS	VVW	---	---	W	W	---	VW	VW
50 V, 30 Min, RT	VS	VS	VVW	---	---	W	---	---	W	W
100 V, 30 Min, RT	VS	VS	VW	VVW	---	W	W	---	W	W
150 V, 30 Min, 41°F	VS	VS	---	---	---	W	VW	---	W	W
150 V, 30 Min, 180°F, 10% Conc.	VS	VS	VVW	---	---	VW	---	---	---	---

INTENSITY OF LINE

VS — Very Strong
S — Strong
M — Medium
MW — Medium Weak
W — Weak
VW — Very Weak
VVW — Very Very Weak

TABLE 10. TABULATION OF AUGER INTENSITIES OBTAINED FROM SURFACES OF AMMONIUM CHROMATE ANODIZED BARE AND CLAD 7075-T6

ANODIZE CONDITION	Al	O_2	Cu	Zn	Mg	Cr	N_2	P	Fe	Ni
Bare										
10 V, 30 Min, RT	VS	VS	W	VW	VW	W	W	---	W	W
50 V, 30 Min, RT	VS	VS	MW	W	VW	VW	---	---	---	---
50 V, 30 Min, 180°F, 10% Conc.	VS	VS	VW	VVW	VW	VW	W	---	W	W
50 V, 30 Min, 41°F	VS	VS	VW	VVW	---	M	VW	---	W	W
Clad										
10 V, 30 Min, RT	VS	VS	VVW	---	---	VW	W	---	---	---
50 V, 30 Min, RT	VS	VS	VW	VW	VW	W	---	---	W	W
150 V, 30 Min, 185°F	VS	VS	VVW	VW	---	W	---	---	VW	VW

INTENSITY OF LINE

VS — Very Strong
S — Strong
M — Medium
MW — Medium Weak
W — Weak
VW — Very Weak
VVW — Very Very Weak

Potassium/Lithium Nitrate Eutectic Salt Anodize System

A total of 4 variable test panels were anodized under varying conditions as described in Table 1. A 60% potassium nitrate/40% lithium nitrate eutectic salt bath was prepared by heating the dry salts at 320F until the entire bath was molten. A total of 64 coupons were anodized at various voltages and times at 315F and 500F. Figures 34 and 35 show the current density versus time plots for the 50 volt anodizing of bare and clad 2024-T3 and 7075-T6. The normal surge of high current occurred immediately after the voltage application and was followed by a gradual decay of the current. The clad material produced lower current density curves than the bare alloys. The 7075-T6 was slightly more reactive than the 2024-T3 during the first portion of the anodizing reaction. The bare 2024-T3 started reacting again after 900 seconds. Raising the bath temperature to 500F resulted in an unstable anodizing bath and arcing occurring periodically. The resultant oxide thickness was, however, proportional to the increased voltage.

The oxide thickness results as measured on the SEM are shown in Table 11. Increased voltage or temperature resulted in an increased oxide thickness. The oxide formation constant appears to be between 50 and 90Å/volt at 315F.

Great difficulty was encountered in rinsing the salt from the surface of the oxide after cool-down. Figures 36 and 37 show representative surface and cross-section photomicrographs of the oxides produced by the eutectic salt anodizing system at 315F. The barrier layer form of this oxide is apparent. However, a "column-like" oxide growth is apparent on the 2024-T3 alloy. Direct viewing of the oxide surface shows that the oxide is cracked as seen on the 7075-T6 alloys. This cracking probably occurs while cooling down to room temperature from the anodizing temperature. The clad alloy surfaces produced a much more even growth of the barrier layer oxide than did the bare alloys which produced a "bubbled" or "column-like" oxide structure. The surface of the 500F anodized specimens showed large pores and severe cracking in the oxide. The electrical arcing probably caused this attack of the oxide.

Using RHEED techniques, the anodic coating formed by this eutectic salt system was determined to be $\alpha\, Al_2O_3$ corundum (see Figure 38).

Auger electron spectrographic analysis was performed on the oxide surfaces and then the oxides were either profiled through to the base metal or they were ion milled below the surface to determine the elemental constituents in the oxide layer. Figures 35 and 36 show representative Auger traces and profiles. The comparative intensity data is tabulated in Tables 12 and 13. The active elements are Cu, Mg and Cr, and Cu,

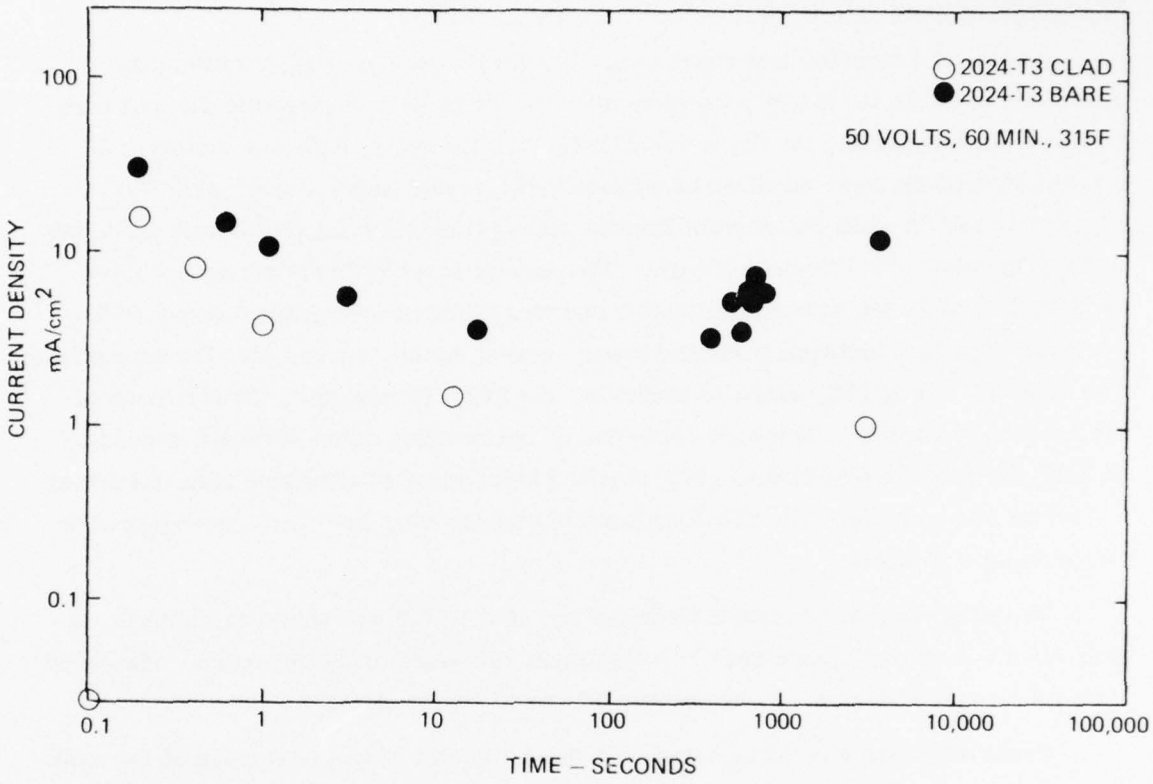

FIGURE 34. CURRENT DENSITY VERSUS TIME CHARACTERISTICS OF BARE AND CLAD 2024-T3 ANODIZED IN POTASSIUM/LITHIUM NITRATE

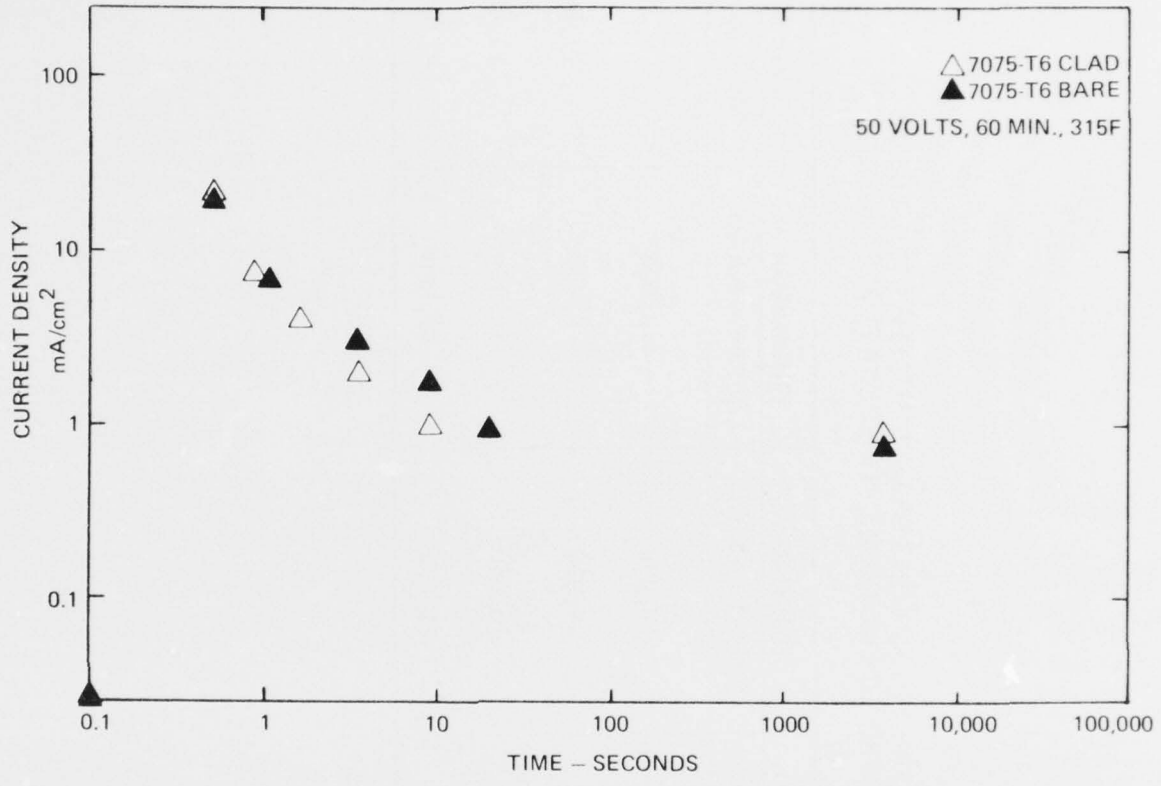

FIGURE 35. CURRENT DENSITY VERSUS TIME CHARACTERISTICS OF BARE AND CLAD 7075-T6 ANODIZED IN POTASSIUM/LITHIUM NITRATE

TABLE 11. ANODIC OXIDE FILM THICKNESS FOR POTASSIUM/LITHIUM NITRATE EUTECTIC SALT ANODIZING WITH VARIOUS VOLTAGES, TEMPERATURES AND TIMES

ANODIZE CONDITION	THICKNESS Å 2024-T3 BARE	THICKNESS Å 2024-T3 CLAD	THICKNESS Å 7075-T6 BARE	THICKNESS Å 7075-T6 CLAD
50 V, 30 Min, 315°F	5,130	10,000	6,050	8,420
50 V, 60 Min, 315°F	6,180	8,950	9,470	11,580
100 V, 10 Min, 315°F	11,050	18,680	15,790	15,660
50 V, 30 Min, 500°F	15,130	71,000	50,500	51,000

50 VOLTS, 30 MIN., 315F 19,000X

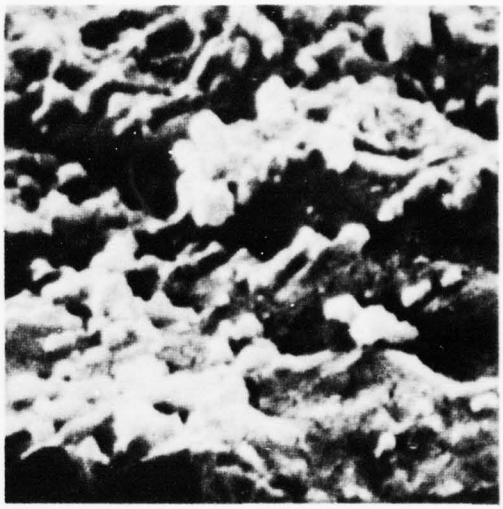

10 VOLTS, 10 MIN., 315F 19,000X

BARE

50 VOLTS, 30 MIN., 315F 19,000X

50 VOLTS, 30 MIN., 315F 19,000X

CLAD

FIGURE 36. SURFACE CHARACTER OF 2024-T3 ANODIZED IN EUTECTIC SALT

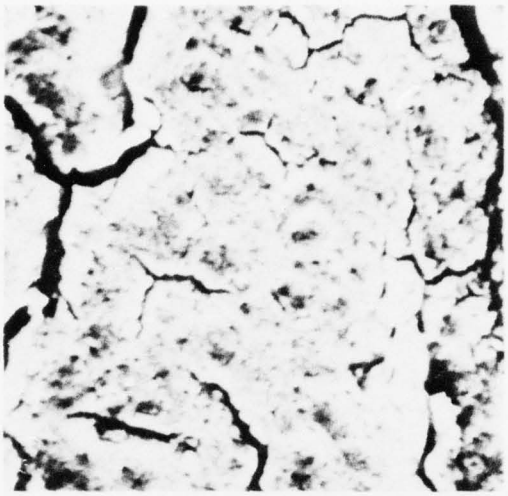

50 VOLTS, 30 MIN., 315F 700X

50 VOLTS, 30 MIN., 315F 19,000X

BARE

50 VOLTS, 30 MIN., 315F 19,000X

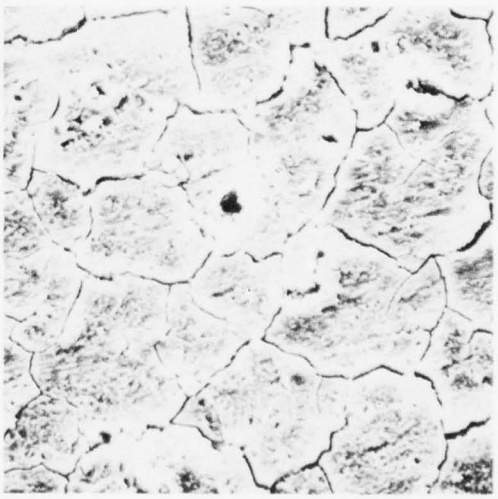

50 VOLTS, 60 MIN., 315F 700X

CLAD

FIGURE 37. SURFACE CHARACTER OF 7075-T6 ANODIZED IN EUTECTIC SALT

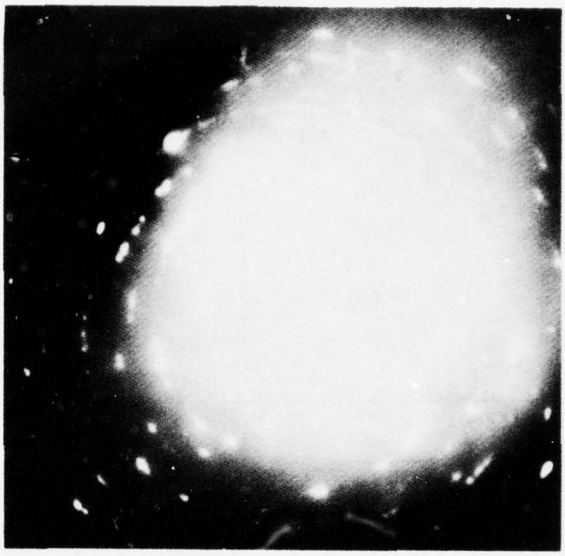

FIGURE 38. RHEED PATTERN FROM OXIDE ON 100 VOLT, R.T., POTASSIUM/LITHIUM NITRATE ANODIZE ON BARE 7075-T6

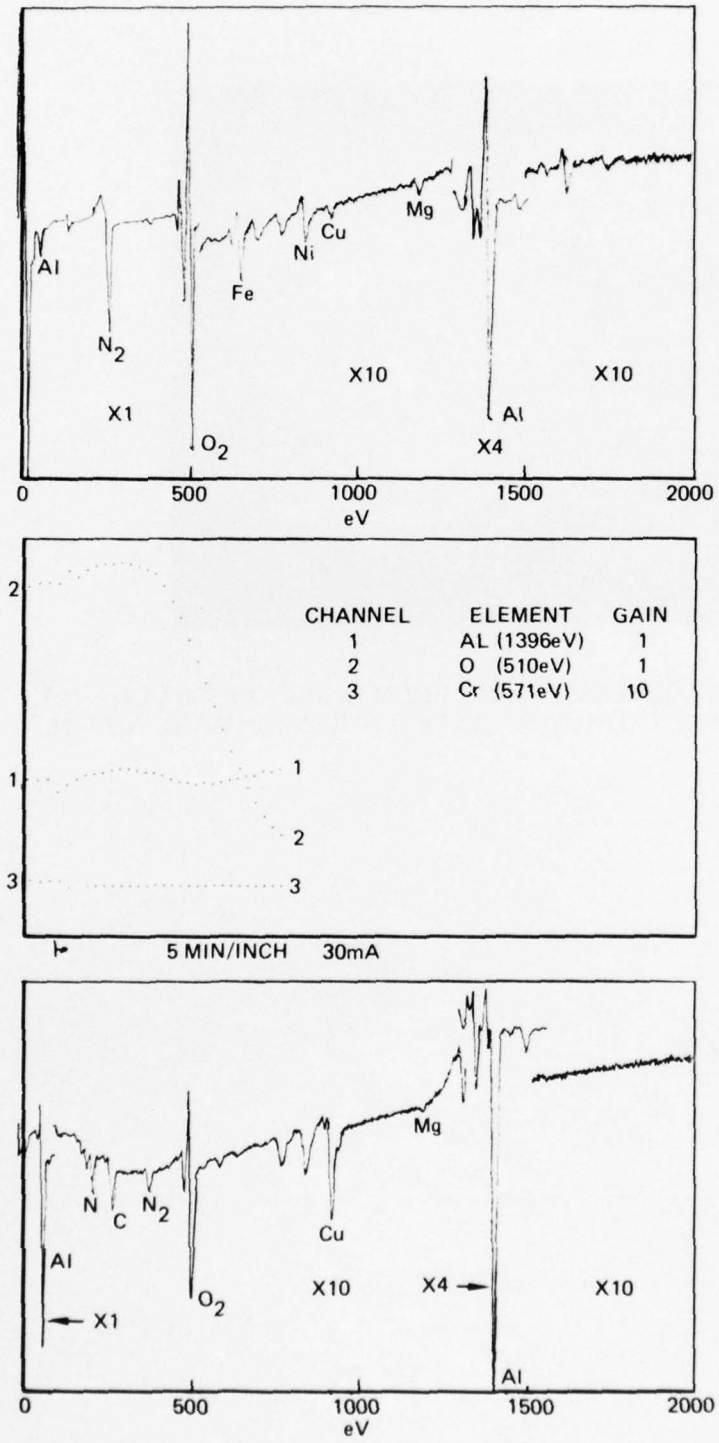

FIGURE 39. AUGER TRACES FROM POTASSIUM/LITHIUM NITRATE ANODIZED BARE 2024-T3-10 VOLTS, 10 MIN, 315F

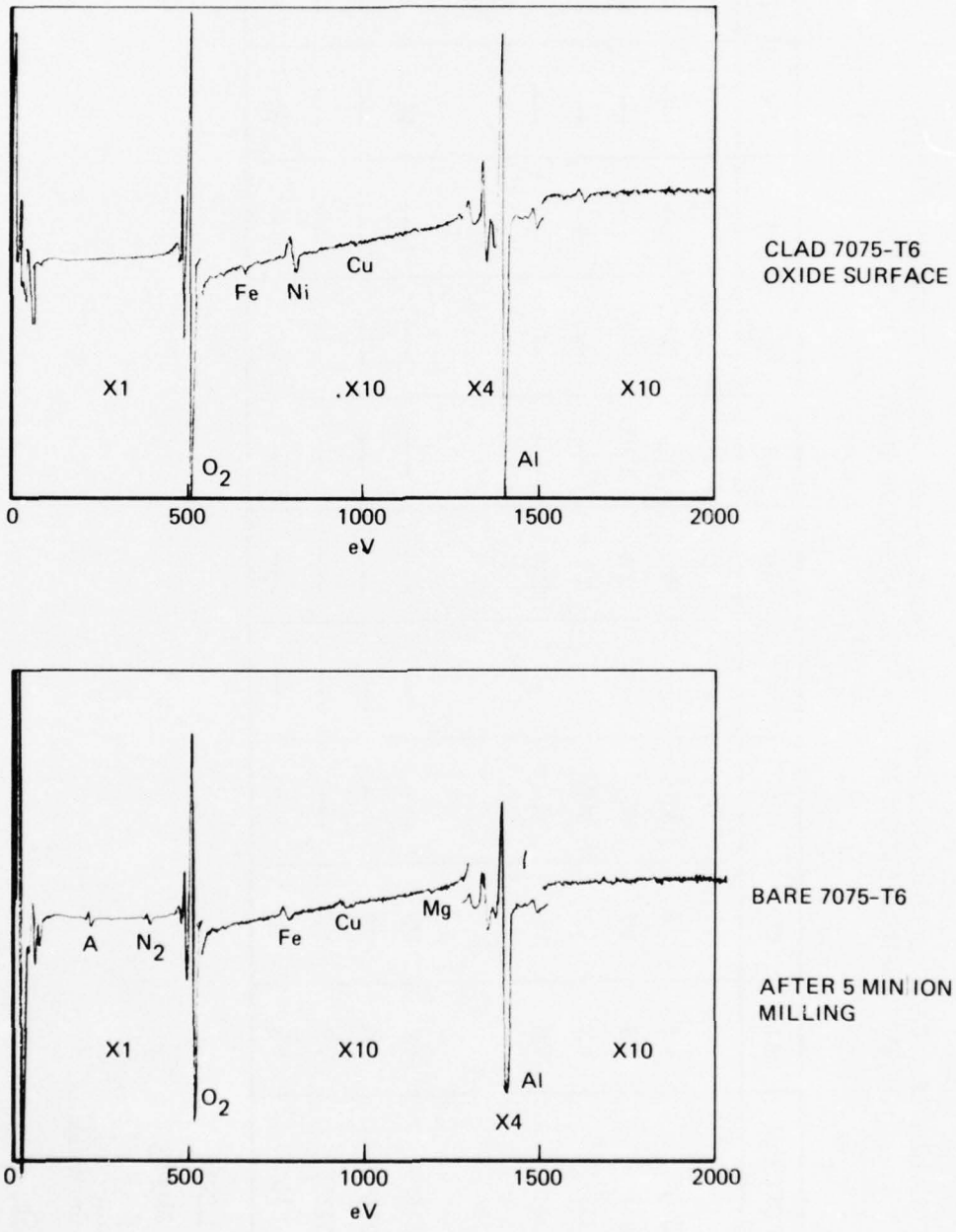

FIGURE 40. AUGER TRACES FROM POTASSIUM/LITHIUM NITRATE ANODIZED BARE AND CLAD 7075-T6, 50 VOLTS, 30 MIN, 315F

TABLE 12. TABULATION OF AUGER INTENSITIES OBTAINED FROM SURFACES OF POTASSIUM/LITHIUM NITRATE ANODIZED BARE AND CLAD 2024-T3

ANODIZE CONDITION	Al	O_2	Cu	Zn	Mg	Cr	N_2	P	Fe	Ni
Bare										
10 V, 10 Min, 315°F	VS	VS	MW	---	W	W	MW	---	---	---
50 V, 30 Min, 315°F	VS	VS	W	---	VW	VVW	---	---	---	---
50 V, 60 Min, 315°F	VS	VS	MW	---	VVW	---	---	---	---	---
100 V, 10 Min, 315°F	VS	VS	M	---	VW	---	---	---	---	---
Clad										
10 V, 10 Min, 315°F	VS	VS	---	---	---	---	---	---	W	W
50 V, 30 Min, 315°F	VS	VS	---	---	---	---	---	---	---	---
50 V, 60 Min, 315°F	VS	VS	---	---	---	---	---	---	---	---
100 V, 10 Min, 315°F	VS	VS	---	---	---	---	W	---	W	W

INTENSITY OF LINE

VS — Very Strong
S — Strong
M — Medium
MW — Medium Weak
W — Weak
VW — Very Weak
VVW — Very Weak

TABLE 13. TABULATION OF AUGER INTENSITIES OBTAINED FROM SURFACES OF POTASSIUM/LITHIUM NITRATE ANODIZED BARE AND CLAD 7075-T6

ANODIZE CONDITION	Al	O_2	Cu	Zn	Mg	Cr	N_2	P	Fe	Ni
Bare										
50 V, 30 Min, 315°F	VS	VS	VVW	---	---	---	---	---	---	---
50 V, 60 Min, 315°F	VS	VS	VVW	---	---	---	---	---	---	---
100 V, 10 Min, 315°F	VS	VS	MW	---	---	---	---	---	VW	VW
Clad										
50 V, 30 Min, 315°F	VS	VS	---	---	---	---	---	---	---	---
50 V, 60 Min, 315°F	VS	VS	---	---	---	---	---	---	VVW	VVW
100 V, 10 Min, 315°F	VS	VS	VW	---	---	---	VW	---	VW	VW

INTENSITY OF LINE

VS — Very Strong
S — Strong
M — Medium
MW — Medium Weak
W — Weak
VW — Very Weak
VVW — Very Very Weak

Zn and Mg for the 2024-T3 and 7075-T6 specimens, respectively. However, the activity does not appear to be as strong as that in the ammonium chromate system as the intensities at the oxide surface were not as strong. The Fe and Ni are believed to be impurities picked up from the stainless steel tank being used. Trace amounts of potassium and lithium were also detected on the oxide surface. They were probably caused by incomplete washing of the bath residues.

Ammonium Pentaborate-Ethylene Glycol Anodize System

A total of 8 variable test panels were anodized at room temperature, 200F, and 41F according to Table 1. Representative current density versus time curves for the 100 volt RT data are shown in Figures 41 and 42. The room temperature 100 volt curves show that all of the alloy conditions had very similar electrical properties. At 41F, the maximum current density dropped slightly, but the shape of the curves was the same. Similarly, at 200F the current density increased. Great care was exercised in running this anodize system to minimize or eliminate exposure to water. Samples were washed before anodizing with ethylene glycol.

The scanning electron microscope (SEM) was used to measure the oxide thicknesses resulting from each anodizing condition. Table 14 shows the measured thickness values. In general, the bare alloys produced slightly thicker oxide layers than did the clad alloys at room temperature. A slightly thicker oxide was produced on the 7075-T6 than on the 2024-T3 at room temperature. At 41F and 200F the oxide thickness appeared to be independent of the base alloy composition but, again, the oxide was thicker on the bare alloy than on the clad. Increased voltage resulted in an increased oxide thickness and the oxide formation constant was found to be between 15 and 20Å/volt at room temperature.

Figures 43 and 44 show representative surface and cross-section photomicrographs of the oxide formed with the ammonium pentaborate-ethylene glycol anodizing system. The expected barrier layer is evident on both the clad 2024-T3 and the clad 7075-T6 with the appearance of the conventional "blocky" type high density oxide. The structure of the oxide on the bare alloys shows a "columnar" nature as compared to the barrier layer growth. This is particularly evident on the specimens anodized at 41F. The layers formed at 200F on both the bare and clad alloys are the high density "block"-type barrier layer oxides. These results indicated that even for barrier layers the oxide formation rate is dependent on base alloy composition.

Using RHEED techniques, the anodic coating on these specimens was determined to be γAl_2O_3 (gamma) (see Figure 45).

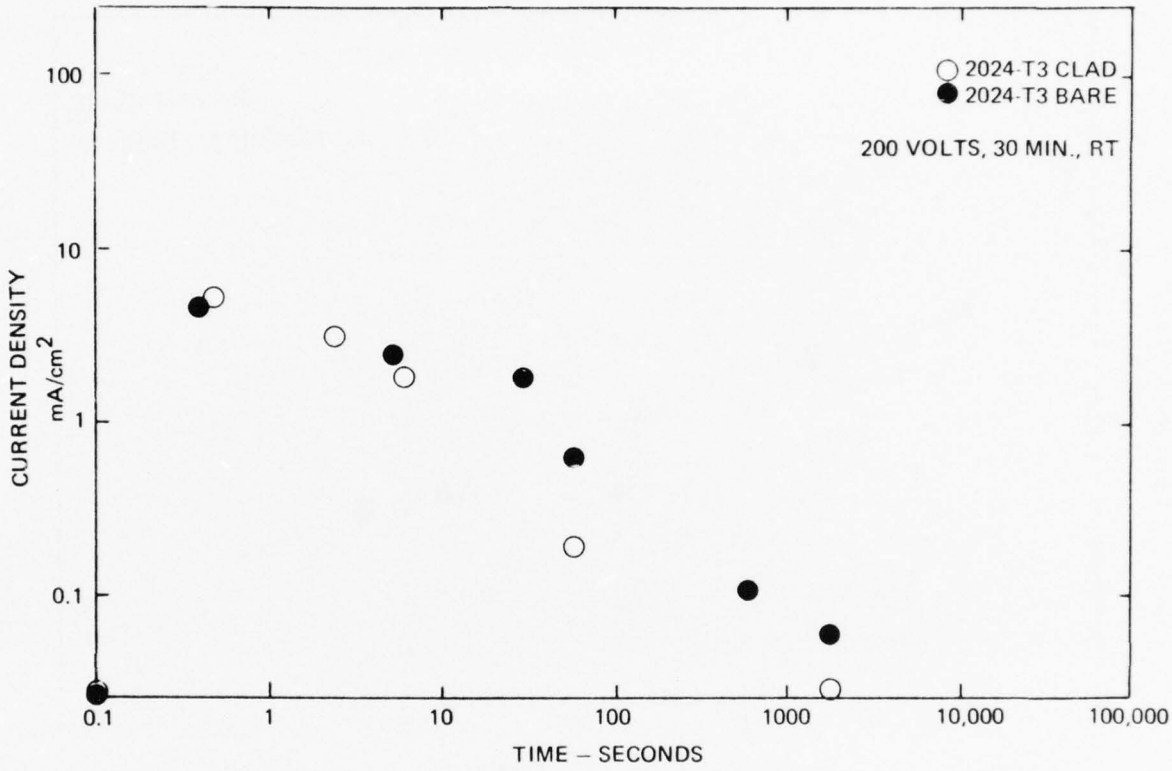

FIGURE 41. CURRENT DENSITY VERSUS TIME CHARACTERISTICS OF BARE AND CLAD 2024-T3 ANODIZED IN AMMONIUM PENTABORATE

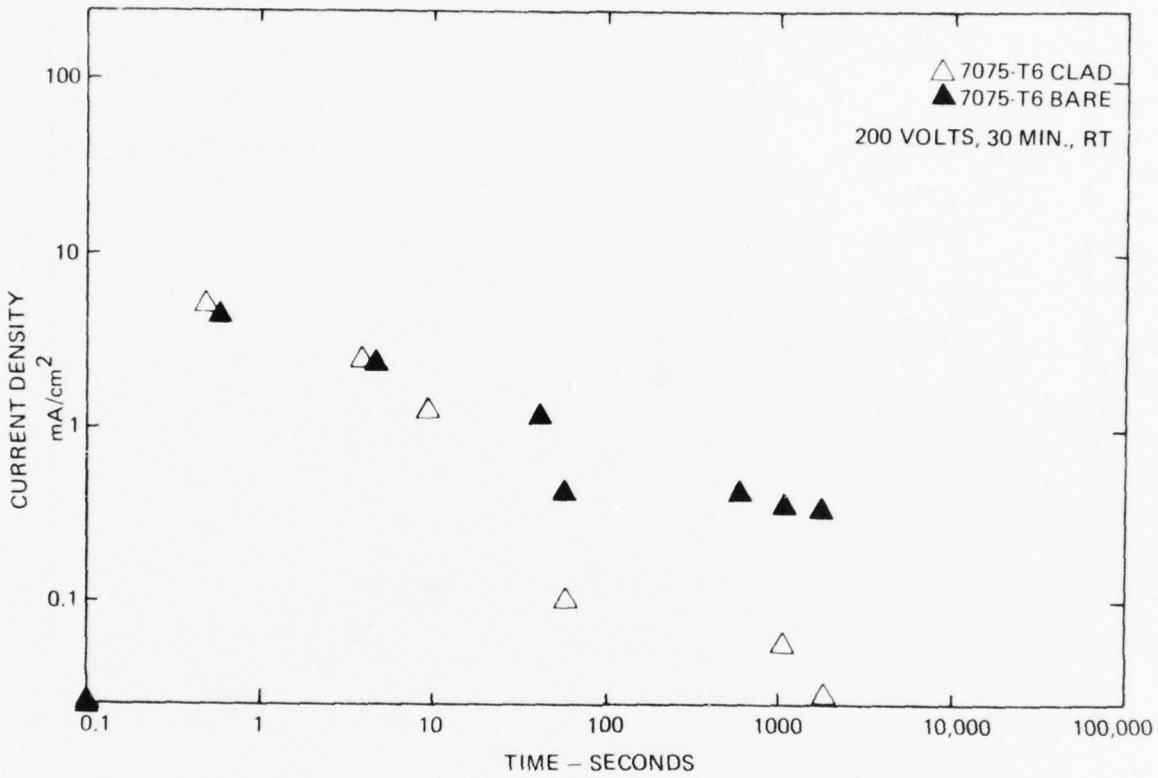

FIGURE 42. CURRENT DENSITY VERSUS TIME CHARACTERISTICS OF BARE AND CLAD 7075-T6 ANODIZED IN AMMONIUM PENTABORATE

TABLE 14. ANODIC OXIDE FILM THICKNESS FOR AMMONIUM PENTABORATE IN ETHYLENE GLYCOL ANODIZING WITH VARIOUS VOLTAGES AND TEMPERATURES

ANODIZE CONDITION	THICKNESS Å 2024-T3 BARE	THICKNESS Å 2024-T3 CLAD	THICKNESS Å 7075-T6 BARE	THICKNESS Å 7075-T6 CLAD
50 V, 30 Min, 41°F	790	950	920	790
100 V, 30 Min, 41°F	1,970	1,580	1,580	1,580
200 V, 30 Min, 41°F	3,680	2,630	3,550	2,630
50 V, 30 Min, RT	1,180	1,050	1,470	1,180
100 V, 30 Min, RT	2,100	1,710	2,100	1,710
200 V, 30 Min, RT	3,050	3,160	3,680	3,290
50 V, 30 Min, 200°F	1,580	1,050	1,450	1,310
100 V, 30 Min, 200°F	2,100	1,970	2,100	1,710

50 VOLTS, 30 MIN., RT 19,000X

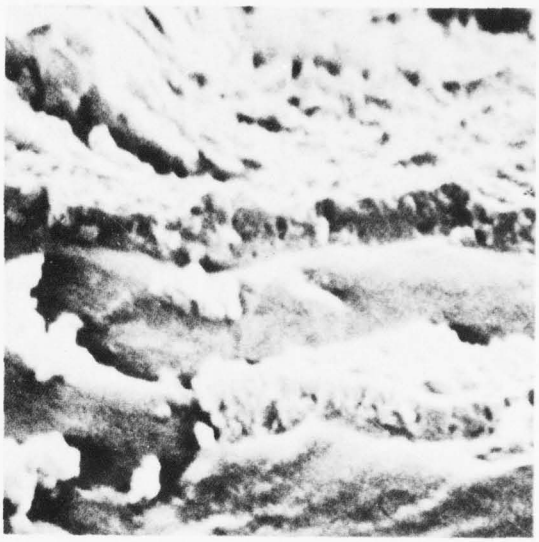

200 VOLTS, 30 MIN., 41F 19,000X

BARE

50 VOLTS, 30 MIN., RT 19,000X

200 VOLTS, 30 MIN., 41F 19,000X

CLAD

FIGURE 43. SURFACE CHARACTER OF 2024-T3 ANODIZED IN AMMONIUM PENTABORATE

AD-A038 068 NORTHROP CORP HAWTHORNE CALIF AIRCRAFT DIV F/G 11/3
FUNDAMENTAL INVESTIGATION OF ANODIC OXIDE FILMS ON ALUMINUM ALL--ETC(U)
AUG 76 R E HERFERT F33615-75-C-5121
UNCLASSIFIED NOR-76-101 AFML-TR-76-142 NL

2 OF 2
AD
A038068

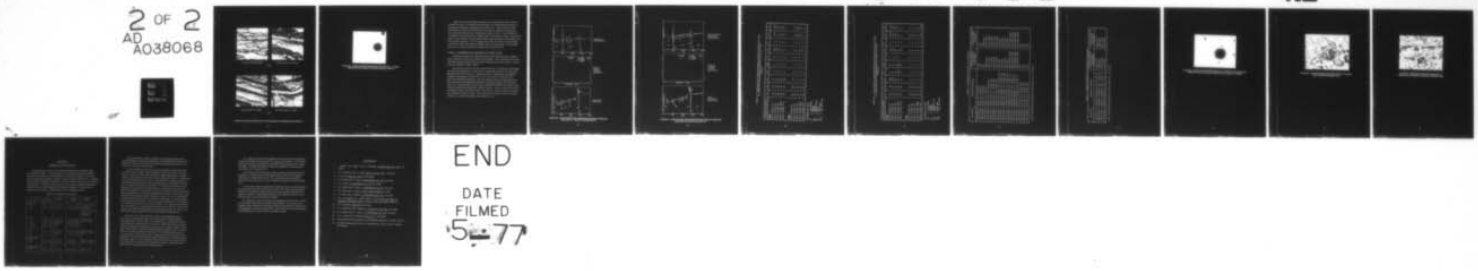

END

DATE
FILMED
5-77

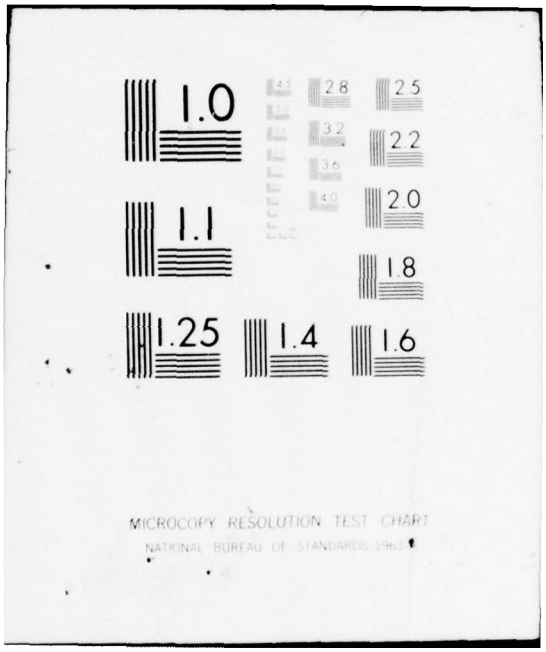
1.0
1.1
1.25
1.4
1.6
1.8
2.0
2.2
2.5
2.8
3.2
3.6
4.0
4.5
MICROCOPY RESOLUTION TEST CHART
NATIONAL BUREAU OF STANDARDS-1963-A

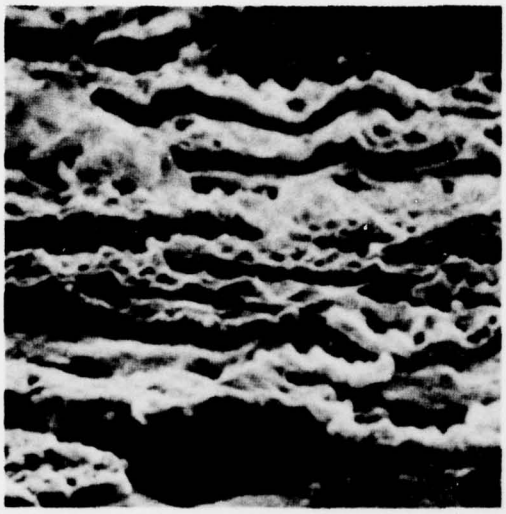

50 VOLTS, 30 MIN, RT 19,000X

200 VOLTS, 30 MIN., 41F 19,000X

BARE

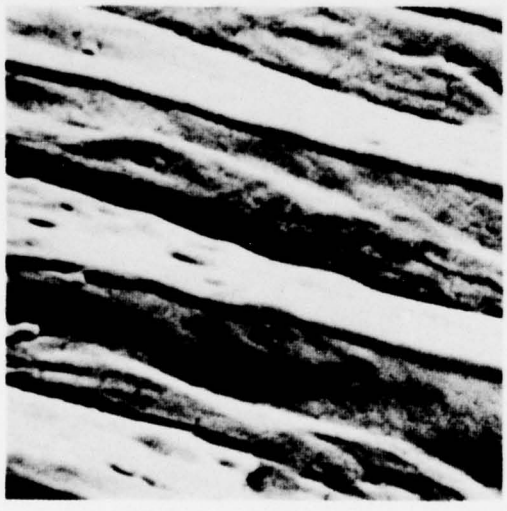

50 VOLTS, 30 MIN., RT 19,000X

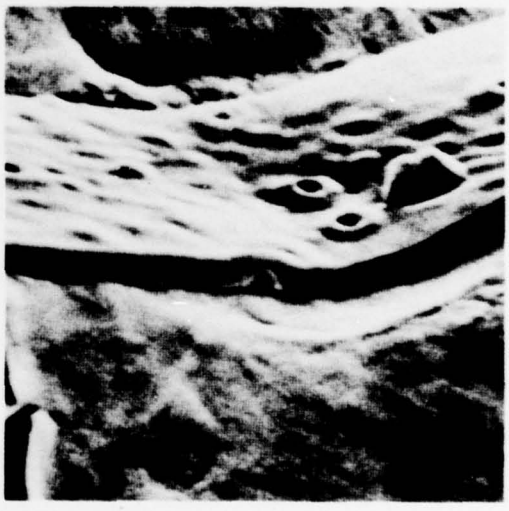

200 VOLTS, 30 MIN., 41F 19,000X

CLAD

FIGURE 44. SURFACE CHARACTER OF 7075-T6 ANODIZED IN AMMONIUM PENTABORATE

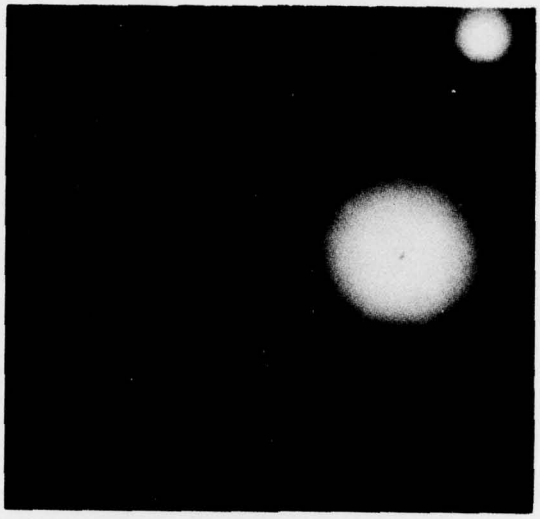

FIGURE 45. RHEED PATTERN FROM OXIDE ON 50 VOLT, R.T., 30 MIN, AMMONIUM PENTABORATE ANODIZE ON BARE 7075-T6

Auger electron spectrographic analysis was performed on the oxide surfaces and then the oxides were either profiled through or ion milled below the surface to determine the elemental constituents in the oxide layer. Figures 46 and 47 show representative Auger traces and profiles for the 2024-T3 and 7075-T6 specimens. The comparative intensity data is tabulated in Tables 15 and 16. The activity of Cu is apparent in the oxides formed on both the 7075-T6 and 2024-T3 alloys. The 2024-T3 shows a large amount of Cu at the surface which slowly decreases to the quantity of Cu in the metallic substrate. The Cu content in the oxide on the 7075-T6 is also higher at the surface than in the metallic substrate, but to a lesser degree. The elements Mg and Zn are also prevalent in the surface oxides on the 7075-T6.

TASK IV — ENVIRONMENTAL DURABILITY OF ANODIC FILMS

Anodized specimens were exposed in both stressed and unstressed condition to both a standard salt spray and a humidity environment. These specimens were evaluated after exposure using the optical and the scanning electron microscopes. Table 17 shows the tabulation of these results.

The stressed series of tests were conducted with a 0.125-inch wire held behind the center of the specimen. In this manner, the specimen surfaces were stressed to approximately 35 ksi in tension. These tests (Table 17) showed the same general ranking, except that the corrosion attack was more severe on these specimens than on the unstressed specimens. Electron diffraction analysis of the severe and heavy attacked oxides showed the formation of a hydrated $\beta Al_2O_3 \cdot H_2O$ oxide (see Figure 48). Scanning electron microscope examination revealed a "scale-like" attack to both the chromic and pentaborate anodized surfaces. Figure 49 shows the chromic acid anodize surface with oxide present on the surface. Figure 50 shows the ammonium pentaborate anodized surface. The attack on the ammonium chromate anodized surfaces was centered around the grain boundary areas.

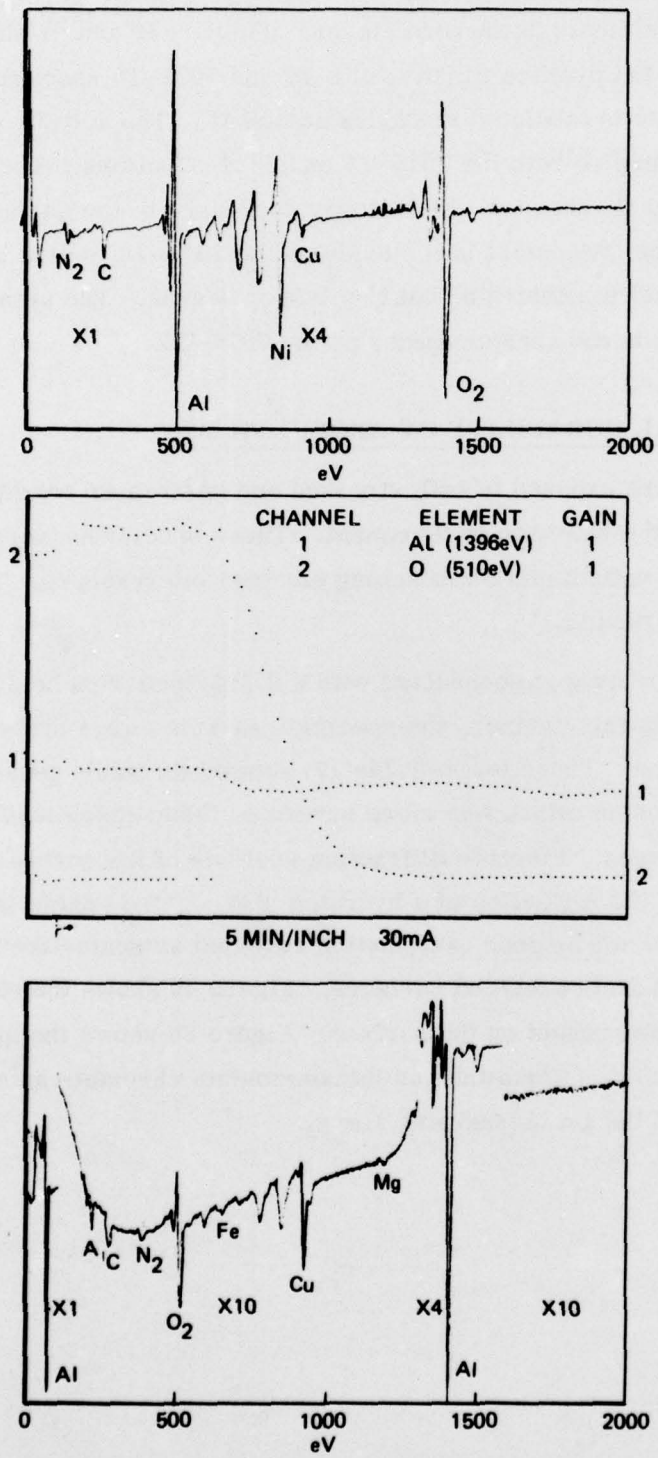

FIGURE 46. AUGER TRACES FROM AMMONIUM PENTABORATE ANODIZED BARE 2024-T3, 100 VOLTS, 30 MINUTES, R.T.

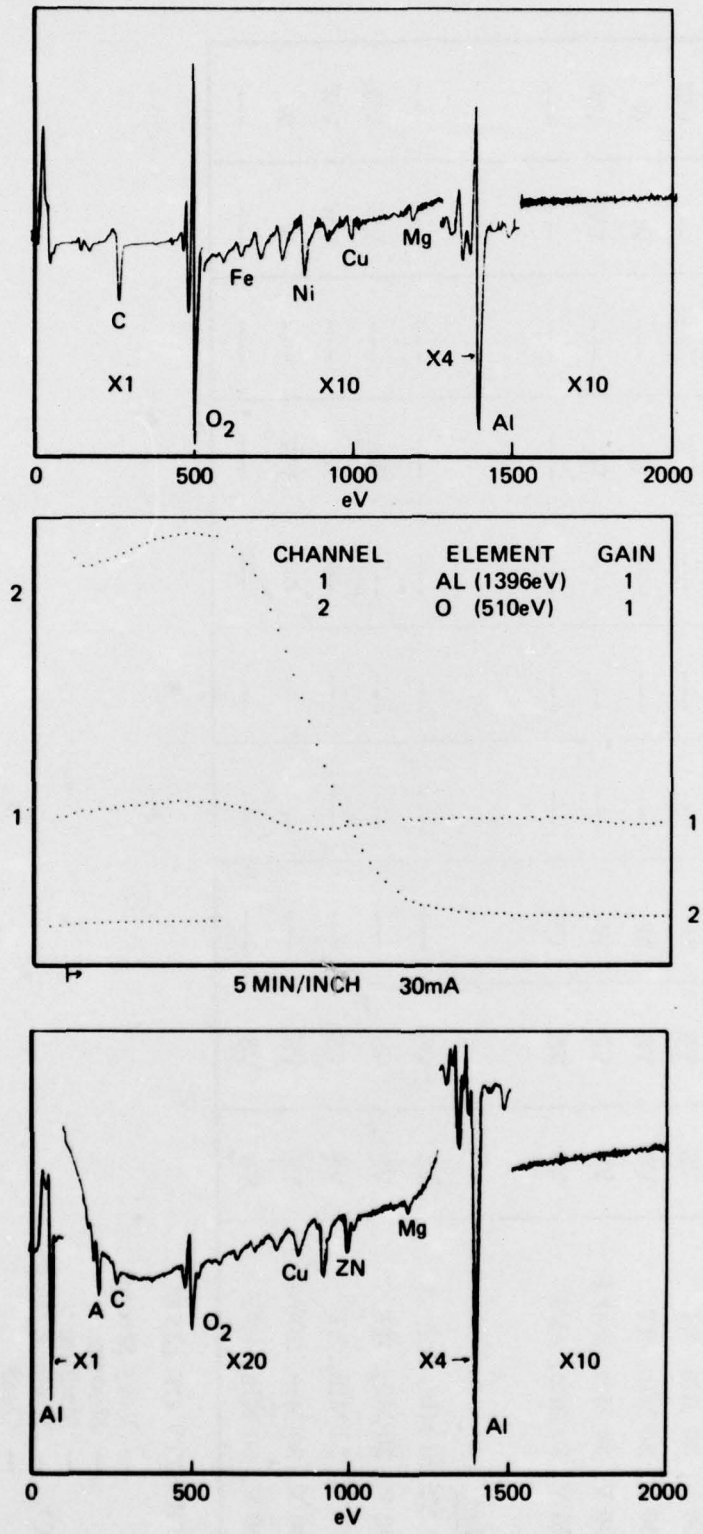

FIGURE 47. AUGER TRACES FROM AMMONIUM PENTABORATE ANODIZED BARE 7075-T6, 100 VOLTS, 30 MIN, R.T.

TABLE 15. TABULATION OF AUGER INTENSITIES OBTAINED FROM SURFACES OF AMMONIUM PENTABORATE ANODIZED BARE AND CLAD 2024-T3

ANODIZE CONDITION	Al	O_2	Cu	Zn	Mg	Cr	N_2	P	Fe	Ni
Bare										
50 V, 30 Min, RT	VS	VS	W	---	---	---	VW	---	VVW	VVW
100 V, 30 Min, RT	VS	VS	M	---	---	---	VW	---	---	VW
200 V, 30 Min, RT	VS	VS	M	---	---	---	W	---	W	W
100 V, 30 Min, 200°F	VS	VS	W	---	---	---	W	---	VW	VW
100 V, 30 Min, 41°F	VS	VS	VW	---	---	---	---	---	---	---
Clad										
50 V, 30 Min, RT	VS	VS	---	---	---	---	---	---	---	---
100 V, 30 Min, RT	VS	VS	---	---	---	---	W	---	VW	VW
200 V, 30 Min, RT	VS	VS	---	---	---	---	W	---	VW	VW
100 V, 30 Min, 200°F	VS	VS	---	---	---	---	VW	---	W	W
100 V, 30 Min, 41°F	VS	VS	---	---	---	---	---	---	---	---

INTENSITY OF LINE

VS — Very Strong
S — Strong
M — Medium
MW — Medium Weak
W — Weak
VW — Very Weak
VVW — Very Very Weak

TABLE 16. TABULATION OF AUGER INTENSITIES OBTAINED FROM SURFACES OF AMMONIUM PENTABORATE ANODIZED BARE AND CLAD 7075-T6

ANODIZE CONDITION	Al	O_2	Cu	Zn	Mg	Cr	N_2	P	Fe	Ni
Bare										
50 V, 30 Min, RT	VS	VS	MW	W	W	---	VW	---	VVW	VVW
100 V, 30 Min, RT	VS	VS	MW	W	W	---	VW	---	VW	VW
200 V, 30 Min, RT	VS	VS	M	W	W	---	W	---	VW	VW
100 V, 30 Min, 200°F	VS	VS	M	MW	MW	---	W	---	W	W
200 V, 30 Min, 41°F	VS	VS	W	W	W		VW	---	---	---
Clad										
50 V, 30 Min, RT	VS	VS	---	---	---	---	W	---	VW	---
100 V, 30 Min, RT	VS	VS	---	---	---	---	W	---	---	---
200 V, 30 Min, RT	VS	VS	---	---	---	---	M	---	W	W
100 V, 30 Min, 200°F	VS	VS	---	---	---	---	M	---	W	W
200 V, 30 Min, 41°F	VS	VS	---	---	---	---	W	---	VVW	VVW

INTENSITY OF LINE

VS — Very Strong
S — Strong
M — Medium
MW — Medium Weak
W — Weak
VW — Very Weak
VVW — Very Very Weak

TABLE 17. CORROSION RESISTANCE TEST RESULTS

MATERIAL	ANODIZED CONDITION	SURFACE CONDITION AFTER TESTING (UNSTRESSED)	SURFACE CONDITION AFTER TESTING (STRESSED)
2024-T3 Bare	H_3PO_4, 10 V, 20 Min RT	Good	Good
2024-T3 Clad	H_3PO_4, 10 V, 20 Min RT	Good	Good
7075-T6 Bare	H_3PO_4, 10 V, 20 Min RT	Good	Slight Attack
7075-T6 Clad	H_3PO_4, 10 V, 20 Min RT	Slight Attack	Severe Attack
2024-T3 Bare	Chromic Acid, 50 V, 40 Min 104F	Severe Attack	Severe Attack
2024-T3 Clad	Chromic Acid, 50 V, 40 Min, 104F	Severe Attack	Severe Attack
7075-T6 Bare	Chromic Acid, 50 V, 40 Min, 104F	Severe Attack	Severe Attack
7075-T6 Clad	Chromic Acid, 50 V, 40 Min, 104F	Severe Attack	Severe Attack
2024-T3 Bare	Chromic Acid, Sealed, 50 V, 40 Min, 104F	Mild Attack	Mild Attack
2024-T3 Clad	Chromic Acid, Sealed, 50 V, 40 Min, 104F	Mild Attack	Mild Attack
7075-T6 Bare	Chromic Acid, Sealed, 50 V, 40 Min, 125F	Heavy Attack	Heavy Attack
7075-T6 Clad	Chromic Acid, Sealed, 50 V, 40 Min, 125F	Mild Attack	Mild Attack
2024-T3 Bare	Ammonium Chromate, 50 V, 30 Min, RT	Spotty Random Attack	Heavy Spotty Attack
2024-T3 Clad	Ammonium Chromate, 50 V, 30 Min, RT	Spotty Random Attack	Heavy Spotty Attack
7075-T6 Bare	Ammonium Chromate, 50 V, 30 Min, RT	Spotty Random Attack	Heavy Spotty Attack
7075-T6 Clad	Ammonium Chromate, 50 V, 30 Min, RT	Spotty Random Attack	Heavy Spotty Attack
2024-T3 Bare	K/Li-NO_3, 50 V, 60 Min, 315F	Good	Good
2024-T3 Clad	K/Li-NO_3, 50 V, 60 Min, 315F	Good	Good
7075-T6 Bare	K/Li-NO_3, 50 V, 60 Min, 315F	Good	Good
7075-T6 Clad	K/Li-NO_3, 50 V, 60 Min, 315F	Good	Good

Note: The corrosion environment was 140F at 100% R.H. for 24 hours.

TABLE 17. CORROSION RESISTANCE TEST RESULTS (Continued)

MATERIAL	ANODIZED CONDITION	SURFACE CONDITION AFTER TESTING (UNSTRESSED)	SURFACE CONDITION AFTER TESTING (STRESSED)
2024-T3 Bare	Ammonium Pentaborate, 100 V, 30 Min, RT	Slight Attack	Slight Attack
2024-T3 Clad	Ammonium Pentaborate, 100 V, 30 Min, RT	Slight Attack	Slithg Attack
7075-T6 Bare	Ammonium Pentaborate, 100 V, 30 Min, RT	Heavy Attack	Heavy Attack
7075-T6 Clad	Ammonium Pentaborate, 100 V, 30 Min, RT	Heavy Attack	Heavy Attack

Note: The corrosion environment was 140F at 100% R.H. for 24 hours.

FIGURE 48. RHEED PATTERN FROM SURFACE OF CHROMIC ACID (UNSEALED) ANODIZE AFTER SALT SPRAY AND RELATIVE HUMIDITY TESTING

FIGURE 49. CORROSION PRODUCTS ON SURFACE OF CHROMIC ACID ANODIZED SPECIMEN, 700X

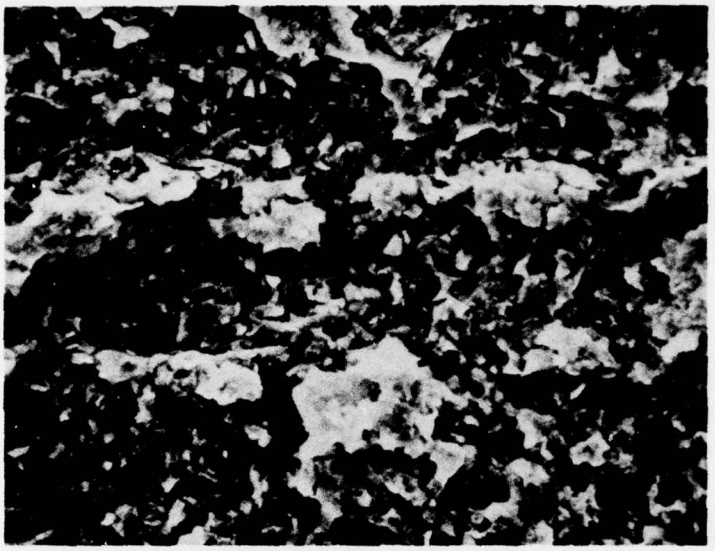

FIGURE 50. CORROSION PRODUCTS ON SURFACE OF AMMONIUM PENTABORATE ANODIZED SPECIMEN, 700X

SECTION IV

SUMMARY AND CONCLUSIONS

The processing variables and the desired results for each anodizing system were outlined in Table I. These parameters were selected in general to establish maximum and minimum in oxide thicknesses; to maximize the density of the oxide; and to maximize the boehmite, corundum or gamma aluminum oxide layer. In addition, the parameters selected were intended to vary the amounts of porous or barrier layers of anodic films. A baseline set of parameters were used to establish the properties obtained from "normally accepted" or commercial conditions. Table 18 shows a summary of the parameters established for the five anodizing systems.

TABLE 18. SUMMARY OF RESULTS

ANODIZING SYSTEM	THICKNESS Min, Å Max, Å	PHYSICAL CHARACTER	CRYSTALLINE CHARACTER RHEED	CHEMICAL CHARACTER AES
Phosphoric Acid				
RT	2,100 - 29,500	Porous Type	α-$Al_2O_3 \cdot H_2O$ Boehmite	Al, O_2 highest intensities in all Oxides Cu high Bare 2024-T3 Cu, Zn, Mg, high in 7075-T6 S, C, N_2, Fe contaminants in most oxides Clad shows mostly contaminants
41°F	1,950 - 4,050	Barrier Appearing	α-$Al_2O_3 \cdot H_2O$ Boehmite	
180°F	520 - 1,670	Porous	α-$Al_2O_3 \cdot H_2O$ boehmite	
Chromic Acid				
42°F	1,390 - 6,900	Porous/Barrier	α-$Al_2O_3 \cdot H_2O$ Boehmite	Same as Phosphoric except, Lower Cu, Zn, and Mg. Cr detected
104°F	5,790 - 187,000	Porous/Barrier	α-$Al_2O_3 \cdot H_2O$ Boehmite	
3 oz/gal	1,400 - 2,500	Porous Barrier	α-$Al_2O_3 \cdot H_2O$ Boehmite	
10 oz/gal	3,160 - 61,000	Porous	α-$Al_2O_3 \cdot H_2O$ Boehmite	
50 oz/gal	5,790 - 187,000	Porous	α-$Al_2O_3 \cdot H_2O$ Boehmite	
Ammonium Chromate				
RT	660 - 2,600	Barrier Type	α-$Al_2O_3 \cdot H_2O$ Boehmite	Similar to Phosphoric but less Cu, Zn, and Mg, High Cr; Fe and Ni from tank
41°F	1,970 - 2,370	Barrier, with porous	α-$Al_2O_3 \cdot H_2O$ Boehmite	
180°F	8,420 - 12,630	Barrier	α-$Al_2O_3 \cdot H_2O$ Boehmite	
Ammonium Pentaborate in Ethylene Glycol				
RT	1,050 - 3,290	Barrier Type	γ-Al_2O_3 (Gamma)	Similar to Ammonium Chromate, No Cr, slightly higher Cu, Zn, and Mg
200°F	1,580 - 2,100	Barrier Type	γ-Al_2O_3 (Gamma)	
41°F	790 - 3,680	Barrier Porous	γ-Al_2O_3 (Gamma)	
Potassium/Lithium Nitrate Eutectic Molten Salt				
300°F	5,130 - 18,680	Barrier Type	α-Al_2O_3 (Corundum)	Similar to Ammonium Chromate, No Cr
500°F	15,130 - 71,000	Barrier Type	α-Al_2O_3 (Corundum)	

During this program, different conditions were evaluated to determine the relationship between voltage, bath temperature, bath composition and anodizing time and the oxide which was produced with five different anodizing systems on bare and clad 2024-T3 and bare and clad 7075-T6.

Two of the anodizing systems which were used produced a porous oxide on top of a thin barrier layer oxide. Both the phosphoric acid and the chromic acid baths were more reactive at higher bath concentrations, higher temperatures, and higher voltages. This greater activity produced a less ordered oxide structure, and entrapped more contaminant elements in the oxide. Low temperatures, voltages and bath concentrations had less chemical activity associated with them which allowed the formation of a regular cell-like porous oxide layer. The oxide layers which formed on the higher purity clad material were composed of a more regular pore structure than those which formed on the bare alloys. The barrier layer film thickness also indicated that the oxide growth rate is largely dependent on alloy content. In each of these cases, the growth rate was greater than the "literature" constant. Of course, the literature constant is based on oxide growth on a 99.99% purity aluminum. Lower bath temperatures resulted in the formation of a barrier layer only on clad 2024-T3 in the phosphoric acid and both clad alloys in the chromic acid bath. The AES analysis indicated that there was a high Cu, Zn, and Mg content in the oxide on bare 7075-T6. Neither of the oxides on the clad alloy contained these elements showing that both the chemical activity of the bath and the composition of the alloy influenced the oxide structure.

The barrier layer baths ammonium chromate, potassium/lithium nitrate eutectic salt, and ammonium pentaborate in ethylene glycol all produced dense or semi-dense barrier layers of oxide. At low temperatures, a small amount of porous oxide developed on the surface of the barrier layer. Higher temperatures frequently changed the baths activity and disrupted the barrier layer. Higher voltages produced thicker barrier layers as expected, but the thickness was different from the constant derived from oxides formed on pure aluminum. The AES indicated the presence of Cu in the barrier layers of 2024-T3, but to a lesser extent than in the porous oxides. The presence of Fe and Ni in the oxides resulted from the use of a stainless steel anodizing tank. Again, Cu, Zn, and Mg were present in the barrier layer oxides formed on the bare 7075-T6 with all of the anodizing baths. However, smaller amounts of these elements were present than in the porous oxides.

The crystalline structures of the phosphoric acid, chromic acid and ammonium chromate oxide films were determined to be $\alpha \cdot Al_2O_3 \cdot H_2O$ (boehmite). The potassium/lithium nitrate eutectic salt produced an oxide film which was analyzed to be $\alpha \cdot Al_2O_3$ (corundum). The oxide film produced in ammonium pentaborate in ethylene glycol was analyzed to be $\gamma \cdot Al_2O_3$ (gamma).

On the whole, all of the stable (low activity) anodizing systems tend toward the formation of a constant thickness oxide depending upon the alloy, bath composition, temperatures and voltage but not time. Thus, given sufficient time (seconds to minutes) the oxide layer which is formed is essentially independent of further holding time.

The corrosion resistance exposure tests showed the chromic acid and ammonium chromate oxides to have the least resistance to 140F, 100% relative humidity testing. Under certain conditions the oxides formed in ammonium pentaborate also showed a hydration breakdown. Testing specimens under stress appeared to hasten the rate of hydration failure, but did not change their ranking.

The significance of this program lies in the subsequent use of this data in studies on the durability of oxide films in conjunction with adhesives. The program has developed the basic relationship between the parameters and the physical, chemical, and crystallographic character of the oxide films. The next step is to use these parameters in the development of a durable interface for adhesive bonding.

REFERENCES

1. F. Keller, M.S. Hunter, and D.L. Robinson, J. Electrochem. Soc., 100, 411 (1953).
2. J.P. O'Sullivan and G.C. Wood, Proc. Roy. Soc. A317, 511 (1970).
3. G. Haas, J. Opt. Soc. Am. 39, 532 (1949).
4. M.S. Hunter and P. Fowle, J. Electrochem. Soc. 101, 481 (1954)
5. R.C. Plumb, J. Electrochem. Soc. 105, 498 (1958)
6. M.S. Hunter and P. Fowle, J. Electrochem. Soc. 101, 515 (1954)
7. T.P. Hoar and J.F. Mott, J. Phys. Chem. Solids 9, 97 (1959)
8. T.P. Hoar and J. Yahalom, J. Electrochem. Soc. 110, 614 (1963).
9. D.T. Arrowsmith, E.A. Culpan, and R.J. Smith, Proc. Int. Symp. on Anodizing, Birmingham, 1967, Aluminum Federation (London, 1967), 17.
10. R.W. Franklin, Nature 180, 1470 (1957).
11. D.J. Stirland and R.W. Bicknell, J. Electrochem. Soc. 106, 481 (1959).
12. M.S. Hunter and P.F. Towner, J. Electrochem. Soc. 108, 139 (1961).
13. J.S.L. Leach and P. Neufeld, Corros. Sci. 9, 413 (1969).
14. "Improved Surface Treatments for Weld-Bonding Aluminum" AF33615-75-C5027.
15. Personal Communication with Dr. Tennyson Smith, Science Center, Rockwell International.

☆ U. S. GOVERNMENT PRINTING OFFICE: 1977 — 757-001/277